NVH HUNGARY

INTERNATIONAL CONFERENCE FOR ACOUSTIC AND VIBRATION ENGINEERS

October 8-10, 2025 – Balatonalmádi, Hungary

CONFERENCE BOOKLET

BOSCH

Invented for life

Bosch NVH Center Budapest
Forming the Future of Mobility NVH

- One of Hungary's most competent NVH teams: acousticians with decades of know-how and diverse background in electrical, mechanical, software and vehicle engineering.
- R&D projects for product and methodology development in cooperation with Bosch product teams, OEM-s and universities
- NVH Facility with state-of-the-art laboratory covering over 1000 m^2, housing Anechoic, Semi-Anechoic and Vehicle Anechoic chambers equipped with a chassis-dynamometer.
- Equipment for every need: multiple Laser Vibrometer Systems, Noise Source Localization and Sound Field Visualization Systems, customized test benches for special needs, etc.

NVH HUNGARY

INTERNATIONAL CONFERENCE FOR ACOUSTIC AND VIBRATION ENGINEERS

Conference Booklet

October 8-10, 2025 – Balatonalmádi, Hungary

ISBN 978-615-5270-85-7

Overview map of the city

(not drawn to scale)

Source: balaton-almadi.hu

About the Conference

NVH Hungary 2025 (NVHH2025) International Conference for Acoustic and Vibration Engineers is the second edition of the biennial NVHH conference series on acoustics, structural dynamics and NVH (Noise Vibration and Harshness) organized by the Budapest University of Technology and Economics, and the University of Győr in close cooperation with industrial partners. The goal of the conference is to provide an international forum for acoustic, vibration, and NVH engineers, researchers, and professionals to share their contributions in the fields of experimental as well as numerical acoustics, vibroacoustics, vehicle NVH, interior acoustics, and entertainment system development. The conference caters to both academicians and professionals, therefore state-of-the-art university research and cutting-edge industrial innovation will be presented side by side, followed by social gatherings that promote the exchange of information and nurture fruitful cooperations between the various fields of the profession.

Conference Chairs:

Prof. Fülöp Augusztinovicz

Prof. Gábor Stépán

Organizing Committee:

Balázs Bank
Zoltan Dombóvári
Bertalan Fukker
Zoltán Gazdagh
Csaba Horváth
Tibor Kimpián
Balázs Vehovszky

Scientific Committee:

Fülöp Augusztinovicz
Balázs Bank
Filip Deblauwe
Zoltan Dombóvári
Steven Dom
Dániel Feszty
Bertalan Fukker
Zoltán Gazdagh
Csaba Horváth
Manfred Kaltenbacher
Tibor Kimpián
Bert Pluymers
Gábor Stépán
Esat Topbas
Balázs Vehovszky

Operative Organizer:

Diamond Congress Kft.
Attila Varga - diamond@diamond-congress.hu
www.diamond-congress.hu

Conference booklet editors:

Balázs Vehovszky, Gergely Szakáts

CONTENTS

Sponsors:

BOSCH
Életre tervezve
www.bosch.hu

thyssenkrupp
thyssenkrupp.com

AVL
www.avl.com

KNORR-BREMSE
www.knorr-bremse.com

Exhibitors:

LB-acoustics Polytec
lb-acoustics.at

HEAD acoustics
www.head-acoustics.com

MÜLLER-BBM
www.muellerbbm.com/hompage

AMC MECANOCAUCHO
www.mecanocaucho.com

sciengineer
sciengineer.com

Organizing Partners:

MŰEGYETEM 1782

MAGYAR MÉRNÖKI KAMARA

SZÉCHENYI EGYETEM
UNIVERSITY OF GYŐR

National Research, Development and Innovation Office
Hungary
PROGRAM FINANCED FROM THE NRDI FUND

Conference Program - Overview

Day 1 (8th of October)			
8:30	10:00	**Registration**, coffee break & exhibition	
10:00	10:20	**Conference opening -** Csaba Horváth, Prof. Fülöp Augusztinovicz	
10:20	11:15	**Opening lecture** - Prof. Gabor Stepan (BME): Vibrations - How has it become a battlefield in R&D? (Chair: Zoltán Gazdagh)	
11:15	12:10	**Plenary lecture 1** - Prof. Klaus Genuit (HEAD Acoustics): Sound character, sound quality, sound design and soundscape – Important acoustical aspects of today and in future (Chair: Fülöp Augusztinovicz)	
12:10	13:30	Lunch break	
13:30	14:50	**Session 1** - Conference room 1 (Békésy) Sound reproduction and audio signal processing	**Session 2** - Conference room 2 (Gábor) Experimental modal analysis
14:50	15:20	Coffee break & exhibition	
15:20	16:20	**Session 3** - Conference room 1 (Békésy) Sound reproduction and audio signal processing	**Session 4** - Conference room 2 (Gábor) Experimental modal analysis
17:10	17:15	Meeting in the hotel's lobby, walking to the ship	
17:30	19:30	**Welcome reception on the Balaton**	
19:45	23:00	Optional social gathering - Rooftop bar	

Day 2 (9th of October)				
8:30	9:25	**Plenary lecture 2** - Håvard Vold (Vold LLC): NVH, a walk down memory lane by an old, applied mathematician (Chair: Csaba Horváth)		
9:25	10:20	**Plenary lecture 3** - Xavier Beudaert Perez (DanobatGroup, Ideko): Active vibration systems for vibration suppression in manufacturing applications (Chair: Zoltán Dombóvári)		
10:20	10:50	Coffee break & exhibition		
10:50	12:50	**Session 5** - Conference room 1 (Békésy) Machine learning and AI approaches	**Session 6** - Conference room 2 (Gábor) Numerical methods and modeling	
12:50	14:10	Lunch break		
14:10	15:50	**Session 7** - Conference room 1 (Békésy): Experimental acoustic and vibration methods	**Session 8** - Conference room 2 (Gábor): Nonlinear structures, processes, and methods	**Session 9** - Conference room 3 (Tobias): Machine-tool vibration
15:50	16:20	Coffee break & exhibition		
16:20	17:40	**Session 10** - Conference room 1 (Békésy): Experimental acoustic and vibration methods	**Session 11** - Conference room 2 (Gábor): Nonlinear structures, processes, and methods	**Session 12** - Conference room 3 (Tobias): Machine-tool vibration
17:40	19:00	Break / Wellness		
19:00	21:00	**Gala dinner**		
21:00	23:00	Optional social gathering - Rooftop bar		

Day 3 (10th October)			
8:30	10:10	**Session 13** - Conference room 1 (Békésy) Vehicle and powertrain NVH	**Session 14** - Conference room 2 (Gábor) Applied substructuring
10:10	10:40	Coffee break & exhibition	
10:40	12:20	**Session 15** - Conference room 1 (Békésy) Noise and vibration of rotating machinery	**Session 16** - Conference room 2 (Gábor) Stability and control of dynamical systems
12:30	12:50	**Closing ceremony -** Best scientific, industrial, and student contribution awards	
12:50	14:20	Lunch	

Conference Program - Sessions

October 8 (Wednesday)		
[Scientific art. / Case study]	Békésy (Room 1)	Gábor (Room 2)
	Session 1 | **Sound reproduction and audio signal processing** *Chairs: Balázs Bank, Tibor Kimpián*	Session 2 | **Experimental modal analysis** *Chair: Zoltán Gazdagh*
13:30 - 13:50	12 | Nóra Nagy - Simulation-based Automotive Sound System Enhancement	7 | Peter Blaschke - Non-mass loaded excitation technique for precise laser measurements
13:50 - 14:10	68 | Géza Balogh - Electroacoustical system of the Puskás Arena	42 | Ákos Miklós - Acoustic excitation for experimental characterization of contact damping in prestressed assemblies
14:10 - 14:30	56 | Péter Szalai - Compensation of inharmonicity of pianos strings with added masses	72 | Tibor Kimpián & Zoltán Dombóvári - Case study on merging dispersed modes due to mass placement using impulse dynamic subspace
14:30 - 14:50	48 | Bence Ország - Overview of nonuniform filter bank design methods	21 | Csaba Horváth & Szilárd Gungl - Rectilinear and torsional modal analysis of a drone propulsion system using optical methods
COFFEE BREAK & EXHIBITION	Session 3 | **Sound reproduction and audio signal processing** *Chairs: Balázs Bank, Tibor Kimpián*	Session 4 | **Experimental modal analysis** *Chair: Zoltán Gazdagh*
15:20 - 15:40	76 | Tibor Kimpián - Crest-factor optimized multisine excitation signal for FRF measurements of lightly damped structures	17 | Simone Gallas - Load dependencies in experimental modal analysis of a hydrogen fuel cell stack
15:40 - 16:00	57 | Balázs Bank - Logarithmic frequency scale filter design using fixed-pole parallel filters	63 | Zoltán Dombóvári - Case study of forming complete FRF from incomplete data using impulse dynamic subspace
16:00 - 16:20	24 | Balázs Vehovszky - Investigation of audio induced squeak and rattle on a car door	66 | Felipe Ponce-Vanegas - On complex mode shapes and their identification

October 9 (Thursday) - Morning		
[Scientific art. / Case study]	Békésy (Room 1)	Gábor (Room 2)
	Session 5 | **Machine learning and AI approaches** *Chairs: Janka Erdélyi, Máté Farkas*	Session 6 | **Numerical methods and modeling** *Chair: Bert Pluymers*
10:50 - 11:10	4 | Karl Janssens - AI-driven solutions to enhance structural dynamics and NVH testing processes	8 | Csaba Huszty - Practical features and performance of the symplectic time-domain and modal FEM methods of Soundy for car interior acoustic predictions
11:10 - 11:30	40 | Davide Carlino - Electric machine stator FRFs prediction using machine learning	62 | Péter Rucz - Computation of sound radiation by moving sources using the convected boundary element method
11:30 - 11:50	33 | Janka Erdélyi - Machine learning approach to the detection and categorization of nonlinear phenomena in electronic components	92 | Timo Giese - Application of the time-domain boundary element method for NVH analysis in automotive gear systems
11:50 - 12:10	73 | Sarai Gonzalez y Gonzalez - Real-time MRI-based transformer model for articulatory speech synthesis	28 | Dániel Serfőző - The effective reduction of spurious oscillations in the valve closure event of an internal combustion engine
12:10 - 12:30	93 | Fatima Ezzahra Akaaboune - Diffusion-based brain-to-speech synthesis decoding intracranial EEG into natural speech	94 | Tamás Turcsán - Analysis of launch-related acoustic loads on a thermal guard assembly
12:30 - 12:50	35 | Máté Farkas & Stephan Pamp - Understanding sound preferences for EVs: A global research collaboration by Bosch, Klangerfinder, and clickworker	39 | Attila Kossa - Exploring stability domains in compressible Ogden's hyperelastic model

Conference Program - Sessions

October 9 (Thursday) - Afternoon			
	Békésy (Room 1)	**Gábor (Room 2)**	**Tobias (Room 3)**
|Scientific art. |Case study	Session 7 | **Experimental acoustic and vibration methods** *Chair: Bertalan Fukker*	Session 8 | **Nonlinear structures, processes, and methods** *Chair: Gábor Stépán*	Session 9 | **Machine-tool vibration** *Chairs: Zoltán Dombóvári, Xavier Beudaert Perez*
14:10 - 14:30	61 | András Kiss - Impact of measurement variables on product sound power levels	5 | Fanni Kádár - Effect of two outlet pipes on the stable pressure relief valve discharge process	10 | Róbert Tóth - NVH Analysis with a vibration monitoring system of a honing machine
14:30 - 14:50	51 | Csongor Báthory - Effect of connection hose on centrifugal coolant pump vibration results	6 | Jum Yi Chan - Effect of modal interaction on close-mode nonlinear structures	54 | András Bártfai - The effect of slowly varying 0th order directional factor in the circular milling of a single degree of freedom flexure
14:50 - 15:10	38 | Kristóf Lakatos & Dániel Ács - Case study of time delay effects on amplitude distortion during sinusoidal sweep excitation	45 | Zoltán Gabos - Graphical interpretation on the formation of isolated resonances in a dissipative nonlinear system	90 | Ferenc Bucsky - Dynamics of low immersion milling process subjected to Coulomb friction
15:10 - 15:30	64 | Gergely Zoltán Horváth - Case study of nonlinear vibration predition via LS-DYNA in airbag ECUs	16 | Ambrus Zelei - Vibroacoustic and sound radiation analysis of a nonlinear plate-cavity system under thermal load	32 | Máté Farkas - Time series failure identification in manufacturing
15:30 - 15:50	60 | Tibor Barsi Palmic - Dynamic sensors and actuators 3D-printed with filament extrusion	79 | János Karsai - Development of tracking methods for nonlinear resonances using a real-time controller	89 | Luka Radulovic - Simulation problems on the state dependent representation of boring bar torsion
COFFEE BREAK & EXHIBITION	Session 10 | **Experimental acoustic and vibration methods** *Chair: Bertalan Fukker*	Session 11 | **Nonlinear structures, processes, and methods** *Chair: Gábor Stépán*	Session 12 | **Machine-tool vibration** *Chairs: Zoltán Dombóvári, Xavier Beudaert Perez*
16:20 - 16:40	31 | Gábor Pór - CT equipment based on sound waves	50 | Csaba Hős - Predicting valve-pipeline instability via impedance equations	75 | Sándor Zalán - Flank contact and the stability of cutting processes
16:40 - 17:00	15 | Manfred Kaltenbacher - Design of acoustic absorbers based on local resonant acoustic metamaterials	81 | Balázs Bauer - Self-excited oscillations in brake systems: can impact-induced bounce trigger sustained vibrations?	77 | Dávid Hajdú - Dynamic force measurements on flexible workpieces
17:00 - 17:20	78 | Jaroslav Hruskovic - Comparision of building sound insulation (R'w) and laboratory values (Rw) in lightweight constructions	55 | Máté Antali - Vibration characteristics of rolling elements in the presence different friction and creep models	52 | Zoltán Dombóvári - Experimental study of self-excited vibrations in broaching operations using strain gauge based stiff load cell technology
17:20 - 17:40	100 | Zoltán Horváth - From concept to construction: how to build fitting noise & vibration test labs	71 | Du Xiaolei - Stochastic shimmy in towed wheels: experimental characterization of road-induced random vibrations	49 | Kristóf Martinovich - Periodic tail stock pressure modulation in turning of flexible workpiece via piezoelectric actuators

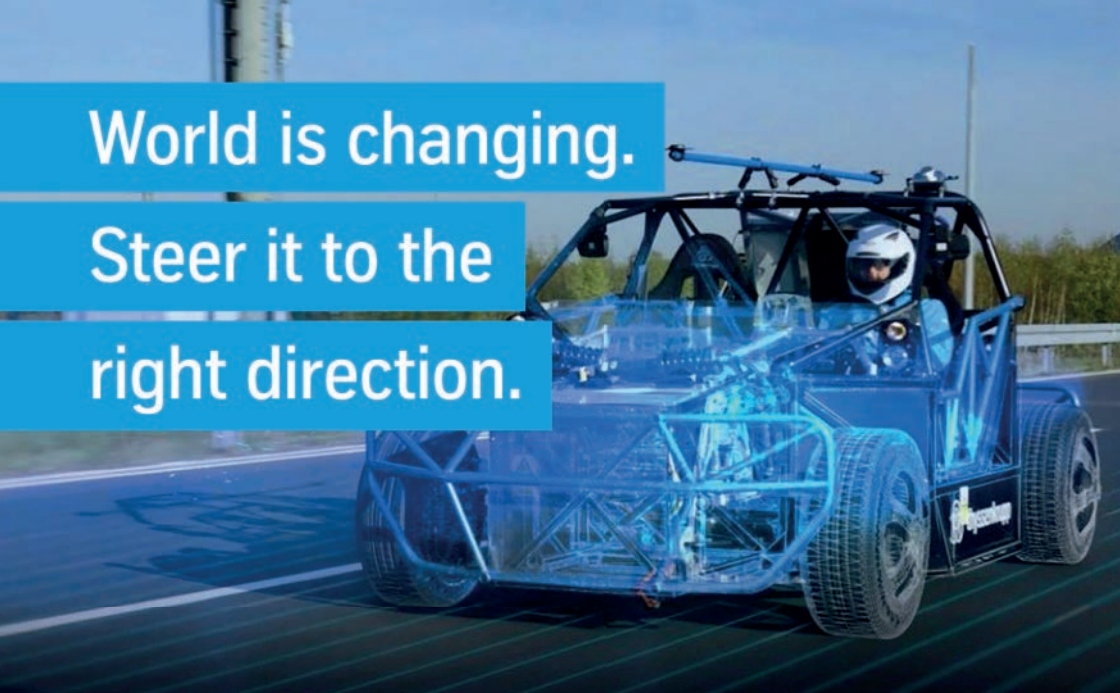

World is changing. Steer it to the right direction.

The thyssenkrupp's E/E Competence Centre in Budapest isn't a just satellite organisation, but literally a real development centre, which has become one of the world's leading centres of expertise in both the software and hardware aspects of electromechanical steering systems based on the ideas of Hungarian engineers and their own intellectual work. We can independently define own development methodology and make the decisions on the basic technical directions. We perform complex development, not outsourced subtasks. Our advanced development department explores distant future solutions that don't even exist today.

For open positions visit thyssenkrupp.hu/karrier.

facebook.com/thyssenkrupphungary

*Please note that by submitting your CV, you consent to the processing of your personal data by thyssenkrupp Components Technolog Hungary Kft (székhely: 1117 Budapest, Budafoki út 56. South Buda Business Park cjsz: 01-09-887088) as data controller in accordance with the Privacy Policy available at https://www.thyssenkrupp.hu/hu/adatvedelem.

engineering.tomorrow.together.

thyssenkrupp

Conference Program - Sessions

October 10 (Friday)		
|Scientific art. |Case study	**Békésy (Room 1)**	**Gábor (Room 2)**
	Session 13 | **Vehicle & powertrain NVH** *Chair: Tibor Kimpián*	Session 14 | **Applied substructuring** *Chairs: Balázs Vehovszky, Zoltán Gazdagh*
8:30 - 8:50	13 | Sándor Varga - Advanced noise reduction strategies in the EDU development	69 | Azat Jolamanov - Case study of long boring bars with passive vibration absorber considering bending and torsion
8:50 - 9:10	27 | Bertalan Fukker & Zoltán Gazdagh - New cooperation model in automotive NVH	14 | Domenico Minervini - High frequency mount stiffness identification for electric powertrains using test driven FE approach
9:10 - 9:30	43 | András Fejér - Optimizing the dynamic behavior of e-Axle test benches by reducing low-frequency vibrations	47 | Tamás Varga - Surface-line contact TPA - Windscreen sensitivity on acoustic transfer at wiper blade positions
9:30 - 9:50	26 | Hongmei Wang - Drivetrain gearboxes NVH modeling and simulation	53 | Bendegúz Gergácz - Investigating passive-side noise in component-based TPA: insights and recent improvements
9:50 - 10:10	88 | Krisztián Horváth - Sensitivity analysis of tooth microgeometric modifications on vibroacoustic behavior in helical gears with harmonically distributed variations	9 | Karl Janssens - Virtual Prototype Assembly (VPA): an overview of the latest technological advancements
COFFEE BREAK & EXHIBITION	Session 15 | **Noise and vibration of rotating machinery** *Chair: Manfred Kaltenbacher*	Session 16 | **Stability and control of dynamical systems** *Chair: Dániel Bachrathy*
10:40 - 11:00	36 | János Vad - Minimal modelling of noise and vibration propensity of fluids engineering equipment due to vortex shedding	83 | Róbert Kristóf Richlik - Human balancing on SUP board
11:00 - 11:20	29 | Hayato Naojima - Electromagnetic vibration and noise analysis of three-phase induction motors	82 | Ádám Kiss - Comfort-Critical Control in vehicle dynamics using Control Barrier Functions
11:20 - 11:40	70 | Szilárd Gungl & Kristóf Horváth - Application of motion magnification in automotive vibration analysis	74 | Dávid Andárs Horváth - Optimization of the position and parameters of a tuned-mass damper for flutter suppression applying Bayesian optimization
11:40 - 12:00	46 | Bálint Kocsis - Exploring theoretical limits in circular microphone array beamforming	85 | Balázs Endrész - Measuring orientation for visual balancing task of Furuta pendulum
12:00 - 12:20	-	95 | Rudolf Tóth - Experimental study of digital force control

Our Predecessors

Prof. György Békésy (Georg von Békésy)

(1899 Budapest, Hungary – 1972 Honolulu, USA)

György Békésy (Georg von Békésy) carried out research in Hungary at the Postal Research Center (acoustics of telephones, function of the human ear). Among his works in Hungary, the acoustic design of the large orchestra studio of the Magyar Rádió plays an important role. He left for Sweden after his laboratory was destroyed (1946) and later moved to Harvard, USA (1948). He received the Nobel Prize in Physiology of Medicine in 1961 for his discoveries of the physical mechanism of stimulation within the cochlea. He received the Nobel Prize in Medicine as a physicist. After his laboratory burned down, he left for the University of Honolulu, where he led the Laboratory of Sensory Sciences, known today as the Békésy Laboratory of Neurobiology. He never married and had no children (2 sisters, 3 brothers, 2 nieces).

Prof. István Albert Tóbiás (Stephen A. Tobias)

(1920 Wien, Austria – 1986 Birmingham, UK)

Stephen Albert Tobias was a leading Hungarian-British mechanical-engineering academic who was a Professor and the Head of the Department of Mechanical Engineering at the University of Birmingham. After his graduation in the war-stricken Budapest in 1945, he worked at the Machine Tool Factory of Weiss Manfred Industries as an engineer. He migrated to the UK in 1948 from the Faculty of Mechanical Engineering of Budapest University of Technology and Economics as a fresh PhD student. Later his research established much of the modern understanding of machine-tool vibration, stability and chatter summarized in his influential book Machine-tool Vibration, and his countless scientific publications. In 1960 he founded the leading scientific journal in the field the International Journal of Machine Tools & Manufacture of which he was the editor-in-chief from the beginning until his death in 1986 establishing high standards for the following two editors up to the present.

Prof. Dénes Gábor (Dennis Gabor)

(1900 Budapest, Hungary - 1979 London, UK)

He began his studies in mechanical engineering at the Budapest University of Technology and Economics and continued them at the Technical University of Berlin. From 1927 to 1933 he worked for Siemens as a research engineer. In 1934, he moved to England, where he joined the research laboratory of British Thomson-Houston, focusing on high-voltage discharge tubes and electron optics. In 1948, he began teaching at Imperial College London. In the same year, he published his paper *"A New Microscopic Principle"* in *Nature*, presenting the wavefront-reconstruction theory (developed mainly in 1947) that states the basic principles of holography.

He is best known as the inventor of holography (Nobel Prize: 1971), but he also revolutionized signal analysis with his 1946 paper: *Theory of Communication*. His idea of analyzing time and frequency jointly – rather than using traditional time-domain or Fourier analysis solely – paved the way for the short-time Fourier transform (STFT) and wavelet analysis. While he initially implemented his ideas with electromechanical devices, the methodology became practically usable with the advent of computers. Today, time-frequency analysis is widely employed in signal processing and data compression applications.

Beyond his technical work, he was deeply concerned about the future of humanity and was one of the founding members of the Club of Rome.

Sources: Wikipedia, ChatGPT, bukowskis.com, University of Birmingham archives, personal memories

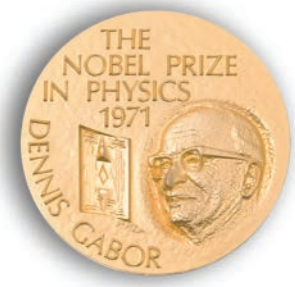

Keynote speakers – plenary lectures

Prof. Dr.-Ing. Klaus Genuit

Sound character, sound quality, sound design and soundscape – Important acoustical aspects of today and in the future

Acoustics does not only mean the presence of sound waves. A sound event can certainly lead to different auditory events. The context, the attitude of the exposed person to the source of the noise, as well as the experience and expectations of the noise exposure, influence the perception and assessment of sounds. Acoustics are determined by spectral composition and temporal patterns. For this reason, the discipline of psychoacoustics has established itself, which can provide more differentiated, meanwhile globally standardized analyses to describe sound character. Parameters such as loudness, sharpness, tonality, roughness, and fluctuation help to classify the sound character of a sound event, but determining the sound quality requires additional information about the meaning and functionality of the sound source with consideration of the context. Only through suitable listening tests can the relationship between sound character and sound quality be recognized, to recommend targeted measures and modifications through sound design to optimize the acoustic effect of a sound event. The international standard ISO 12913 "Soundscape" describes this relationship of perceived sound quality considering the context, while also considering that there are usually several spatially distributed sound sources that determine the entire sound event. The aurally correct recording of a complex sound event for the purpose of psychoacoustic analysis and auditory assessment is therefore normatively based on the use of binaural measurement technology. Psychoacoustics, sound quality and cognition provide information on how humans perceive and interpret their surrounding world. With psychoacoustics alone it is only possible to describe sound character. Whereas the perceived sound quality depends on the context of how people experience the sound situation. While the overall noise measured at a specific location can be analyzed in terms of several acoustic parameters, the annoyance or pleasantness level of a complex soundscape composed of several sound sources cannot be determined solely from the values obtained through such analyses. Even if the acoustic

contribution of a single sound source to the overall noise does not appear significant in a physical sense, the influence of this sound source on the soundscape can be relevant perceptually. The definition was part of ISO 12913-1 (2014): Soundscape is the acoustic environment as perceived or experienced and/or understood by a person or people, in context. Two major components like pleasantness and eventfulness describe soundscape. This concept allows to consider sound quality aspects beyond noise annoyance, a good soundscape quality is not simply identical to the absence of annoyance. Judgments cannot be fully understood by only considering acoustic quantities, since contextual parameters and interactivity are relevant for assessment of a soundscape as well. The description of complex sound quality, how it is created, how it is assessed, how it becomes predictable through simulation, will be explained in this article using examples.

Prof. Dr.-Ing. Klaus Genuit

Founder of HEAD Acoustics GmbH

Member of the supervisory board of HEAD Acoustics

Chairperson of the board of directors of HEAD-Genuit-Foundation

Klaus Genuit led the psychoacoustic working group at the Institute "Elektrische Nachrichtentechnik" at the RWTH Aachen. In cooperation with a German car manufacturer, he developed a new, improved binaural measurement system for the advanced diagnosis and analysis of sound. In 1986 he founded the company HEAD acoustics GmbH which is today a leading contributor in areas of binaural signal processing, analysis, auralization of virtual environments, NVH analysis, and telecommunication measurements. In 2010 he published at Springer “Sound Engineering im Automobilbereich”. He is a member of various associations, such as AES, JAS, JSAE, SAE, DEGA and ASA. He has participated in different EU-supported research projects like OBELICS, SVEN, Q-CITY and CITYHUSH, all of them focusing on improved sound quality of vehicle interior and exterior noise.

Alma Mater/Degrees:

Diploma Electrical Engineering, RWTH Aachen, 1976

Diploma Economic Science, RWTH Aachen, 1979

PhD Engineering Science, RWTH Aachen, 1984

Honorary Professor Psychoacoustics, RWTH Aachen, 2008

Prof. Gábor Stépán:

Vibrations – How has it become a battlefield in R&D?

Noise, vibration and harshness – while the composition of these three topics present a relatively well-defined notion today especially in the automative industry, this lecture focuses on the historical aspects of **vibrations** from the perspective of the essential changes that have been taking place in the Hungarian industry, also in the related training of our engineers for the last five decades. This lecture is a subjective report about an Odyssey of returning to the research and development community.

In Hungary, the 1980's looked quite controversial from engineering viewpoint. Our schools provided an internationally competitive theoretical background, while the flagship industrial companies struggled with R&D, started using increasing number of western licenses instead of trusting the knowledge and ideas of their own engineers. My experience across the local industry, academia, followed by international settings in the field of mechanical engineering, especially in dynamics and vibrations, has presented the source of the above controversy. Theoretical knowledge alone does not guarantee success in industrial research and development. High level of expertise in production technology, well organized cooperation of engineers and research groups are also essential conditions, prerequisites.

This picture was sharpened by international politics back in 1981. Ronald Reagan became the president of the USA. His government decided to extend the so-called CoCom list that maintained an embargo on high-tech products and equipment that could support military of the Soviet Union and its Eastern Bloc either directly or indirectly. This extension included bans on importing glass and carbon fiber, function analyzers, and even 5-axis CNC machining centers. For my surprise, many of these were related to dynamics and vibrations.

Since I worked on related projects in the industry and at the university equipped with all the necessary theoretical background, the whole extended embargo issue looked awkward and irrelevant, and this view was strongly supported by the media at that time. First, this situation led to many new, high-tech oriented R&D projects, since our companies could not buy these products and/or licenses from the west anymore.

The lecture will discuss such examples from a historical perspective, highlighting moral lessons for future generations working in NVH. The failure of the R&D efforts of the 1980's was followed by the large-scale collapse of relevant Hungarian industrial companies that were internationally recognized ones in the mid-20th century. The newly established western factories planted ready-made technologies and products, while Hungarian engineers were employed to maintain the production, being far away from the design and the R&D centers of these international companies.

The first positive trends showed up at the millennium when the knowledge of our engineers was needed in vibration-related problems, like vibration monitoring at the production lines, at modal testing of the products, then at improved design of the products in a market where the competition from energy efficiency has slowly shifted to the fields of NVH. Learning the up-to-date technology and the high-tech products, accompanied by the theoretical foundation in differential equations, complex analysis, Fourier and Laplace transformations, informatics and digital measurement techniques, led to professional meetings like the actual international conference.

Prof. Gábor Stépán

Budapest University of Technology and Economics, Faculty of Mechanical Engineering, Department of Applied Mechanics

Dr. Stépán is currently professor emeritus at Budapest University of Technology and Economics, former dean of the Faculty of Mechanical Engineering and head of the Department of Applied Mechanics. He is member of the Hungarian Academy of Sciences, the Academy of Europe, and the Chinese Academy of Sciences. He is an ERC Advanced Grant holder, which was followed by an ERC Proof-of-Concept Grant. His research interests include nonlinear vibrations in delayed dynamical systems with applications in mechanical engineering and biomechanics such as wheel dynamics (rolling, braking, shimmy), robotic force control, machine tool vibrations, human balancing, and traffic dynamics.

Alma Mater/Degrees:

MSc in Mechanical Engineering, Budapest University of Technology and Economics

PhD and Doctor of Science, Hungarian Academy of Sciences

Dr. Xavier Beudaert:

Active vibration systems for vibration suppression in manufacturing applications

Chatter vibrations remain one of the most critical challenges in machining, often resulting in poor surface quality, reduced dimensional accuracy, accelerated tool wear, and lower productivity. These self-excited vibrations arise from the complex interaction between the cutting process and the dynamic response of the machine tool, imposing strict limits on achievable material removal rates. Hence, suppressing chatter becomes essential to ensure product quality and process efficiency.

This talk introduces the development and industrial implementation of active vibration suppression systems designed to address these challenges. By integrating feedback control, and dedicated actuators, these systems can adaptively counteract vibrations under varying operational conditions. This presentation covers novel active damping module designs, real-time vibration monitoring using embedded accelerometers, and advanced algorithms for automatic tuning. Case studies demonstrate significant improvements, including suppression of chatter vibrations and reduction of forced vibration amplitude, enhanced surface quality, and increased machining stability. Finally, the presentation explores practical integration strategies, scalability, and the future role of active vibration suppression in next-generation manufacturing systems.

Dr. Xavier Beudaert

Head of the Dynamics and Control department,
IDEKO research center, Member of BRTA
Elgoibar, Spain

Dr. Xavier Beudaert, is Head of the Dynamics and Control Department in the research center IDEKO, Spain, and an Associate Member of the CIRP Academy. He has authored over 30 peer-reviewed publications on machine tool dynamics, feed drive control, chatter suppression, and CNC trajectory optimization. Xavier's research focuses on active damping, feed drive control, and control-based strategies to boost productivity in large machine tools. He received the prestigious CIRP Taylor Medal in 2020 for his contributions to active vibration control. As a lead researcher in multiple European innovation projects, he combines modelling, experimentation, and real-world industrial experience.

Alma Mater/Degrees:

MSc in Machine Tools and Robotics

PhD in Mechanical engineering, Ecole Normale Supérieure de Cachan, France

https://www.linkedin.com/in/xavier-beudaert-b41328278/

Dr. Håvard Vold:

NVH, a walk down memory lane by an old, applied mathematician

My career began in **Oslo**, where I studied applied mathematics at the University of Oslo while serving as a conscript officer in the Norwegian Army. Balancing military duties with academics slowed my progress, but the experience taught me how to follow and give orders – skills that proved valuable throughout my later work in academia and industry. During this time, I became deeply involved in numerical and scientific computing and helped develop **Simula 67**, a pioneering object-oriented language that became an ancestor of C++.

I was then invited to **Stuttgart**, Germany, to work with Professor John Argyris at the Institut für Statik und Dynamik der Luft und Raumfahrts-konstruktionen (ISD). There I shifted from pure computer science toward the **finite element method (FEM)** and solid mechanics, implementing assembly and solvers for large linear systems and eigenproblems. This was my first real exposure to structural dynamics and to how structures respond to environmental loads.

After three years, I returned to **Oslo** to join a team bringing FEM technology to Norway's emerging North Sea offshore oil industry. Much of my work focused on stress analysis in concrete and steel structures under wave spectra and environmental forces. Less than two years later, I accepted an invitation to write a new dynamics-oriented finite element program in the United States.

In **Cincinnati, Ohio**, I joined **Structural Dynamics Research Corporation (SDRC)** to create a cutting-edge finite element program compatible with MSC Nastran and integrated into the I-DEAS CAD suite. While there, I discovered experimental modal analysis and acoustics, and seeing animated mode shapes derived from test data completely hooked me. Drawing on my background in matrix methods, I worked with colleagues to develop the **Polyreference Complex Exponential algorithm**, a new modal parameter estimation method that used multiple inputs and outputs to identify closely spaced or repeated resonances efficiently. Around the same time, our University of Cincinnati collaborators pioneered simultaneous incoherent excitation, which fit perfectly with our method. NASA took notice and invited us to perform the 1982 **ground vibration test of the Space Shuttle Orbiter Enterprise**. I also served as an adjunct professor at the University of

Cincinnati until 1992, working with students from Cincinnati and from other U.S. and European universities.

Seeking a more physics-oriented environment, I founded **Vold Solutions, Inc.** in 1992 in Cincinnati. We specialized in driveline and rotating/reciprocating equipment analysis, developing the **Vold-Kalman Filter** for accurate order tracking of machinery with rapidly changing speeds. However, after the 9/11 attacks and the outsourcing boom, combined with software piracy of our Rotate program, the small company's market declined sharply.

I then joined **ATA Engineering** in San Diego, where I focused on aerospace and acoustics projects, including jet and rocket noise research, beamforming, and acoustic holography. We pioneered robotic data acquisition along continuous lines for high-resolution acoustic measurements, and once again the Vold-Kalman Filter proved invaluable for extracting tonal content from jet engine recordings.

In **2016**, my family and I returned to Norway, where I took over our ancestral farm on the northwest coast. Since I am not really interested in farming, I established **Vold LLC**, continuing to consult and develop methods in areas ranging from acoustic jet-engine liners to rolling mills—remaining active in advanced engineering to this day.

Håvard Vold

Vold LLC, Romsdalen, Norway

Dr. Vold runs this solo practitioner consultancy since 2017 from his ancestral farm in the fjord landscape in Northwestern Norway. Advises on numerical and statistical methods in acoustics and experimental mechanics.

Alma Mater/Degrees:

MSc in Applied Mathematics

PhD in Mathematics, University of Oslo

Infantry officer in the Norvegian Arma Reserves

MotionScope

Visualizing the invisible

Camera-based measurement systems for precise and intuitive full-field results in under a minute!

Get the trial software! Includes examples.

(expires 10th Nov 2025)

www.motion-scope.com/nvhh25

Software and/or hardware

A low-cost R&E license / set is available for non-commercial use in academia.

For small and large structures

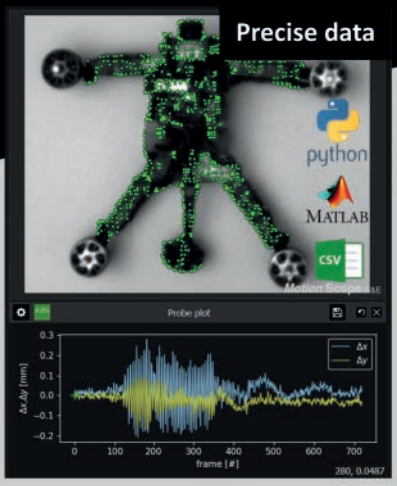

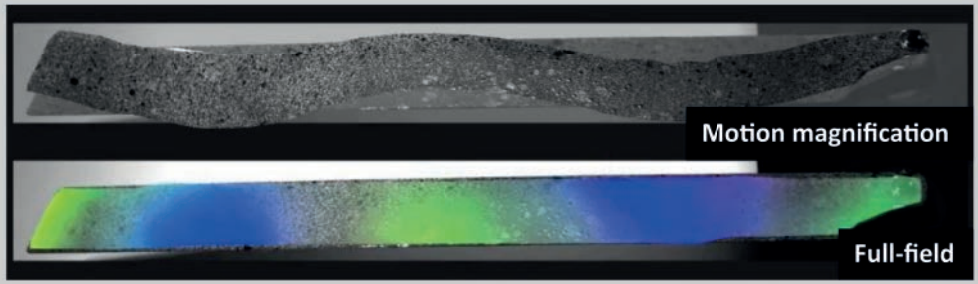

Motion magnification

Full-field

Web: www.motion-scope.com

email: info@motion-scope.com

Industrial case studies

Due to the sensitivity of certain data and information, only a summary of the presentation is published in some cases.

NVHH2025-0005

Effect of two outlet pipes on the stability of pressure relief valve discharge process

F. Kadar [1,2*], R. Sipahi [1]

[1]Northeastern University, Mechanical and Industrial Engineering, Boston, USA
[2]Budapest University of Technology and Economics,
Departement of Applied Mechanics, Hungary
[*]Corresponding author, e-mail: fanni.kadar@mm.bme.hu

Summary

Two outlet pipes of different lengths are utilized with the specific aim of avoiding pressure relief valve vibrations. The arising mathematical model of this system is next analyzed for stability, considering a set-up of a vessel, the valve, and two pipes. The analysis reveals that certain ratios of pipe lengths substantially extend the stable domains of the discharge process, compared to a single-pipe case.

Pressure relief valve vibration and pipe dynamics

Pressure relief valves (PRVs) are the last line of failure prevention in high-pressure systems. In these valves, the closing body is equipped with a precompressed spring that keeps the valve closed until the system pressure reaches the so-called set pressure. When the fluid force exceeds the spring force, the valve opens allowing discharge. Although PRVs are safety critical devices, suddenly appearing vibrations in their operations incapacitate their reliable operation. Besides causing noise and fatigue, vibrations inhibit the discharge process, and moreover high-pressure peaks can rise in the protected system. Although the mitigation of these vibrations is crucial, industrial standards forbid the application of external damping elements on the valve since the viscous dampers can get stuck easily due to the rare interventions of the valve. Thus, alternative design aspects have to be defined to avoid dangerous oscillations.
Previous studies [1] revealed a great potential in the design of the hydraulic environment of the valve for avoiding valve vibrations. Fig. 1 shows how the research about the system of a constantly charged vessel and a PRV evolved, which highlights the powerful effect of the wave reflections in the pipe that

can meet the valve vibrations such that they force the valve disc to return to the equilibrium state. The amount of time it takes for these waves to travel in the pipe, i.e., the time delay is the critical factor: in the single-pipe case, the presence of delay helped extend the parametric space for which the vessel-valve equilibrium is stable [1]. However, stabilizing downstream pipe length, hence the amount of delay, has an ultimate upper-bound in realistic circumstances.
The stabilizing effect arises through the backpressure of the valve that is dynamically influenced by the backward wave. That being so, two pipes of different lengths can further modify the backpressure, potentially, in a beneficial way. The aim of this study is to show how the two-pipe cases can improve the size of the stable region of the parametric settings, in particular, for various time-delay ratios induced by different pipe lengths. One opportunity in this direction is whether both pipe lengths can be made larger than the upper-bound of a stabilizing single-pipe, without sacrificing stability. Fig. 1 shows how these findings extend the existing studies and how the results contribute to deepening our understanding of PRV vibrations in specific environments.

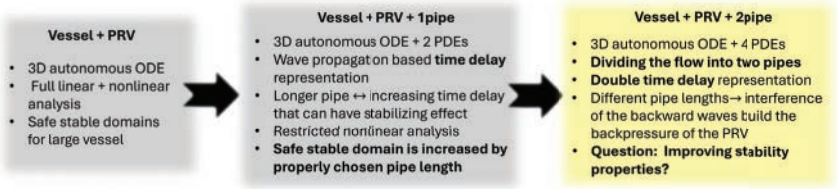

Figure 1: The present two-pipe model extends the existing models and results of analyzing vibrations in vessel-valve systems.

Mathematical model

The state variables are summarized in Fig. 2, where yellow shows the present two-pipe (two-delay) model. The pressure variables are denoted by p, while the velocity variables by v, for specific notations, see Fig. 2. On the basis of the single-pipe model, the valve dynamics is described as a 1 degree-of-freedom

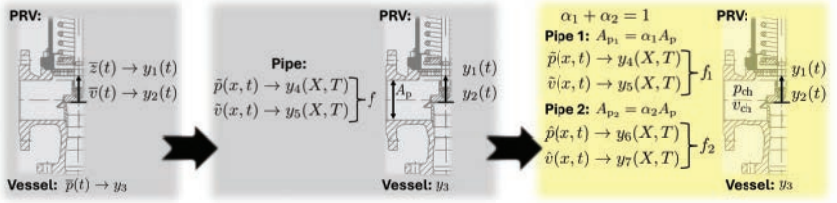

Figure 2: Mathematical model of the two-pipe case in the yellow box as an extension of the single-delay case.

oscillator and it is combined with the mass balance equation of the vessel as

$$\frac{\mathrm{d}\overline{z}(t)}{\mathrm{d}t} = \overline{v}(t)\,, \tag{1}$$

$$\frac{\mathrm{d}\overline{v}(t)}{\mathrm{d}t} = -2\zeta\omega_\mathsf{n}\overline{v}(t) - \omega_\mathsf{n}^2(\overline{z}(t)+\overline{z}_0) + \frac{A}{k}\omega_\mathsf{n}^2\Delta\overline{p}(t)\,, \tag{2}$$

$$\frac{\mathrm{d}\overline{p}(t)}{\mathrm{d}t} = \frac{K}{V}\left(Q_\mathsf{in} - \overline{Q}_\mathsf{out}(\overline{z}(t), \Delta\overline{p}(t))\right), \tag{3}$$

with the constant inlet flow rate Q_in of the liquid with density ρ and bulk modulus K into the rigid vessel of volume V. The spring is precompressed with $\overline{z}_0$, and closes the outflow cross section area A, while after opening $\overline{Q}_\mathsf{out}$ is the flow through the valve. The valve has the angular natural frequency ω_n with spring stiffness k. The damping ratio ζ on the valve comes from internal damping effects. For this new two-pipe model, the chamber pressure p_ch is introduced as an internal variable, see the corresponding chamber in Fig. 2. This is the backpressure of the valve appearing in the pressure drop $\Delta\overline{p} = \overline{p} - p_\mathsf{ch}$. The main challenge here is the proper definition of the boundary conditions, such that the backward wave interference can be captured. The wave propagation is described by the dimensionless continuity and Navier-Stokes equations with neglected convective and friction terms:

$$\frac{\partial\tilde{p}(x,t)}{\partial t} = -\rho a^2\frac{\partial\tilde{v}(x,t)}{\partial x}\,, \qquad \frac{\partial\tilde{v}(x,t)}{\partial t} = -\frac{1}{\rho}\frac{\partial\tilde{p}(x,t)}{\partial x}\,, \tag{4}$$

$$\frac{\partial\hat{p}(x,t)}{\partial t} = -\rho a^2\frac{\partial\hat{v}(x,t)}{\partial x}\,, \qquad \frac{\partial\hat{v}(x,t)}{\partial t} = -\frac{1}{\rho}\frac{\partial\hat{p}(x,t)}{\partial x}\,, \tag{5}$$

where a is the speed of sound in the pipe. Both pipes deliver to the atmospheric pressure, thus the pressures at lengths $l_{1,2}$ are $\tilde{p}(l_1,t) = \hat{p}(l_2,t) = 0$. The valve outlet flow is divided between the two pipes as $A_\mathsf{p}(\alpha_1\tilde{v}(0,t) + \alpha_2\hat{v}(0,t)) =$

$\overline{Q}_{\text{out}}(\overline{z}, \Delta\overline{p})$ based on the Bernoulli's Law

$$p_{\text{ch}} + \frac{\rho}{2} v_{\text{ch}}^2 = \tilde{p}(0,t) + \frac{\rho}{2}\tilde{v}^2(0,t) = \hat{p}(0,t) + \frac{\rho}{2}\hat{v}^2(0,t)\,. \tag{6}$$

The dimensionless system can be derived based on [1] with the variables in Fig. 2. The travelling wave solution of the PDEs with the state variables f_1 and f_2 can be substituted into the dimensionless boundary conditions, and the system of Delay Differential Algebraic Equations (DDAEs) can be formulated with the time delays τ_1 and τ_2 as follows

$$\dot{y}_1 = y_2\,, \tag{7}$$

$$\dot{y}_2 = -2\zeta y_2 - (y_1 + \delta) + \Delta y_3\,, \tag{8}$$

$$\dot{y}_3 = \beta(q - \frac{1}{\phi}\left(\alpha_1(f_1 + f_{1\tau_1}) + \alpha_2(f_2 + f_{2\tau_2})\right)\Big)\,, \tag{9}$$

$$\alpha_1(f_1 + f_{1\tau_1}) + \alpha_2(f_2 + f_{2\tau_2}) = \phi y_1\sqrt{\Delta y_3}\,, \tag{10}$$

$$f_1 - f_2 = f_{1\tau_1} - f_{2\tau_2} + \nu((f_2 + f_{2\tau_2})^2 - (f_1 + f_{1\tau_1})^2)\,, \tag{11}$$

where $\nu = p_0/(2\rho a^2)$ is a new parameter. The inlet flow rate q, the set pressure δ, the hydraulic system stiffness β, and the pipe inlet parameter ϕ are used consistently with the single-pipe case [1]. The subscripts $\tau_{1,2}$ refer to the delayed variables as $f_1(T-\tau_1)$ or $f_2(T-\tau_2)$ with the dimensionless time T.

Stability analysis

For the stability analysis of the equilibrium state, the system has to be linearized around the equilibrium, that can be calculated from the following equations in a flow rate dependent form:

$$\Delta y_3^* = y_3^*,\; y_1^* + \delta = y_3^*,\; q = y_1^*\sqrt{y_3^*},\; f_{1,2}^* = f^* = \frac{\phi}{2}q\,. \tag{12}$$

In the following analysis, the set pressure is 3 bar gauge pressure corresponding to $\delta = 3$ and the pipe inlet parameter can be calculated for a realistic dataset based on [1] as $\phi = 48.2$. After the linearization and introduction of $\mathcal{F}(\tau) = 1 - \mathrm{e}^{-\lambda\tau} + F(1 + \mathrm{e}^{-\lambda\tau})$, the characteristic equation is derived as

$$\mathcal{F}(\tau_2)\sum_{i=0}^{3}\left(a_i\lambda^i + \mathrm{e}^{-\lambda\tau_1}b_i\lambda^i\right) + \mathcal{F}(\tau_1)(1 + \mathrm{e}^{-\lambda\tau_2})\sum_{i=0}^{3}c_i\lambda^i = 0\,, \tag{13}$$

where λ is the characteristic root, $F = 4\nu f^*$, and the coefficients depend on $\phi, \beta, \zeta, \alpha_{1,2}, F, y^*_{1,3}$, while they are coupled to each other. The characteristic equation is neutral, and the two time delays present a cross-talk effect with the term $e^{-\lambda(\tau_1+\tau_2)}$. Stability analysis is performed next. We first compute the delay pairs in the (τ_1, τ_2) plane for which the system has characteristic roots at $\lambda = \pm i\omega$. For this, we revisit CTCR [2] and implement the Rekasius substitution

$$e^{-\lambda\tau_j} = \frac{1 - T_j\lambda}{1 + T_j\lambda}, \quad j = 1, 2, \tag{14}$$

on (13). This substitution creates two algebraic equations in terms of the real quantities T_1 and T_2, obtained as the real and imaginary part of (13). One then performs ω-sweep in both equations, see [3], to solve for $T_{1,2}$, and ultimately compute the delay values

$$\tau_j = \frac{2}{\omega}(\arctan(\omega T_j) + k_j\pi), \quad j = 1, 2, \quad k_j = 0, \pm1, \pm2, \ldots \tag{15}$$

The collection of these delay values will then form boundaries (see the blue, red and dark green markers in Fig. 3b), which decompose the (τ_1, τ_2) plane into regions, where in each region the number of unstable characteristic roots is fixed. Wherever this number is zero, those regions are labeled as 'stable'.

Next, we utilize QPmR [4], which provides a MATLAB package to calculate the rightmost roots of a quasi-polynomial and the spectral abscissa of the essential spectrum, for a given set of delays. QPmR showed that the essential spectrum associated with the valve dynamics is stable, and provided the real part of the rightmost characteristic root for pairs of delays selected on a dense mesh in the (τ_1, τ_2) plane, see the color coding in Fig. 3b.

Clearly, the boundaries obtained based on Rekasius substitution very well match the stable/unstable regions found using QPmR. Moreover, the intensity of the grey color associated with the real part of the rightmost stable roots is inversely proportional to system's settling time. Next, in Fig. 3b, we present large red and blue dots corresponding to the single delay stability boundaries, see [1]. Since the $\tau_1 = \tau_2$ case recreates the single-pipe case, the stability boundaries appear on the line with slope 45°, so they match with the horizontal cut of the stability chart for the single delay case shown in panel a). This means that the shaded red region corresponds to pipe lengths that are above the upper-bound of the stabilizing single-pipe length, and the black stars show two examples of (τ_1, τ_2) combinations that lead to longer stable outlet piping than the single delay case.

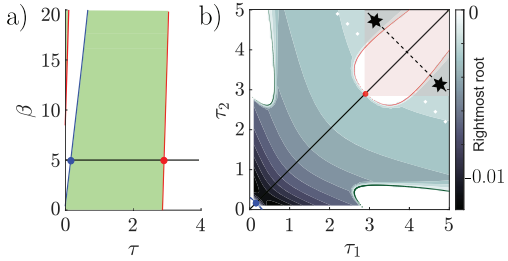

Figure 3: Stability charts for $q = 6$, $\beta = 5$ and $\zeta = 0.39$ for a) the single-pipe case, b) the two-pipe case of $\alpha_1 = \alpha_2 = 0.5$. Panel b) depicts the real parts of the rightmost root in the stable domains in grey, white domains are unstable. The shaded red region corresponds to longer piping than the allowable single-pipe upper-bound. Stars show example time-delay combinations for stabilizing with longer outlet piping than in the single delay case.

Acknowledgements

Dr. Kadar was supported by the Rosztoczy Foundation, and the BME EKÖP scholarship funded by the National Research Development and Innovation, Fund of the Ministry of Culture and Innovation. Dr. Kadar conducted this research in the Department of Mechanical and Industrial Engineering at Northeastern University, Boston.

References

[1] F. Kadar, C. Hos, and G. Stepan, "Delayed oscillator model of pressure relief valves with outlet piping," *Journal of Sound and Vibration*, vol. 534, p. 117 016, 2022, ISSN: 0022-460X.

[2] R. Sipahi and N. Olgac, "Complete stability robustness of third-order LTI multiple time-delay systems," *Automatica*, vol. 41, no. 8, pp. 1413–1422, 2005, ISSN: 0005-1098.

[3] R. Sipahi and I. I. Delice, "Advanced clustering with frequency sweeping methodology for the stability analysis of multiple time-delay systems," *IEEE Transactions on Automatic Control*, vol. 56, no. 2, pp. 467–472, 2010.

[4] T. Vyhlídal, J.-F. Lafay, and R. Sipahi, *Delay systems: From theory to numerics and applications*. Springer Science & Business Media, 2013, vol. 1.

NVHH2025-0010

NVH Analysis with a vibration monitoring system of a honing machine

R. Tóth[1*], A. Urbán[1]

[1]Audi Hungaria Zrt., Development - Acoustics, Győr, Hungary

[*]Corresponding author, e-mail: robert2.toth@audi.hu

Summary

This paper shows an opportunity to analyse a gear acoustic issue at the earliest phase of production. Using the gear manufacturing machine's preventive maintenance system, not only can the machine itself be protected as originally intended, but the gear's acoustic quality can be forecast. An ongoing topic was used to investigate the excited vibrations of the processing machine and the downstream effect caused on a component- (gear) and subassembly- (electric drive) level.

Introduction

As part of the competition in the automotive industry, Audi Hungaria Zrt. aims to solve problems as quickly as possible, with minimal waste. From an acoustic perspective, this means that the earlier a harmful excitation can be detected, the better. In this case, the detection occurs during the gear processing phase.

Motivation and goals

With the knowledge of so-called "ghost orders" it was already revealed, that the excitation originates from the imperfections on the gear face surface. These imperfections mean tiny waves on the face, leading to an inappropriate gear contact. The question was whether the formation could be observed throughout the manufacturing process, and if so, how?

Methods

The production line provided everything necessary for the analysis. There was a gear processing machine equipped with a built-in vibration monitor system and a component acoustic test bench for measuring the product after the processing.

The only requirement was to validate whether the preventive maintenance system was suitable for acoustic purposes and to conduct experiments to reproduce the acoustic phenomenon.

Results and discussion

The vibration monitoring system proved to be completely suitable for analysing the excited vibrations during gear processing. Additionally, it provided further information that was useful in subsequent cases.

After gear manufacturing, the measured results were compared to the component acoustic test bench evaluations and in the observed excitation (ghost order) they showed a convincing correlation.

At the end of the experiment, a Modal Analysis was conducted to examine the resonance properties of the manufacturing machine and identify the potential root cause.

Conclusions

The developing of modern machines used by the industry opens up new ways to solve old problems.

The examined evaluation method was integrated into the fault elimination process and used since the analyses.

References

[1] PRÄWEMA Antriebstechnik GmbH, “Process Monitoring with HRI® & HRIexpert®”

NVHH2025-0012

Simulation-based Automotive Sound System Enhancement

N. Nagy[1*], D. Sipos[1]

[1]Audi Hungaria Zrt, G/GF-3 Acoustic Simulation, Győr, Hungary

[*]Corresponding author, e-mail: nora.nagy@audi.hu

Summary

To enhance the prediction of a vehicle's audio system performance, we developed a model using FEM and Raytracing techniques. This model allowed us to simulate the loudspeaker frequency responses at various listening positions throughout the entire audible spectrum. Different methods for modelling the boundaries of the car cavity to ensure accuracy was employed. The simulated frequency responses were also measured in the actual vehicle and compared with the simulation results to refine and improve the model. The FRF serves as a vital instrument in comprehending how sound is perceived under various broadband excitations, and it plays a pivotal role in the early phases of automotive sound system development. FRFs help in determining the ideal parameters and locations for the speakers, ensuring a balanced and immersive auditory experience. Furthermore, by accurately simulating the FRF, sound system filter presets can be created to accelerate the actual tuning of the vehicle.

NVHH2025-0013

Advanced noise reduction strategies in the EDU development

P. Horvat[1*], S. Varga[1], M. Mehrgou[2]

[1]AVL Hungary Kft., Structural and MBS simulation, Érd, Hungary

[2]AVL List GmbH, Multibody Dynamics, NVH & Electromagn., Graz, Austria

[*]Corresponding author, e-mail: Peter.Horvat@avl.com

Summary

As the demand for electric drive units (EDUs) grows, achieving superior noise, vibration, and harshness (NVH) performance has become a critical development goal. This paper presents advanced noise reduction strategies tailored for EDU applications, focusing on a holistic approach that integrates source mitigation, path optimization, and advanced acoustic treatments. Key topics include gear whine and electromagnetic whine, as well as structural optimizations and damping solutions. Here mainly, we explore the role of numerical simulations in refining NVH performance. By leveraging these strategies, we demonstrate a systematic methodology to enhance acoustic comfort and meet stringent industry requirements for next-generation electric powertrains.

Introduction

Thanks to the intensive development of computer aided engineering, NVH performance of power units is possible to be measured very precisely. With these simulations several issues can be highlighted in the development phase, those would lead to high noise radiation [1]. However, then comes the most challenging part of the task: NVH issues need to be solved with minimum cost in other measures like efficiency, weight or price. To achieve this, computer-aided optimization technologies are inevitable. Neural networks, DoE, gradient based methods and several other technologies are used in the daily work, but with the spread of AI tools this trend is becoming even more important, to make the customers satisfied.

Source Optimization

Excitation forces can be caused by errors in the system, but also as side effect of the normal operation. In this paper, optimization processes are collected those

are targeting the second one. The main sources of these harmonic excitations are the E-machines, gears, inverters and in case of very high-speed EDU-s, bearings as well. With the optimization of the varying forces indicated by these components, the NVH performance of a drive unit can be efficiently reduced.

Reducing Electromagnetic excitations

The excitation forces in an E-machine are results of the periodic change of the electromagnetic field during the rotation of the rotor. The shape of the electromagnetic excitation is a very complex shape, but it can be break down to sum of several sinus wave excitations with different orders and orientations based on Fourier transform, this is so called space-orders. The contribution of these components can be calculated with the electromagnetic tool, and the system can be loaded by them, with unit amplitudes and be investigated the sensitive of the structure by the responses. Main occasions of high excitations are considering to orders from pole number and teeth number [2]. Usual NVH issue, when radial force components exciting the eigenmodes of the stator (2-pole, 4-pole, 6-pole, breathing mode, etc…). In this case high response can be detected in the higher frequency range. Numerous industrial cases and studies have shown high response for tangential forces in the lower frequency range, where is also audible and important for target setting [3]. High efficiency panel modes of components with flat surfaces like inverter and transmission cover are typical issues in this lower frequency range [4].

With a well optimized rotor and stator geometry, the force components, those are mostly responsible for the excitation, can be significantly reduced. The goal of the optimization is to find the best from thousands of variants, that has better NVH performance, without significant efficiency degradation or cost increase. Significant reduction in the simulation times and remarkable increase in the result quality can be achieved with introducing Design of Experience (DoE) optimization combined with neural network [5]. The optimization tool AVL Cameo, which is builds a mathematical model based on a generated design matrix, has been used to predict results from a several simulated case to billions of additional possible combinations. As result of the optimization, the most relevant geometries can be picked from the pareto front and validated.

Reducing gear excitations

The teeth of loaded gears have a deflection that indicates a difference in the gears theoretical and real angular position. This effect is called to transmission error. The source of the excitation is the periodic change of the meshing stiffness

due to varying number of teeth in contact [6]. As main target of the optimizations the amplitude of the transmission error needs to be reduced and a smoother transition between the extremums should be provided. The development process is started already at the concept phase. Beside efficiency and safety requirements, NVH performance it is very important to be considered during the definition of the full layout dimensions, the bearing types and positioning and the main gear parameters. In the later design phases, further improvements can be achieved with the flank microgeometry modifications, but it is significantly more efficient if the system is already designed with attention for NVH from the beginning.

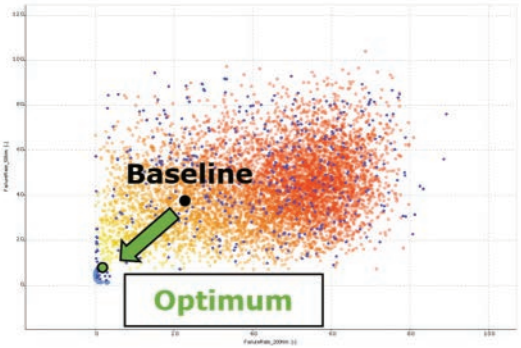

Figure 1: Pareto front in DoE optimization

Transfer path optimization

The next step where it is possible to intervene to avoid noise radiation is the transfer path, the rout of the vibration from the source to the radiation. There are several good practices in the EDU development for this purpose, those are working in each case, like the decoupling of the stator in the housing, to minimize the transition of the electromagnetic excitation forces to the outer surfaces. Structural modifications also can be classified into this section, those are focusing on the stiffening of the components to reduce the amplitudes of the vibrations and shift them into higher frequencies.

However, the situation in case of EDUs get significantly more complicated than for ICEs, where it was possible to shift out the critical eigenmodes from the excitation range. Since the rotational speed of the E-machines can easily reach 20000 rpm, and the excitation orders existing over 60, the full frequency spectra of the human hearing is excited. To handle this phenomenon, a completely new workflow has been developed, that targeting directly the reduction of the noise

radiation during the optimization of the structure. A proper measure for this, is the equivalent radiated power (ERP), that represents the NVH performance with the surface integral of the velocities on the outer surface in normal direction. See Eq. (1). Since ERP is a sound power level value, it directly describes the EDU as sound source and not dependent on the measurement environment. It helps comparison between variants and to other products. However, sound pressure level or air borne noise can be calculated or simulated from ERP if required [7].

$$P_{ERP} = \frac{1}{2} \varrho_f c_f \sum_{\mu=1}^{N_e} S_\mu v_{n_\mu} v_{n_\mu}^* \tag{1}$$

With computer aided structural optimization, significant reductions were achieved for components, those were already designed by well experienced engineers. Besides NVH performance, always very important factor is the added mass. The need for advanced optimization is not just because of the noise reduction but also for doing it from the minimum added, or even from less weight. During the iterations, the gradient of the objective function is calculated by the solver and varied the density of the design elements in a way to minimize or maximize it, until the optimization is converged.

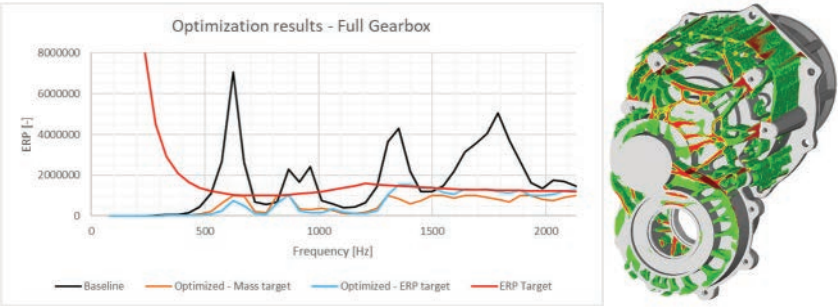

Figure 2: Topology optimization for ERP target

Reduction of noise radiation

As last step of the NVH development, the radiating surfaces of the EDU can be covered with special noise absorbing, or high damping material. These expensive solutions are not always ordered by the customers, mostly only in the premium segment. The so-called encapsulation, when the full EDU or the critical components are covered by a special foam to absorb the noise that would spread out of the surfaces, has less potential to achieve additional improvement by using optimization. Not like damping pads, those are built up from several

layers with different material properties and behavior. Final performance can also be improved by parameter optimization based on neural networks.

Conclusion

Significant noise reductions could be achieved at the developed EDUs, where all the optimization processes from source to radiation could be implemented. The described computer aided methods are actively used and developed in different industrial cases, for both E-machine and gear trains. As goal in the future, a fully automatized working process needs to be developed, that combines the experience and knowledge in simulation and optimization with the most recent technologies.

Acknowledgement

I would like to thank all the representatives from AVL List GmbH in Austria and AVL Hungary GmbH in Hungary making possible to prepare this paper.

References

[1] M. Mehrgou, I. Garcia de Madinabeitia Merino, J. Pohn, J. Garmendia Gutierrez, C. Priestner, F. Zieher “Robustness and Variability Prediction of Electric Machine Noise Using CAE” W. Siebenpfeiffer (Hrsg.): Automotive Acoustics Conference 2019, Proceedings, S. 200–210, 2020

[2] K. Degrendele, J. L. Besnerais, R. Pile, P. Gning and E. Devillers, "Characterization of EV/HEV NVH issues using electrical machine tooth FRF," *PROCEEDINGS OF ISMA2020 AND USD2020,* 2020. Leuven, Belgium.

[3] Ulz, A., Graf, B., Priestner, C., and Mehrgou, M., “Criteria for the NVH Development of Electric Drive Units,” ATZ Worldw. 123(7–8):26–31, 2021, doi:10.1007/s38311-021-0684-8.

[4] Mehrgou, M., Garcia de Madinabeitia, I., Graf, B., Zieher, F. et al., "NVH Aspects of Electric Drives – Integration of Electric Machine, Gearbox and Inverter," SAE Technical Paper 2018-01-1556, 2018

[5] Mehrgou, M., Garcia de Madinabeitia, I., and Ahmed, M., "Synergizing Efficiency and Silence: A Novel Approach to E-Machine Development," SAE Technical Paper 2024-01-2914, 2024, https://doi.org/10.4271/2024-01-2914.

[6] R. W. Gregory, S. L. Harris and R. G. Munro, Torsional motions of a pair of spur gears, 1963

[7] M. Klaerner, M. Wuehrl, L. Kroll and S. Marburg, "FEA-based methods for optimising structure-borne sound radiation," *Mechanical Systems and Signal Processing,* vol. 89, pp. 37-47, 2017

NVHH2025-0014

High Frequency Mount Stiffness Identification for Electric Powertrains using Test driven FE Approach

D. Minervini[1*], M. Stoica[1], B. Forrier[1], F. Bianciardi[1]

[1]Siemens Digital Industries Software, Interleuvenlaan 68, 3000 Leuven, Belgium

[*]Corresponding author, e-mail: domenico.minervini@siemens.com

Summary

Rapid electrification of the automotive industry presents new challenges in noise, vibration, and harshness (NVH). Stiffer bushings and higher frequency ranges push conventional mount testing to their limits, with test rig resonances often compromising accuracy and requiring timeconsuming setups. This work introduces a hybrid framework leveraging high-frequency testing and simulation to develop a parametric finite element mount model. This technique eliminates the need for support structures, extends the usable frequency range, and enables efficient design modifications. By frontloading the NVH optimization process, the proposed method allows virtual prototyping, reducing effort compared to conventional testing while maintaining accuracy.

NVHH2025-0017

Load dependencies in experimental modal analysis of a hydrogen fuel cell stack

S. Gallas[1,2*], H. Denayer[1,2], G. Kosova[3],
G. Fasulo[4], M. Barbarino[4], O. Ekblad[5], F. Naets[1,2], B. Pluymers[1,2]

[1]KU Leuven, Department of Mechanical Engineering, Heverlee, Belgium
[2]Flanders Make, Flanders Make@KU Leuven, Belgium
[3]Siemens Digital Industries Software, Leuven, Belgium
[4]Italian Aerospace Research Centre (CIRA), Capua, Italy
[5]PowerCell Group, Gothenburg, Sweden
[*]Corresponding author, e-mail: simone.gallas@kuleuven.be

Summary

When designing hydrogen fuel cell stacks for aircraft propulsion, it is essential to analyse their response to in-flight dynamic loads, particularly in terms of structural resonances. Finite element (FE) models can efficiently predict this response across design iterations, but require validation against experimental modal analysis (EMA). EMA results are generally considered independent of the excitation type. However, this assumption does not hold for highly nonlinear systems like fuel cell stacks. Therefore, in this industrial case study, shaker-based EMA is repeated for various excitation directions and amplitudes to assess their impact on modal frequencies and shapes.

1. Introduction

Hydrogen fuel cell technology enables aircraft propulsion with zero CO_2 emissions. To support the adoption of this technology in aviation, the mechanical design of fuel cell stacks must not only maximize power density but also ensure structural resistance under in-flight dynamic loads [1]. The structural resistance can be analyzed with numerical models reducing the need for time-consuming and expensive of physical prototypes. In this context, the goal of this work is to evaluate the accuracy of a linear finite element model for predicting the vibration response of a fuel cell stack developed by PowerCell. The accuracy is evaluated in terms of percentage errors on the modal frequencies, using experimental results obtained from shaker testing as a reference. Since the fuel cell

stack is expected to show nonlinear behavior, this work particularly focuses on the load dependencies in experimental modal analysis of a hydrogen fuel cell stack. To capture these effects, the shaker test is repeated under various excitation amplitudes, directions and degrees-of-freedom and the model's accuracy is re-evaluated for each case.

2. Methods

2.1. Finite Element modeling

The linear finite element model, developed by the co-authors from CIRA, consists of a combination of 3D elements with homogenized orthotropic material properties for the cell package, and 2D and 1D elements for the end-plates and structural connections. The model also includes the fixture used to attach the stack to the shaker table, to verify that it can be considered rigid within the frequency range of 5-300 Hz. Regarding the boundary conditions, all the nodes lying at the interface between fixture and shaker table are constrained in all their degrees-of-freedom. The resulting model is used to simulate the eigenfrequencies and eigenshapes.

2.2. Experimental modal analysis

The top and bottom plates of the fuel cell stack are bolted into a cage-like fixture, which is mounted on top of the CUBE, a six degrees-of-freedom shaker, as shown on the left in Fig. 1. On the right side of the same figure, 54 triaxial accelerometers are distributed among the stack (green), the compression bands (purple), the fixture (red and blue) and the shaker (orange). At these locations, the frequency response functions are measured with respect to a selected accelerometer positioned on the shaker. For single axis tests, the reference acceleration is aligned with the excitation direction. For multiaxial tests, the three translation measured at the selected accelerometer on the shaker are used instead. The first test is executed with pseudo-random excitation in Z direction, with RMS of 0.04 V. The test is then repeated for various excitation levels and degrees-of-freedom, as listed in Tab. 1, to investigate the load dependencies of the modal frequencies. For each test, the frequencies and shapes of the first six modes are estimated using Polymax algorithm [2]. The data acquisition and modal estimation are realized using respectively Siemens Scadas and Simcenter Testlab.

3. Results and discussion

The mode shapes obtained from the first experimental test are described in Tab. 2. These modes are correlated with the numerical modes and with those

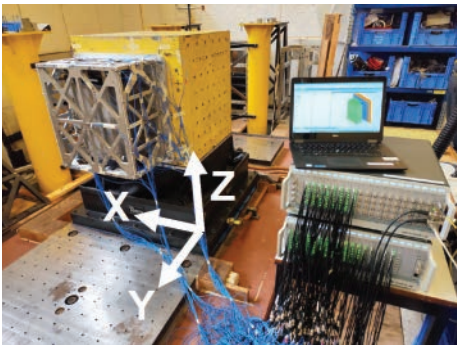

Figure 1: Shaker setup (left) and geometry discretized at accelerometer locations (right)

Table 1: Test runs and excitation type

Test number	Exc. signal	Exc. level	Exc. DOF
1 (ref.)	Pseudo-Random	0.04 VRMS	Transl. in Z
2	Pseudo-Random	0.02 VRMS	Transl. in Z
3	Pseudo-Random	0.08 VRMS	Transl. in Z
4	Pseudo-Random	0.04 VRMS	Transl. in X
5	Pseudo-Random	0.04 VRMS	Transl. in Y
6	Pseudo-Random	0.02 VRMS	Rot. around X
7	Pseudo-Random	0.04 VRMS	Rot. around X
8	Pseudo-Random	0.08 VRMS	Rot. around X
9	Pseudo-Random	0.04 VRMS	All transl.
10	Pseudo-Random	0.04 VRMS	All transl. and rot.

estimated from the other test runs using the modal assurance criterion (MAC) [3]. Two modes are considered paired only when the MAC value is higher than 70%. The accuracy of the modal frequencies prediction is shown in in Fig. 2 for each test run. The following observations can be made:

1. The numerical prediction significantly underestimates the frequency of the ”stack modes” 1, 2 and 6 (max error 30%), indicating a potential stiffness underestimation in the stack part of the model. The bands modes are predicted with a better accuracy instead (max error 2%).
2. The increase of excitation amplitude leads to a negligible decrease of modal frequencies (1% decrease).
3. When exciting the rotation around X or the translation in X, or when exciting multiple degrees-of-freedom contemporaneously, the estimation of

some modes is not possible.

4. The direction of the excitation has a non-negligible impact on the modal frequencies (max error 4%).

Table 2: Description of the experimental modes

Mode number	Shape description
1	Stack, first bending in Y direction
2	Stack, axial in Z direction
3	Compression band 1, first bending in Y direction
4	Compression band 2, first bending in Y direction
5	Compression band 3, first bending in Y direction
6	Stack, first bending in X direction

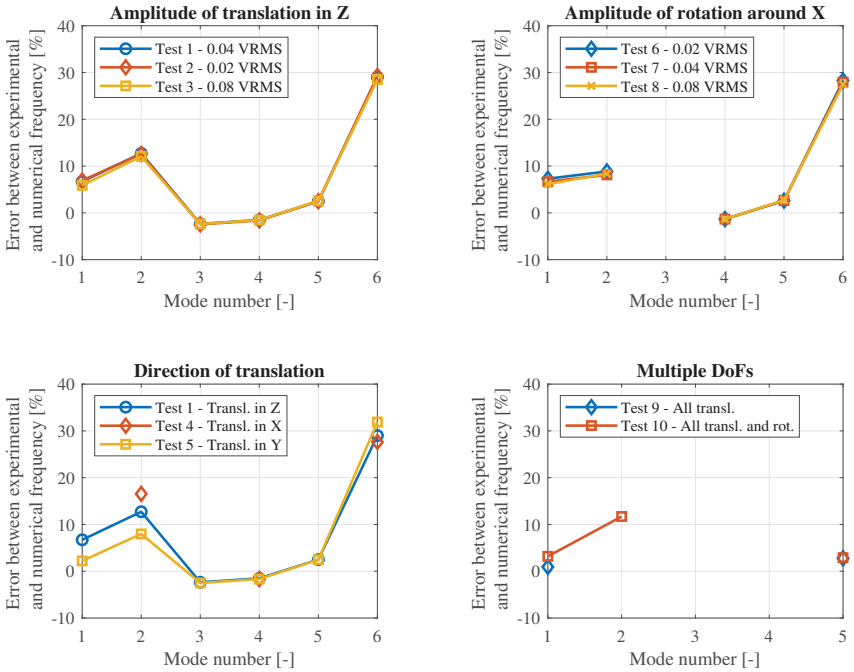

Figure 2: Percentage errors between test runs and numerical prediction

4. Conclusion

In this work, the modal analysis of a fuel cell stack is conducted both numerically with finite element modeling, and experimentally with shaker testing using various excitation types. On the one hand, the considered excitation amplitudes have a negligible influence on modal frequencies. On the other hand, the direction of the excitation shows a more noticeable impact. However, both effects are considerably smaller than the prediction error of the initial finite element model, highlighting the need for model update.

5. Acknowledgements

The European Commission is gratefully acknowledged for their support of the NEWBORN project (GA number 101101967). Views and opinions expressed are however those of the authors only and do not necessarily reflect those of the European Union. The European Union cannot be held responsible for them. Internal Funds KU Leuven are gratefully acknowledged for their support.

References

[1] Fuel Cells and Hydrogen 2 Joint Undertaking, *Hydrogen-powered aviation – A fact-based study of hydrogen technology, economics, and climate impact by 2050*. Publications Office, 2020. DOI: doi/10.2843/471510.

[2] P. G. B. Peeters H. Van Der Auweraer and J. Leuridan, "The polymax frequency-domain method: A new standard for modal parameter estimation?" *Shock and Vibration*, vol. 11, no. 3, pp. 395–409, 2004.

[3] S. L. W. Heylen and P. Sas, *Modal analysis theory and testing.* 1st. Heverlee: KUL. Faculty of engineering. Department of mechanical engineering. Division of production engineering, machine design and automation, 1997.

HEAD acoustics

meet US

optimize SOUND & VIBRATION

Your NVH partner for sound and vibration, psychoacoustics, sound quality, soundscape, end-of-line testing, and more.

We are looking forward to your visit!

REAL-LIFE-PROOF.

www.head-acoustics.com

NVHH2025-0024

Investigation of vibration-based noises generated by the sound system in the interior of modern vehicles

Zs. Hidegföldi[1,2*], B. Vehovszky[1], P. Á. Gajdátsy[2]

[1]Széchenyi István University, Department of Whole Vehicle Engineering, Győr, Hungary

[2]Jaguar Land Rover Hungary, Digital Product Platform, Budapest, Hungary

[*]Corresponding author, e-mail: zhidegf1@jaguarlandrover.com

Summary

In premium vehicles, a low noise level in the interior is an important expectation. Previously, the main challenge was to reduce the engine- and road noise, but with technological advancements, there are now largely refined solutions for these. Simultaneously, vehicle sound systems have become significantly more complex and powerful. Consequently, the vibrations due to their operation may introduce new noise sources in the cabin. The focus of this paper is to get a better understanding of the relationship between structure-borne and airborne noise of an automotive door induced by the built-in woofer. To achieve this goal, a set of acoustic measurements should be performed following by the corresponding evaluation. All this in terms of the fact that the results obtained can later form the basis of a subsequent simulation.

Introduction

The overall driving experience in a vehicle is significantly impacted by the acoustic and tactile feedback it produces. Automotive engineers utilize NVH to analyse sounds and vibrations, aiming to reduce undesirable occurrences and enhance beneficial ones through simulation and physical testing. NVH broadly encompasses noise (sound propagation from components like engine or door operations), vibration (oscillations felt through contact points like steering wheel or seats), and harshness (the subjective perception of unpleasant sounds and vibrations). While NVH initially focused on mitigating mechanical noises in combustion engine vehicles, it has evolved into a critical performance metric, particularly for premium automotive brands where superior NVH performance is a key differentiator and a fundamental aspect of brand image.

The increasing demand for enhanced audio experiences in automotive cabins has led to more powerful sound systems, which in turn pose a challenge by inducing unwanted structural vibrations and audible rattling noises. This paper specifically addresses the problem of rattling noise excited by the sound system. Amplified sound levels from the vehicle's audio system, especially from low-frequency drivers like door-mounted woofers, can generate sufficient airborne and structure-borne vibrations to excite loosely coupled components or panels, leading to intermittent contact loss and rattling. The study focuses on vehicle doors as a representative subsystem to understand and mitigate this issue, with the primary goal of formulating assumptions about the structural and acoustic excitation caused by the built-in woofer to serve as a foundation for vehicle audio development simulation. Understanding the complex interplay between airborne sound pressure within the door cavity and the resulting structure-borne vibrations of the door panels and associated components is essential for this problem.

Measurement setup

The experimental investigation utilized a 2003 Lexus IS200 front right door, fully assembled with its functional components, including the window mechanism, door opening apparatus, and electric harness. Elements like the right rearview mirror and tweeter were removed. The latter having no notable effect as it is outside the door cavity, while the former facilitated the free-free hanging of the door. A compatible plastic trim with an Alcantara cover closed the door cavity from the passenger side, secured by factory plastic fasteners and bolts.

The original speaker was replaced with an OEM woofer. This replacement speaker was secured with self-locking nuts for easier refitting. Additional foam padding was placed to eliminate gaps between the trim and the speaker. The door's structure, including the inner metal plate, was deemed suitable for acoustic measurements despite minor lower-part damages. Moreover, cables and wires were covered in plastic by the manufacturer to prevent rattling. Potential noise sources were identified around the cavity, including vibrations transmitted from the woofer to the holding plate via bolted connections, and resonance of plate elements due to increased sound pressure inside the door. The larger outside panel was also noted as a potential drum-like membrane due to internal sound pressure and its thinner construction.

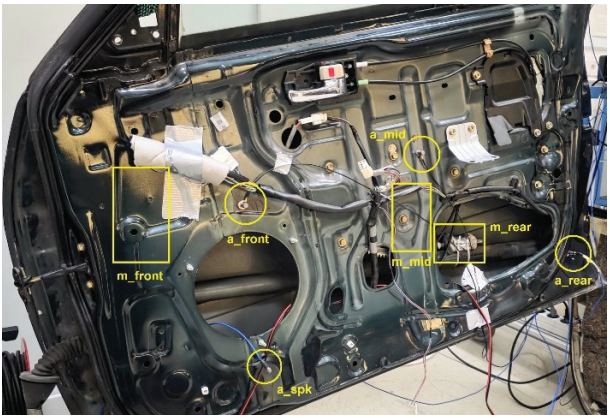

Figure 1: Location of sensors in passenger side panel

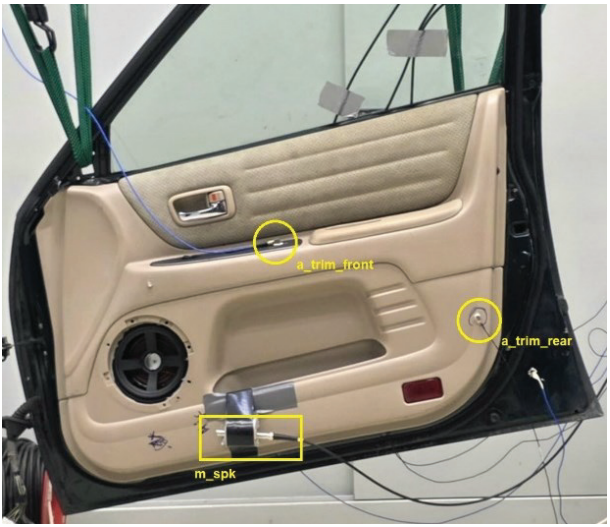

Figure 2: Location of sensors in door trim

A total of 12 sensors – 8 single axis accelerometers and 4 free-field condense measurement microphones – were used across the door assembly for measurements. A reference accelerometer was glued to the magnet of the excited speaker in all setups. Three accelerometers were fitted on the inner side of the door; near the speaker; in the middle of the panel; and at the rear bottom, visible outside the trim. Three microphones were located inside the door cavity, and a reference microphone on the trim. Two accelerometers were positioned on the trim panel, and two on the outside panel.

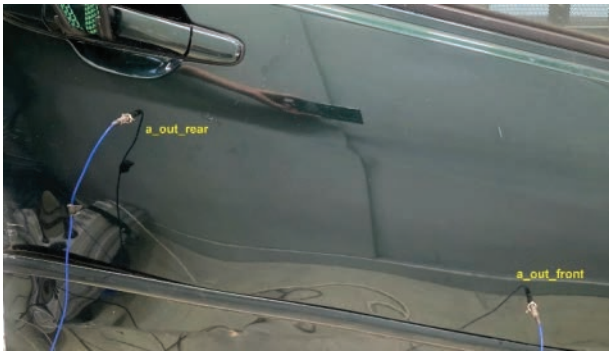

Figure 3: Location of sensors in outside panel

The measurement process involved Siemens Simcenter Testlab suite and Simcenter SCADAS data acquisition systems for data recording and analysis. The MIMO FRF Testing module was employed for comprehensive excitation and response measurement. The excitation signal was a logarithmic sweep of 'periodic chirp' from 20 Hz to 8192 Hz with 0.125 Hz resolution, and with the average of four sweeps constituting the measurement output. The excitation signal was amplified by a TIRA power amplifier.

Three distinct measurement setups were utilized:

Setup 1 - The Conventional Layout: The door assembly replicated its in-vehicle configuration, with the OEM speaker providing combined airborne and structure-borne excitation via a logarithmic sweep signal. The door was in a free-free hanging state.

Setup 2 - The Structure-Borne Excitation: Similar to Setup 1, but the speaker's membrane was cut, leaving only four 1.5 cm wide strips. This modification significantly reduced airborne sound pressure while maintaining speaker excitation, allowing for the isolation and recording of structure-borne excitation. The reference speaker vibration level was kept consistent with other setups.

Setup 3 - The Airborne Excitation: This setup used two speakers. The damaged internal speaker remained in place, but excitation came from an external speaker positioned to generate airborne noise into the door cavity. The external speaker was held by a separate stand to minimize physical connection to the door. Insulation and tapes covered gaps to reduce sound pressure loss. This setup aimed to measure vibrations primarily induced by airborne noise, allowing for comparison with previous setups to determine the dominant excitation form for different panels.

Results

Validation of the measurement setups confirmed consistent excitation levels across all three cases. A reference accelerometer placed at the back of the active speaker ensured that the root mean square (RMS) value of the vibration was approximately 0.3 g during calibration with white noise. For the measurements, a logarithmic sweep from 20 Hz to 8192 Hz was applied, which had a higher excitation effect and less disturbance in the output signal compared to white noise. The sound pressure levels confirmed expected behaviour: Setup 2 – the structure-borne excitation – exhibited the lowest sound pressure levels, while Setup 1 – the conventional layout – had the highest overall levels.

An initial examination of the overall sound behaviour within the door assembly in Setup 1 revealed generally higher sound pressure levels within the door cavity compared to the passenger side of the trim. This suggests that the trim panel provides a degree of soundproofing, though this effect appeared less effective in the lower-middle frequency range of approx. 450 Hz to 600 Hz. The sound pressure level on the passenger side was largely confined to a range between 64 dB and 74 dB, indicating a more controlled acoustic environment compared to the more variable noise levels within the door cavity.

Analysing the inside panel vibrations, the first diagram compares the vibrations at the inside front location and demonstrates the dominance of structure-borne vibrations at this point. This is anticipated due to the accelerometer's proximity to the speaker and its bolted connections, which form a direct vibration path. A noteworthy observation is that in the frequency range of 375 Hz to 825 Hz, the structure-borne excitation – Setup 2 – registers higher vibration levels than the combined excitation – Setup 1. This anomaly might be attributed to the repeated installation and removal of the speaker, potentially altering the seating or effectiveness of the speaker connection padding. However, at lower frequencies, the close tracking of the conventional and structure-borne curves suggests that the measurement integrity is generally good. Furthermore, in several instances at the inside front location, distinct vibrational peaks align across all three setups, indicating frequencies where all excitation paths contribute or where structural response is particularly sensitive.

Turning to the outside panel vibrations, the second diagram below compares the vibrations at the outside front location, suggests that this panel is particularly responsive to the airborne setup – Setup 3. This effect is especially pronounced at lower frequencies, where substantial differences are observed between the vibration magnitudes induced by structure-borne and airborne excitation. This

supports the premise that where airborne excitation induces a stronger vibrational response at a given frequency compared to structure-borne excitation, airborne sound is the presumable dominant excitation mechanism for that specific panel response.

Diagram 1: Comparison of the vibrations at inside front location (dB/level)

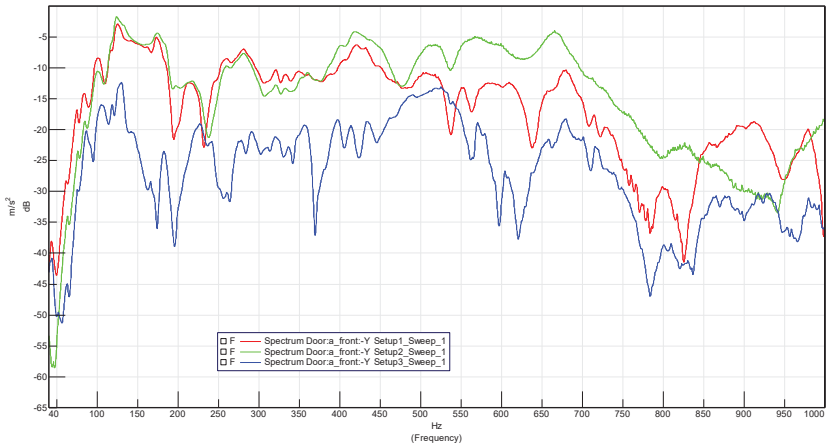

Diagram 2: Comparison of the vibrations at outside front location (dB/level)

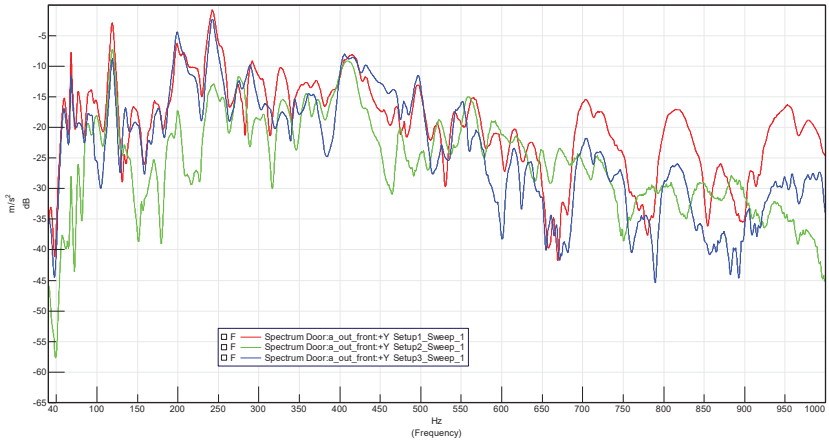

The trim panel vibrations exhibit differing characteristics by location. Structure-borne excitation appears more influential at the trim's front location, while airborne excitation has a greater effect at the trim's rear location. This observation should be contextualized by the age of the door assembly (over 20 years), as the plastic components and connections may have degraded, potentially leading to a less secure fit and increased susceptibility to airborne excitation at the rear.

Diagram 3: Comparison of the vibrations at trim rear location (dB/level)

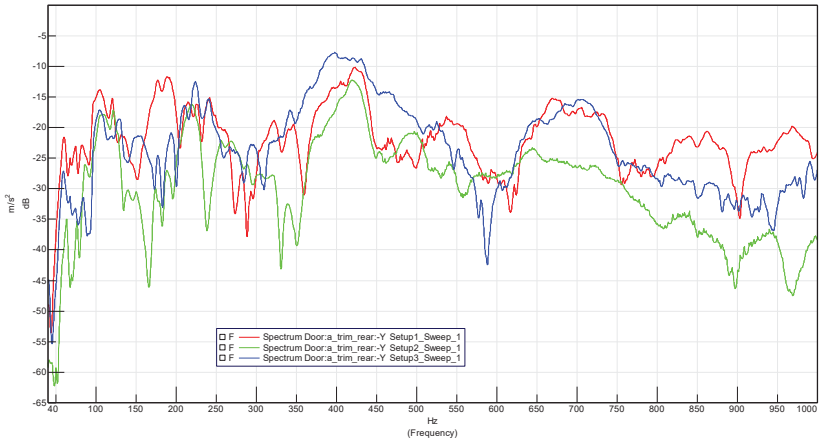

Conclusions

This paper successfully investigated the excitation mechanisms of an automotive door assembly due to its built-in woofer, with a specific focus on differentiating between airborne and structure-borne sound and vibration transmission paths. Through a three-setup measurement methodology valuable insights were gained into the vibro-acoustic behaviour of the door components.

Key findings include at the inside front location, structure-borne vibrations were found to be dominant, as expected due to proximity to the speaker's mounting points. While structure-borne excitation remained the primary driver at the inside middle location, airborne excitation also demonstrated clear contributions, resulting in a mixed excitation scenario at specific frequencies. Notably, both the large outside panel and the trim panel were significantly excited in the airborne setup, particularly at lower frequencies, supporting the interpretation that airborne excitation predominantly influences frequencies more strongly excited by airborne paths than structure-borne paths.

The study reinforced that airborne sound primarily transits through the door cavity, while structure-borne sound propagates via the physical structure. The primary contribution of this research lies in the detailed experimental separation and analysis of airborne and structure-borne sound and vibration transmission from a door-mounted woofer. These findings and the dataset itself provide a valuable foundation for the development and validation of simulation models aimed at predicting and mitigating audio-induced vibro-acoustic phenomena in automotive doors.

Acknowledgement

I would like to express my gratitude to my professors at Széchenyi István University, who guided me through the final stage of my semesters. I am also grateful to my colleagues at Jaguar Land Rover Hungary for all the support and knowledge I gathered from them during this period.

NVHH2025-0027

New cooperation model in automotive NVH

B. Fukker[1*], Z. G. Gazdagh[1]

[1]Robert Bosch Kft, Engineering Acoustics –
Noise Vibration and Harshness
Budapest, Gyömrői út 104. H-1103 Hungary

Summary

The European automotive industry is adapting to competition by shifting from passive strategies to collaborative approaches. Companies are increasingly forming strategic partnerships and joint ventures to leverage manufacturing efficiency and innovation speed. For instance, one major player has acquired a significant stake in a local Asian firm to access cost-effective electric vehicle (EV) technology, enabling production in Europe while avoiding tariffs. Shared manufacturing capacities are also being explored, allowing both European and other firms to optimize resources and reduce costs through joint facilities. Furthermore, technology and innovation transfer is crucial, as European expertise in design and marketing complements the rapid development cycles of Asian automakers. This collaboration aims to produce high-quality EVs at lower prices, benefiting all parties involved. The new cooperative model fosters a "win-win" strategy, enhancing production efficiency and competitiveness in the global market. In the realm of noise and vibration (NVH), European automakers are focused on improving vehicle comfort, particularly in electric vehicles. Collaborations with partners are driving innovative solutions that not only cut manufacturing costs but also accelerate development. Ultimately, these partnerships ensure that the European automotive industry remains competitive.

Introduction

The European automotive industry is increasingly facing fierce global competition, compelling a strategic shift from traditional, independent operational models towards collaborative frameworks. Noise, Vibration, and Harshness (NVH) management, an essential aspect of automotive comfort, especially in electric vehicles (EVs), is at the forefront of these new cooperation initiatives. The necessity for improved NVH performance arises from increased

consumer expectations for vehicle comfort, particularly pronounced in quiet electric propulsion systems. Collaboration among European automakers and Asian partners aims to integrate the manufacturing efficiencies, rapid innovation cycles, and cost-effectiveness prevalent in Asian markets with Europe's advanced technological expertise and stringent quality standards [1].

The core objectives driving this collaborative model include accelerated innovation, optimized production efficiency, reduced costs, and enhanced global competitiveness. Strategic partnerships, joint ventures, and technology transfers characterize this evolving cooperative landscape, contributing significantly to the production of competitively priced, high-quality electric vehicles [2].

Discussion

Recent collaborative examples underscore the effectiveness of the new cooperation model. Stellantis, one of Europe’s automotive giants, has strategically partnered with China's Leapmotor, acquiring approximately 20% ownership. Through this cooperation, Stellantis started EV production at its Polish plant, leveraging Leapmotor’s cost-efficient EV technology and avoiding EU tariffs [1]. This partnership exemplifies how strategic international collaborations enable European production facilities to remain competitive against global automotive giants.

Additionally, Stellantis and Contemporary Amperex Technology Co. Limited (CATL) established a €4.1 billion joint battery manufacturing facility in Spain, each holding an equal stake. This collaboration highlights how strategic resource pooling can optimize investments, share risks, and reduce operational costs, making European automotive manufacturers competitive against dominant Asian battery producers [2].

Changan, another prominent Chinese automaker, also announced plans to establish European manufacturing facilities, indicative of a broader industry trend of cross-regional investment and cooperation. This move aims to tap into European technological excellence and market access while enabling efficient localization of production, demonstrating how the cooperative model serves mutual strategic interests [3].

In the specific context of NVH, European automakers are capitalizing on partnerships with specialized suppliers and technology companies, facilitating knowledge transfer, especially in active noise cancellation, advanced acoustic insulation materials, and simulation technologies. The European Hybrid and EV NVH Summit 2025 notably emphasizes collaborative approaches to integrate smart mounting solutions, modular drivetrain architectures, and predictive

simulation tools, enhancing vehicle comfort and NVH performance while reducing developmental timelines and costs [4].

Conclusion

The new cooperation model in automotive NVH represents a significant evolution in how European automakers address global competition. By forging strategic alliances, particularly with Asian companies, European manufacturers leverage complementary strengths, such as cost efficiency, rapid innovation cycles, and advanced technological capabilities. Joint ventures and shared manufacturing capacities allow European automakers to optimize resources, cut costs, and accelerate market entry. This collaborative approach ultimately delivers high-quality electric vehicles with superior NVH characteristics at competitive prices, ensuring continued relevance and competitiveness in the global automotive industry.

References

[1] Reuters (2024). China's Leapmotor started EV production at Stellantis' Polish plant. Retrieved from: https://www.reuters.com/business/autos-transportation/chinas-leapmotor-started-ev-production-stellantis-polish-plant-jefferies-says-2024-06-17

[2] Financial Times (2024). China's CATL to build €4.1bn battery factory with Stellantis in European expansion. Retrieved from: https://www.ft.com/content/b2c41a7d-02fa-4846-ab50-dd27e534dcf5

[3] Reuters (2025). China's Changan plans European factory, executive says. Retrieved from: https://www.reuters.com/business/autos-transportation/chinas-changan-plans-european-factory-executive-says-2025-07-02

[4] ECV International (2025). European Hybrid and EV NVH Summit 2025. Retrieved from: https://www.ecvinternational.com/european-hybrid-and-ev-nvh-summit-2025

NVHH2025-0029

Electromagnetic Vibration and Noise Analysis of Three-Phase Induction Motors

H. Naojima[1*], K. Ohno[1]

[1]Fuji Electric Co. Ltd., Corporate R&D Headquarters, Digital Innovation Laboratory, Digital Engineering Dept., Hino-city, Tokyo, Japan

[*]Corresponding author, e-mail: naojima-hayato@fujielectric.com

Summary

The miniaturization and improved efficiency of rotating machines have increased the demand for noise reduction. Electromagnetic vibration and noise caused by the resonance between the stator's electromagnetic force and its eigenmode are often problematic. To predict electromagnetic vibration and noise during the design stage using numerical analyses, it is essential to reproduce accurately vibration characteristics. Traditionally, the vibration characteristics of the stator's laminated steel sheets and windings were identified through experiments. We are developing an analytical method to determine these characteristics. This study validates the proposed method by comparing numerical analysis results with experimental data for a three-phase induction motor.

Introduction

To improve motor performance, noise reduction is a key challenge. The sources of motor noise can be classified into three types: fluid pressure fluctuations by cooling fan, mechanical vibrations resulting from bearing movements, and vibrations caused by electromagnetic forces in stator. Electromagnetic vibration spans a wide frequency range and becomes more pronounced when the electromagnetic forces resonate with the stator's eigenmodes. To estimate and reduce the electromagnetic vibration and noise, it is necessary to accurately predict the electromagnetic force generated in the stator and its natural modes, for which a finite element method (FEM) is widely used. In [2,3], accurate modal analyses of the stator, considering the effects of laminated cores and windings, have been presented. However, the mechanical properties of the stator are often identified through correlations between experimental data and analytical results, but the derived properties are not generally applicable. Furthermore, there are few cases of motor electromagnetic vibration and noise

analysis conducted using mechanical properties identified analytically without experiments.

In this paper, we propose an analytical method to determine equivalent mechanical characteristics of the stator without experiments. Electromagnetic-structural-acoustic analysis is conducted with FEM, and the proposed method is validated by comparing the analysis results with experimental results of a three-phase induction motor during no-load operation.

Analysis model

Fig. 1 illustrates the analysis model of the target motor, which is a 1.5 kW, 6-pole three-phase induction machine. The motor is mainly composed of a stator and a rotor. The stator includes a stator core and windings, while the rotor consists of a shaft, a rotor core, and bars. In the structural analysis, the impact of the rotor on electromagnetic vibrations was considered minimal and thus ignored. In the FEM, JMAG®, ANSYS®, and Actran® have been used.

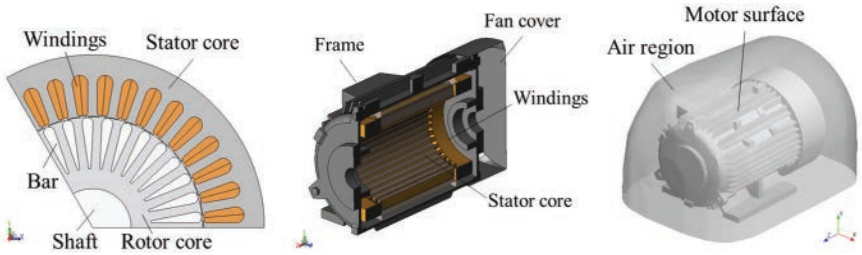

Figure 1: Electromagnetic analysis model (left), structural analysis model (center), and acoustic analysis model (right).

Analysis method

Structural Analysis

In structural analysis using finite element analysis, when the mass, mechanical properties, and damping ratio are known, the discrete equation is expressed as

$$(-\omega^2\mathbf{M} + j\omega\mathbf{C} + \mathbf{K})\boldsymbol{u}(\omega) = \boldsymbol{f}(\omega) \tag{2}$$

where ω is the angular frequency, $\mathbf{M}$ is the mass matrix, $\mathbf{C}$ is the damping matrix, $\mathbf{K}$ is the stiffness matrix, $\boldsymbol{u}(\omega)$ is the displacement vector, and $\boldsymbol{f}(\omega)$ is the force vector. In this case, $\boldsymbol{f}(\omega)$ corresponds to the Fourier transform results of the electromagnetic force obtained through electromagnetic analysis.

Modelling of Stator

Fig. 2 shows the modelling of laminated core and windings of the stator. The stator core model is created by stacking electromagnetic steel sheets, and the contact stiffness k_{N} in the normal direction and k_{T} in the tangential direction between the sheets are determined by surface pressure applied during the lamination process [3]. Equivalent orthotropic properties of the bulk model are identified to match the results of the laminated model. For the windings, based on Voigt and Reuss rules commonly used in composite material modelling, the equivalent properties are calculated by

$$E'_x = E'_y = \frac{E_{\mathrm{c}}E_{\mathrm{v}}}{P_{\mathrm{v}}E_{\mathrm{c}}+P_{\mathrm{c}}E_{\mathrm{v}}}, \tag{2}$$

$$E'_z = P_{\mathrm{c}}E_{\mathrm{c}} + P_{\mathrm{v}}E_{\mathrm{v}} \tag{3}$$

where E_{c} is the Young's modulus of copper, E_{v} is the Young's modulus of varnish, P_{c} is the volume ratio of copper, and P_{v} is the volume ratio of varnish. The obtained material properties are applied to (1), and the sound pressure can be calculated by solving the wave equation with the resulting vibration acceleration as the boundary condition.

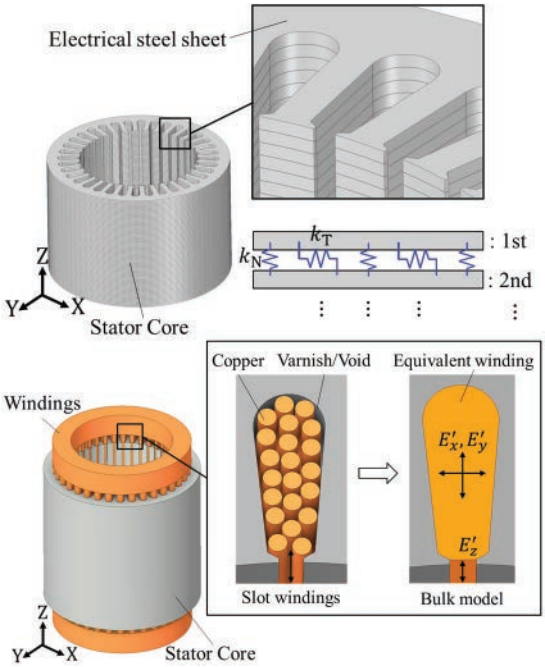

Figure 2: Modelling of laminated core (upper) and modelling of windings (lower).

Numerical Results

The average vibration acceleration levels on the motor surface and the average noise levels at 8 evaluation points positioned 0.5 m from the center of the motor are shown in Fig. 3. In the analysis, the vibration and noise values are reproduced qualitatively, and the difference in OA values is less than 2 dB. The relatively large errors below 500 Hz and around 1000 Hz are likely caused by differences in boundary conditions and the connection conditions of components.

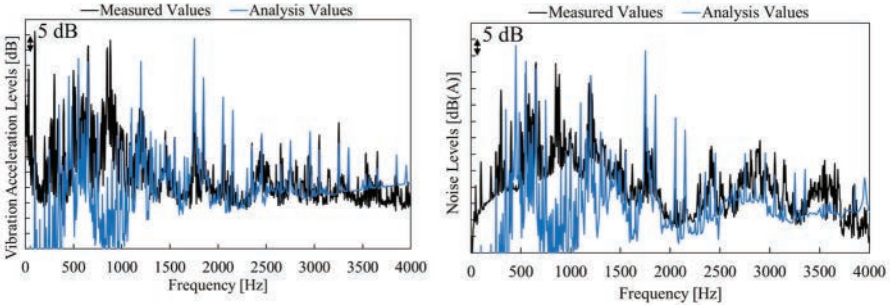

Figure 3: Vibration acceleration levels (left) and noise levels (right).

Conclusion and Future Work

This paper provided an analysis method to determine the vibration characteristics of the stator in induction motors without experiments and its effectiveness by mostly reproducing the vibration and noise.

In the future, we will conduct analysis reflecting the connection states between components to improve accuracy.

References

[1] F. Chai, Y. Li, Y. Pei, and Z. Li, *Accurate modelling and modal analysis of stator system in permanent magnet synchronous motor with concentrated winding for vibration prediction*, IET Electric Power Applications, Sep. 2018, vol. 12, no. 8, pp.1225-1232.

[2] H. Yin, X. Zhang, F. Ma, C. Gu, H. Gao and Y. Wang, New Equivalent model and Modal Analysis of Stator Core-Winding System of Permanent Magnet Motor With Concentrated Winding, in IEEE Access, 2020, vol. 8, pp. 78140-78150.

[3] N. Back, M. Burdekin, and A. Cowley, Analysis of Machine Tool Joints by the Finite Element Method, in Proc. 14th Int. MTDR Conf., UK: Macmillan Education, pp.529-539.

NVHH2025-0032

Time Series Failure Identification in Manufacturing

M. Farkas[1*], J. A. Erdélyi[1]

[1]Robert Bosch Kft., Engineering Acoustics – Noise Vibration and Harshness, Budapest Gyömrői út 104, H-1103, Hungary,

[*]Corresponding author, e-mail: mate.farkas2@hu.bosch.com

Summary

In the automotive manufacturing and development sectors, vast amounts of time-series data are collected, making manual evaluation increasingly impractical. Traditional models that rely on predefined thresholds or historical data require frequent adjustments to remain effective, which is not feasible in dynamic manufacturing environments. To address this challenge, we propose a self-training pipeline that can autonomously identify failures across various manufacturing processes without the need for extensive retraining or manual intervention. This domain-independent solution offers a powerful and scalable approach to anomaly detection, ensuring robust performance even in the face of data drifts and adjustments.

Method

The model proposed in [1] was used for detecting anomalies in a manufacturing process. The periodic nature of the data is given by recording a time-signal relevant to the process execution (eg. vibration acceleration, pressing force, current, etc.) for each part that goes through that manufacturing process. A detected anomaly consequently belongs to one specific manufactured part.

The proposed model begins with a single input parameter: the reference window size. Initially, a slice of the input signal is used as the reference window to start the algorithm. The sliding correlation between the input signal and the reference window is then calculated to determine the step size. As the algorithm progresses, the reference window is updated with new input data segments at a set learning rate, allowing the prediction to adjust dynamically to changing period shapes. This process ensures that the model remains adaptive to variations in the input data. In our case the reference window size needs to cover exactly the recording length made at one physical part at the manufacturing

process. As the selected process outputs a time signal of constant length for each part, the automatic period detection part of the algorithm could be turned off.

Next, the model predicts a new slice of the input signal using the shifted reference window and calculates the error between them. To enhance the accuracy of anomaly detection, previous windows are stored, and the standard deviation for each sample point within the window is computed. A weighted error is then derived from the standard deviation window and the error window. This approach ensures that signal areas with consistently higher noise ratios are not mistakenly detected as anomalies.

Dynamic Time Warping (DTW) is employed to calculate the optimal match between the reference window and the input signal segment. Enabling DTW enhanced the model's ability to accurately identify anomalies, due to improved temporal alignment of the manufacturing process data.

The algorithm also includes a bidirectional run feature, which allows it to be executed in both directions on the input time signal. It is making use of the fact that the anomaly score will increase only after a profile change, and by combining the two anomaly score signals, profile change-related anomalies are effectively eliminated. This bidirectional approach can be used periodically in manufacturing to check impact of changes in raw material, etc.

By integrating these advanced techniques, the proposed model offers a robust and scalable solution for time series failure identification in manufacturing, capable of adapting to various data conditions and providing reliable anomaly detection without the need for extensive retraining or manual intervention.

Conclusion

The self-training pipeline presented in this study offers a robust and scalable solution for time series failure identification in manufacturing. By eliminating the need for extensive retraining and manual intervention, this model provides an out-of-the-box approach to anomaly detection, capable of adapting to various manufacturing processes and data conditions.

References

[1] J. A. Erdélyi, M. Farkas, B. Fukker, “Self-training anomaly detection in vibrational and acoustic data” in *ISMA2024, Leuven, 9 to 11 September 2024*, Editors: W. Desmet, B. Pluymers, D. Moens, J. del Fresno Zarza, Place: Publisher, 2024, pp. 3335-3342, ISBN 978-90-82893-17-5

NVHH2025-0033

Machine learning approach to the detection and categorization of nonlinear phenomena in electronic components

J. Erdelyi*[1]

[1]Robert Bosch Kft.,
ME/ECF-NVH, Budapest, Hungary

*Corresponding author, e-mail: erdelyi.jankaanna@hu.bosch.com

Summary

Nonlinear phenomena within electronic components in an automotive setting can lead to functional problems. The root-cause analysis of these phenomena is therefore an important task during the product development phase, which can be accelerated by the use of data-driven methods and machine learning approaches. The two main topics of this presentation are the detection and categorization of nonlinearities. Detection can be aided by models which help differentiate between sample specific nonlinearities and those originating from the measurement environment. Once the nonlinearities are detected, either by previous models or thresholds set by engineers, classification algorithms can be used to identify the type of nonlinearity present in the structures. The nonlinearity type can give valuable information regarding the location, or the materials associated with the phenomena. Acquiring a trained classifier requires large amounts of labelled data from numerous measurements and sample types to create a robust model, capable of predicting not only in a known environment, but in new settings too. In some cases, generated data can help take this burden off the measurement and labelling process but poses an added risk when it comes to ensuring data quality. This presentation aims to show these principles of data-driven nonlinearity detection and categorization in use.

Introduction

The first step in the identification process is a well-rounded measurement workflow capable of giving information relevant to the nonlinearity in question. A measurement sequence consisting of sweep, impact and burst measurements,

each targeting different features, is needed. Using different time-signal processing methods, these features can be computed and a Nonlinearity signal feature – Nonlinearity type dictionary can be created, to use in further evaluations.

One measurement type that is vital in the identification process is the nonlinear resonance backbone curve measurement. Due to nonlinear phenomena, the resonance frequency a certain mode can shift when the excitation amplitude used in the measurement is altered. This frequency-amplitude dependency can characterize the measured nonlinearity, giving insights into the type, and parameters of the phenomena. An automated measurement of the entire system, consisting of a low excitation measurement of the underlying linear system and backbone curves of all resonances can show a complete picture of the component in question.

Once all measurements are completed, features acquired through time signal processing and domain knowledge help identify the nonlinearity. To provide a data driven solution, machine learning models can be utilized, making use of past measurements as well. A machine learning workflow is used to combine simulated nonlinearities and real nonlinearities from historic data to form a well-rounded dataset of phenomena present in components and predict the type of nonlinearity occurring in new samples. The use of a parametrized physics-based model enables the creation of labelled classes of phenomenon types such as impact rattling, friction or geometric nonlinearities to be predicted.

An alternative approach is the localization of the source through coordinate prediction. This technique is indifferent to the cause of the nonlinearity, but instead aims to predict either its XYZ coordinates or its distance from various measurement points and calculates the source through triangulation. To achieve this, a measurement based digital twin of the component must be created, the nonlinearity measured at a high enough excitation level to activate it, features transformed into the same format as the digital twin. An AI model can then be trained on the digital twin and the location of the nonlinearity predicted.

The two approaches, identification and localization, give a rounded solution to the root-cause analysis of nonlinear phenomena and together they accelerate the design process. The use of data driven methods, as seen in the ML workflow applied to historic data, enables the exploitation of information in past measurements otherwise unaccessed. This presentation aims to showcase the benefits of using these approaches in nonlinearity identification.

NVHH2025-0035

Understanding Sound Preferences for EVs: A Global Research Collaboration by Bosch, Klangerfinder, and clickworker

M. Farkas[1*], B. Fukker[1], Prof. F. Käppler[2], Prof. Dr. C. Zenk[2], L. Münter[2], S. Pamp[3], I. Maione[3]

[1]Robert Bosch Kft., Engineering Acoustics – Noise Vibration and Harshness, Budapest Gyömrői út 104, H-1103, Hungary,

[2]Klangerfinder GmbH & Co KG,
Humboldtstraße 4, 70178 Stuttgart, Germany

[3]clickworker Germany GmbH,
Theodor-Althoff-Str. 41, 45133 Essen, Germany

[*]Corresponding author, e-mail: mate.farkas2@hu.bosch.com

Summary

How does the sound of a vehicle influence user perception – and can this impact vary across cultures? This was the guiding question behind a recent collaborative research project conducted by Bosch, Klangerfinder, and clickworker. The initiative aimed to identify regional preferences for electric vehicle (EV) start-up sounds, providing data-driven insights to support product development and culturally aligned sound design.

In this collaboration, Klangerfinder was responsible for creating the sound concepts across three categories – Sport, Eco, and Classic vs. Futuristic – bringing in their deep expertise in emotional and brand-driven audio design. Bosch Engineering translated these into testable formats and oversaw the technical design of the study, while clickworker enabled the large-scale online testing and global user segmentation. Participants across continents evaluated sound pairs in controlled A/B comparisons, with preferences directly quantified for statistical analysis.

Main Challenges

Sound is deeply cultural. What's perceived as sporty or elegant in one region might be considered inappropriate or even unpleasant in another. One key challenge was designing sounds that could evoke emotional associations such

as performance, sustainability, or innovation – while still being accepted across markets.

Another challenge: collecting meaningful data at scale without sacrificing quality. The team implemented an innovative "gold data" quality control mechanism and rigorous contextualization strategies to ensure responses reflected genuine, considered preferences.

Results

The study uncovered striking regional and demographic differences in sound preferences – and perhaps more surprisingly, a disconnect between what participants thought they preferred and the choices they actually made in controlled comparisons. These insights underline the importance of grounding sound design in real user data rather than assumptions.

If your products rely on sound – whether in mobility, smart devices, or consumer goods – this project offers key lessons on how user expectations and perceptions vary across the globe. Join our presentation to discover how a data-driven approach to sound design can improve product resonance, emotional impact, and market fit.

Company Introductions & Contact

Bosch

The Bosch Group is a leading global supplier of technology and services. Its operations are divided into four business sectors: Mobility, Industrial Technology, Consumer Goods, and Energy and Building Technology.

The Engineering Center Budapest was founded in 2005 and now more than 3500 experts are shaping the future of mobility – making Hungary Bosch's fourth-largest R&D center in the world after Germany, India, and China.

The NVH team in Budapest is one of Hungary’s most competent, comprising acousticians with decades of know-how and diverse backgrounds in electrical, mechanical, software, and vehicle engineering. They engage in R&D projects for product and methodology development in collaboration with Bosch product teams, OEMs, and universities. The NVH facility boasts a state-of-the-art laboratory covering over 1000 m2, housing Anechoic, Semi-Anechoic, and Vehicle Anechoic chambers equipped with a chassis-dynamometer. The team utilizes advanced equipment such as multiple Laser Vibrometer Systems, Noise

Source Localization, and Sound Field Visualization Systems, along with customized test benches for special needs.

Contact: bertalan.fukker@hu.bosch.com

Klangerfinder

Klangerfinder GmbH & Co KG, founded in 2009 by Prof. Florian Käppler, is an award-winning agency for holistic audio experience design based in Stuttgart. The transdisciplinary team designs and realises national and international projects in the fields of culture and digitality, technology and art, brands and music as well as science and business.

The work of Klangerfinder became known to a wider public through the globally successful sound brands Audi and Deutsche Telekom. Klangerfinder researches and develops new forms of communication, learning and experience with a focus on participation, democratisation, accessibility and inclusion.

A constantly growing field of activity are often long-term research co-operations with universities, institutes and partners from the fields of business, technology and culture.

Contact: info@klangerfinder.de

clickworker

clickworker, now part of LXT.ai, is one of the largest global providers of crowdsourced data, with over 7 million freelancers across Europe, America, and Asia. As an integral part of LXT's industry-leading AI data solutions, clickworker offers scalable services for AI training data, categorization and tagging, surveys, store audits, web research, text creation, and product data digitalization – in 18 languages and across more than 30 target markets.

Its powerful technology platform supports mobile-first and desktop task execution, with options ranging from self-service to fully customized, managed solutions. Tasks are divided into micro jobs, completed by qualified Clickworkers, and delivered with built-in quality assurance. In 2024, clickworker successfully completed over 800 million jobs, serving top-tier technology clients with high throughput, scalability, and cost-efficiency.

Learn more at clickworker.com
Contact: stephan.pamp@clickworker.com

NVHH2025-0036

Minimal modelling of noise and vibration propensity of fluids engineering equipment due to vortex shedding

J. Vad[1*], M. Mizsei[1], E. Balla[1]

[1]Budapest University of Technology and Economics,

Department of Fluid Mechanics, Budapest, Hungary

[*]Corresponding author, e-mail: vad.janos@gpk.bme.hu

Summary

Vortex shedding from blades of low-speed, axial-flow, air-handling rotors has been considered from two complementary perspectives: as an undesirable cause of noise and vibration in an NVH view – and also as a potential tool for diagnostics and condition monitoring purposes.

Introduction

The blades of low-speed axial-flow air-handling turbomachinery, such as ventilating and cooling fans, and rotors for drone propulsion, are discussed herein. The shedding of vortices from an axial-flow rotor blade profile, initiated already upstream of the blade trailing edge (**TE**), is termed herein as profile vortex shedding (**PVS**). The effects of PVS related to Noise, Vibration and Harshness (**NVH**) are twofold. a) PVS causes a fluctuation in lift force acting on the blade section, and, as such, it generates a bending moment, causing blade vibration. b) PVS generates a dipole noise in association with the TE.

PVS can be characterized by a universal Strouhal number $St^* \approx 0.17$ [1]:

$$St^* = \frac{f \cdot b}{U} \tag{1}$$

Where f is the vortex shedding frequency, b is the transversal distance between the two rows of shed vortices, and U is the flow velocity. In [2], the authors provided a method for brief empirical estimation for b as function of geometrical and operational parameters.

In addition to the negative aspects of noise and vibration in terms of NVH, they can also be considered as valuable tools for turbomachinery diagnostics, condition monitoring, and predictive maintenance. In [3], the actual flow rate of turbomachinery has been retrieved from vibrometer data. In [4], acoustic measurements were exploited in prediction of faulty machine behaviour. [5] reports on utilization of pressure sensor data in condition monitoring.

The departmental turbomachinery research group has been maintaining active research in PVS related to blade elements of low-speed axial flow air-handling turbomachinery rotors [1, 6-7], with extensive involvement of Computational Fluid Dynamics (**CFD**). A brief, order-of magnitude estimation of PVS-related noise and vibration has been performed by minimal modelling of PVS effects. The most developed modelling state is reported in [7].

Motivation and goals

The authors outline the following concept for future industrial consideration / utilization of the phenomenon of PVS in relationship with low-speed axial flow gas-handling turbomachinery rotors, such as ventilating and cooling fans (in e.g. automotive applications), and for drone propulsors.

Depending on the availability of inputs to Eq. (1), two ways of the utilization of the equation is envisaged, after further development of the related empirics. **A)** Already in the preliminary design phase of the rotor blades, the rotor noise is to be moderated for reducing the human annoyance. Furthermore, blade vibration is to be moderated for enhancing the operational safety of the rotor. As a substantial input data for both of these goals, the order of magnitude of f can be estimated as output, if the operational data for the design state U and b are provided as input. **B)** PVS is considered as contributor to the complex acoustic and vibrational "fingerprint" of the machine. For an actually operating turbomachine, PVS has a signature in the apparent noise and vibration due to PVS providing a measurement-based means for estimating the actual f as input. This data correlates the operational state via U and b, and thus, it can contribute to monitoring the operational state of the rotor, eg. flow rate estimation – as in a classic "vortex shedding flowmeter" application.

Toward these goals, the PVS minimal modelling in [7] is to be further developed, and the errors due to modelling simplifications are to be quantified.

Results and discussion: examples

An airfoil and a circular-arc cambered plate profile, being representative for low-speed axial flow rotor applications, were modelled using CFD from the perspective of PVS [1][6]. **Figure 1** provides a CFD example [7] for PVS from the airfoil, in terms of velocity magnitude for a given angle of attack α and chord-based Reynolds number Re_c. **Figure 2** demonstrates the vortices identified using the Lagrangian-Averaged Vorticity Deviation (***LAVD***) downstream of the TE of the airfoil [1][6], in terms of the coordinates x and y being parallel to and normal to the inflow direction, respectively, normalized by

the chord length c, having the origin located at the TE. In minimal modelling of noise and vibration caused by PVS [7], the vortices were considered as circular-shaped coherent structures, associated with a rotationally symmetrical tangential relative velocity field around the vortex centre, superimposed on the temporal mean wake velocity field. Fig. 2 illustrates, however, that the detected vortices usually differ from the circular shape. For quantification of non-circularity of the individual vortices, the vortex asymmetry indicator A has been introduced as follows [1][6]. The vortex radius R of a circular equivalent vortex for any detected, non-circular vortex (see Fig. 2) was determined using area equality. The actual distance between the vortex centre and each point lying on the detected vortex boundary over the CFD grid was determined, and the standard deviation R_{SD} of these data was calculated. The asymmetry indicator was calculated for each vortex as $A = R_{SD}/R$. The A dataset incorporating each shed vortex in each studied Case for the airfoil profile, presented in [1], was considered as a statistical multitude, and was modelled as a normal distribution with a mean value of $\bar{A} = 0.30$, and variance of $\sigma_A = 0.12$. **Figure 3** shows the probability density function as well as the cumulative distribution for the A dataset. The figure suggests that the mean deviation from the circular shape is in the order of magnitude of 30 % of vortex radius R. Furthermore, 50 % as well as 95 % of the detected vortex multitude is characterised by an asymmetry of $A \leq 0.3$ as well as $A \leq 0.5$, respectively.

In analogy to Figs. 1 to 3, Figs. 4 to 6 provide data on PVS related to a circular-arc cambered plate blade profile [6-7]. **Figure 4** is a CFD example for the distribution of velocity magnitude, accompanied by **Figure 5** presenting vortices detected using LAVD [6]. Based on the data in [6], **Figure 6** presents the A statistics related to the cambered plate, modelling the A dataset as a normal distribution with a mean value of $\bar{A} = 0.21$, and variance of $\sigma_A = 0.09$. The figure shows that the mean deviation from the circular shape is in the order of magnitude of 20 % of vortex radius R. Furthermore, approximately 50 % as well as 95 % of the detected vortex multitude is characterised by an asymmetry of $A \leq 0.2$ as well as $A \leq 0.35$, respectively.

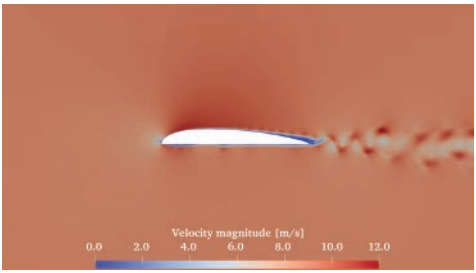

Figure 2: PVS from an airfoil blade profile, illustrated using the CFD-resolved velocity magnitude, for the Case of $\alpha = 0.0°$, $Re_c = 0.60 \cdot 10^5$ [7].

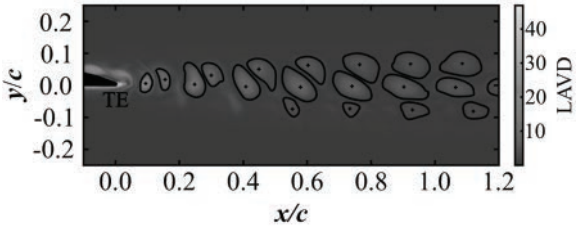

Figure 2: Vortices identified downstream of the TE for the airfoil Case of Fig. 1. Dots: vortex centres. Contours: vortex boundaries [1].

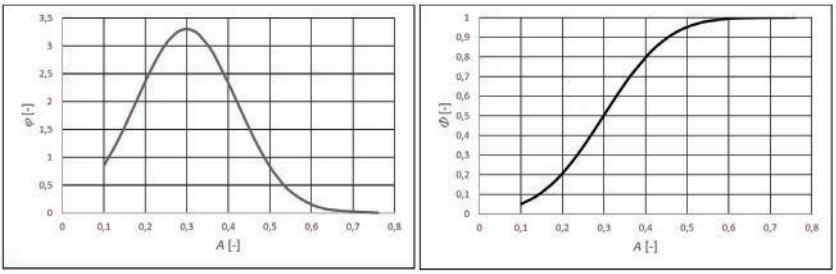

Figure 3: Statistics for the vortex asymmetry indicator A for the airfoil of Fig. 1 [1]. *Left: probability density function* $\varphi = N(\bar{A}, \sigma_A^2)$ *. Right: cumulative distribution function* Φ *for* $\varphi = N(\bar{A}, \sigma_A^2)$.

The statistics in Figs. 3 and 6 will serve as input to the future estimation of the modelling error due to the PVS minimal modelling approximation of vortex circularity and rotational symmetry, in terms of modelling both lift force fluctuation and noise caused by PVS.

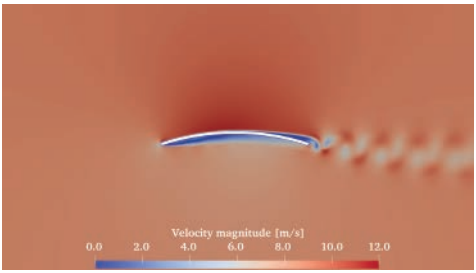

Figure 4: PVS from a circular-arc cambered plate profile, illustrated using the CFD-resolved velocity magnitude, for the Case of $\alpha = 1.1°$, $Re_c = 0.60 \cdot 10^5$ [7].

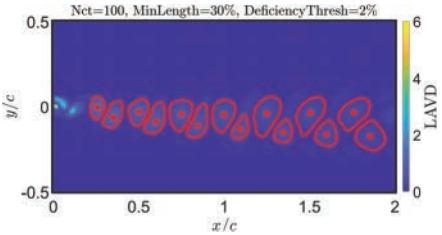

Figure 5: Vortices identified downstream of the TE for the cambered plate Case of Fig. 4. Dots: vortex centres. Contours: vortex boundaries [6].

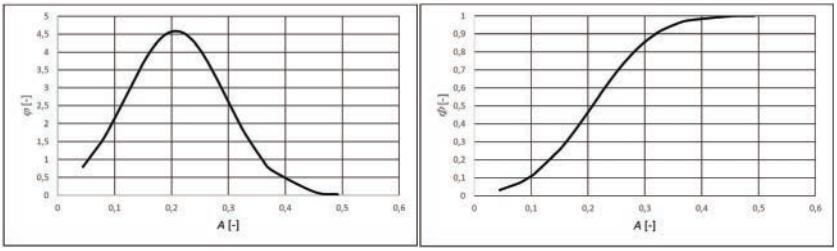

Figure 6: Statistics for the vortex asymmetry indicator A for the cambered plate blade of Fig. 4 [6]. *Left: probability density function* $\varphi = N(\bar{A}, \sigma_A^2)$. *Right: cumulative distribution function* Φ *for* $\varphi = N(\bar{A}, \sigma_A^2)$.

Conclusions

A twofold concept has been outlined for moderating blade noise and vibration due to PVS in the preliminary design phase of low-speed axial-flow rotors, as well as utilizing the remaining noise and vibration for rotor condition monitoring purposes. Preparatory steps for future estimation of PVS modelling errors due to vortex asymmetry have been taken.

Acknowledgement

This work has been supported by the NRDI Fund under contract No. NKFI K 143204. Gratitude is expressed to Mr Gábor DAKU and to Ms Kinga Andrea KOVÁCS for providing the CFD data related to references [1][6] for further processing.

References

[1] G. Daku, and J. Vad, "Enhanced modelling of the phenomenon of vortex shedding from a low-speed axial flow rotor blade profile," *ASME Paper* GT2024-123991, 2024.

[2] E. Balla, and J. Vad, "Refinement of a semi-empirical method for the estimation of profile vortex shedding frequency from low-speed axial fan blade sections," Paper ID: ETC2021-591, in proc. *14th European Turbomachinery Conference (ETC14)*, 2021 (online).

[3] H. Ma, O. Kirschner, and S. Riedelbauch, S., "Systematic comparison of sensor signals for pump operating points estimation using convolutional neural network," in proc. *15th European Turbomachinery Conference (ETC15),* 2023, Budapest, Hungary.

[4] N. Linnemann, and D. Brillert, "Detection of faulty machine behavior using acoustic measurements: A predictive maintenance approach demonstrated by means of of IGV misalignment," Paper ID: ETC2025-141, in proc. *16th European Turbomachinery Conference (ETC16),* 2025, Hannover, Germany.

[5] D. Hummer, and J. Hermann, "AI-based condition monitoring of gas turbine combustors using high-resolution dynamic pressure sensor data," Paper ID: E25-21, in proc. *11th EVI-GTI Conference*, in conjunction with the *ETC16 Conference,* 2025, Hannover, Germany.

[6] K. A. Kovács, G. Daku, E. Balla, G. Janiga, and J. Vad, "Numerical investigation of the vortex shedding phenomenon from a circular-arc-cambered plate profile relevant to low-speed axial flow rotor blades," Paper ID: ETC2025-185, in proc. *16th European Turbomachinery Conference (ETC16),* 2025, Hannover, Germany.

[7] M. Mizsei, E. Balla, and J. Vad, "Minimal modelling for noise and vibration propensity of low-speed axial flow rotor blades due to vortex shedding," *ASME Paper* GT2025-153711, in proc. *2025 ASME Turbo Expo*, 2025, Memphis, Tennessee, USA.

NVHH2025-0038

Case study of time delay effects on amplitude distortion during sinusoidal sweep excitation

Ács Dániel[1], Gazdagh Zoltán Gábor[2,3] , Lakatos Kristóf[4]

[1]Robert Bosch Kft.,
Electrified Motion – eAxle Validation, Budapest Gyömrői út 104. H-1103, Hungary

[2]Robert Bosch Kft.,
Engineering Acoustics – Noise Vibration and Harshness, Budapest Gyömrői út 104. H-1103, Hungary

[3] Széchenyi István University ,
Dept. of Whole Vehicle Engineering, Győr, Egyetem tér 1. H-9026, Hungary

[4]Robert Bosch Kft.,
Environmental Validation Special Testing, Budapest Gyömrői út 104. H-1103, Hungary

[*]Gazdagh Zoltán Gábor, e-mail:gazdagh.zoltan.gabor@sze.hu

Summary

This study examines the importance of sinusoidal sweep testing in the automotive industry for assessing the performance and durability of components. It highlights the critical role of selecting an optimal sweep rate, as this affects both the accuracy of results and testing efficiency. The research identifies a significant time delay effect that occurs at resonance frequencies, which can lead to amplitude distortion. By simplifying the testing device, the study clarifies the relationship between sweep rates and time delay. Ultimately, the findings aim to enhance testing protocols, improving the reliability and performance of automotive components.

Introduction

Sinusoidal sweep testing plays a crucial role in the automotive industry, as it generates various excitations that are essential for evaluating the performance and durability of automotive components. This testing method simulates the loads that rotating machinery experiences during operation, reflecting their behaviour through periodic motions that closely mimic real-world conditions. A critical aspect of these tests is the sweep rate, which defines the speed at which the Device Under Test (DUT) moves through the designated testing range. Selecting the optimal sweep rate is vital and requires meticulous optimization,

especially since these tests are performed at the resonance frequencies of the product being evaluated, where the system is most sensitive to changes in input.

The importance of sinusoidal sweep testing has grown significantly with the rise of electric drive systems in the automotive industry. Electric motors operate at higher rotational speeds and involve large, heavy rotating components, necessitating careful consideration of factors such as imbalance and higher frequency excitations. Sinusoidal sweep testing offers a reliable method for examining these dynamic factors, ensuring the performance and reliability of modern electric vehicles.

Effects of sweep rate on testing results

If the sweep rate is excessively fast, it can lead to distortion in the response amplitudes, which may compromise the accuracy and reliability of the test results. On the other hand, if the sweep rate is too slow, it can result in prolonged testing durations and increased costs, which are undesirable in a competitive industry where efficiency is paramount. Our research has uncovered a significant time delay effect that manifests when the excitation signal traverses through the resonance frequencies. This study aims to delve deeper into this phenomenon, particularly focusing on the ratio of amplitude distortion that arises from rapid sweeps and the corresponding time delay. This is crucial because the system does not respond instantaneously to an excitation, which can affect the overall test outcomes and lead to misinterpretations of the component's performance.

Advancement in Testing Protocols

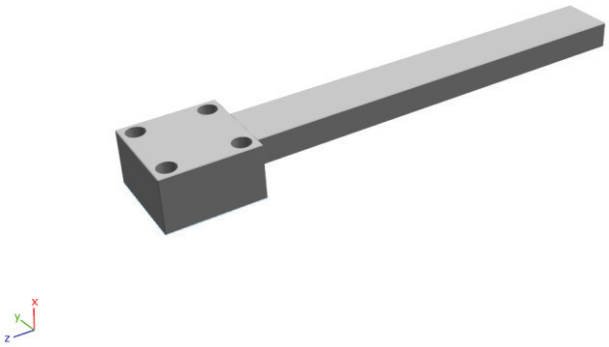

Figure 1: Test specimen

Building on this analysis, previous research has primarily focused on the eAxle level, which is too complex to clearly identify the main parameters affecting the time delay. This complexity can obscure the relationships between various factors, making it challenging to draw definitive conclusions. Following the selection of the resonance frequency based on experimental modal analysis, tests were conducted using constant amplitudes at various sweep rates on a shaker. The device under test was designed to maintain simplicity, resulting in the test specimen being manufactured from a single aluminium block. This design choice not only facilitated the testing process but also ensured that the results were more easily interpretable. Based on the measurement outcomes, the time delay can be defined, which aids in understanding the dynamic system while also refining the equations related to distortion caused by the sweep rate.

Understanding the implications of these findings can lead to enhanced testing protocols, crucial for improving the reliability and performance of automotive components. By characterizing the time delay effect for each product, we can refine our testing methodologies for greater accuracy and efficiency. This research contributes to existing knowledge and has practical applications in optimizing automotive testing processes, benefiting both manufacturers and consumers. The insights gained can also serve as a foundation for future research and development efforts in advancing automotive technology.

Acknowledgement

Project no. KDP-2023-C2254459 has been implemented with the support provided by the Ministry of Culture and Innovation of Hungary from the National Research, Development and Innovation Fund, financed under KDP-2023 funding scheme.

References

[1] Z. Gazdagh, D. Ács, B. Vehovszky, B. Fukker, “Control of transfer function distortion during RPM-sweep testing of e-drive systems”. In: Conference Proceedings of ISMA2024 - USD2024. 2024, pp. 3779–3787. URL: https://m2.mtmt.hu/api/publication/35498927

[2] A Lalanne, C. (2009). Sinusoidal Vibration: Mechanical Vibration and Shock Analysis, Volume 1, Print ISBN:9781848211223, Online ISBN:9780470611906, DOI:10.1002/9780470611906

[3] Dániel Ács and Zoltán Gazdagh. “Exploring the impact of RPM related excitation on transfer function distortion in E-Drive systems”. In: NVHH 2023: International Conference for Acoustic and Vibration Engineers. 2023, pp. 54–55. URL: https://m2.mtmt.hu/api/publication/34780200

LB-acoustics Messgeräte GmbH

Sound and vibration measurement
From compact sensors to comprehensive measurement systems

With over 40 years of experience and expertise, LB-acoustics Messgeräte GmbH offers solutions in sound and vibration measurement technology. LB-acoustics sells measuring instruments from major manufacturers as well as the associated evaluation and documentation software and combines these into systems tailored to the specific needs of the user.

LB-acoustics Messgeräte GmbH emerged in October 2001 from the former measurement technology group of LB-electronics, by concentrating on core competencies in sound and vibration measurement technology.

Laser vibrometers from Polytec Germany – leading in optical metrology for the measurement and analysis of acoustics, dynamics and vibration. Their Laser Doppler Vibrometers are established tools in research, development and production testing control of DUTs from micro to macro – optically: no contact, no wear, no pseudo-rejects. Laser vibrometers are established precision sensors for vibro-acoustic characterization – whether on prototypes or for in-line and end-of-line testing. Single-point vibrometers operate according to the simple point-and-measure principle for fast measurement results and evaluation. Scanning vibrometers enable reliable, efficient modal analysis, FE model validation, structural analysis by full-field measurement with high spatial resolution, visualized as 2D and 3D vibration modes, covering frequencies from DC to 32 MHz. Micro System Analyzers enable the comprehensive study of MEMS and microsystems - whether in 3D, with IR laser through intact MEMS encapsulation, optional topography analysis of form parameters and roughness, or measuring up to the super high frequency range of 8 GHz.

Quality meets Service

NVHH2025-0045

Graphical interpretation on the formation of isolated resonances in a dissipative nonlinear system

Z. Gabos[1,2*], Z. Dombovari[1,2]

[1]Department of Applied Mechanics, Faculty of Mechanical Engineering,
Budapest University of Technology and Economics,
Műegyetem rkp. 3 H-1111 Budapest, Hungary

[2]MTA-BME Lendület Machine Tool Vibration Research Group,
Department of Applied Mechanics,
Budapest University of Technology and Economics, Budapest H-1521

[*]Corresponding author, e-mail: zoltan.gabos@mm.bme.hu

Summary

Backbone curves (BBC) describe the amplitude-dependent behaviour of a nonlinear vibration mode. However, the concept of BBCs that depend solely on frequency does not explain the formation of isolated resonances (isoli) in specific nonlinear structures. This study extends the definition of BBCs to the dissipative domain. Visualising this concept in an analogous space to the linear Laplace transform domain, it can be shown that this new definition of BBCs can 'curve' the nonlinear resonance so that isoli, closed branches of periodic stationary solutions, can emerge at specific forcing levels. The results highlight that the BBC is not solely governed by the frequency but by a combination of local attenuation and vibration properties.

Introduction

In this work, we propose a visualisation technique, similar to that in [1], formed in the space of local attenuation and frequency properties analogously to the Laplace-domain for linear systems (Fig. 1). This technique is capable of demonstrating and explaining the appearance of isolated resonances (isoli) in a structure caused by a form of dissipative nonlinearity [2]. A general concept for understanding nonlinear vibrations is through the observation of nonlinear frequency-response (NLFR) curves, defined by the system's response amplitude and phase lag as a function of the forcing frequency with constant forcing amplitude [3]. The features of the NLFR curves provide meaningful insights into the system's dynamics [4], allowing for the prediction of safe operating parameters for non-

linear structures.

The core idea comes from the concept of damped linear systems and their relation to frequency (Fourier) and transfer (Laplace) responses, where the transient and stationary behaviour are strictly connected by the inverse Fourier and Laplace transform of the so-called impulse response function (IRF). In the linear case, the free (transient) decay follows a straight 'vertical' path in the Laplace domain described by constant attenuation (σ) and constant oscillation frequency (ω), where the response is lagging $\pi/2$ behind the excitation.

1. Extension od BBC with dissipation

For the linear consideration, the mentioned constant parameters are the real and imaginary parts of the so-called poles ($s = \sigma + \omega \mathrm{i}$) at which the Laplace response has singularity or mathematical resonance for the $\mathrm{e}^{s\mathrm{i}}$ excitation. Note that the Fourier response is limited in the damped case, since it can be considered as an intersection of the Laplace response at zero attenuation when ($\sigma == 0$). In this case, the Fourier response is the rounded section of the singularity, also suggesting that mathematical resonance (singularity) occurs only in the Fourier domain if no damping is involved. For physical (Newtonian) systems, this happens when the phase lag is $\pi/2$, where the inertial forces cancel the elastic forces, and the injected power through excitation cannot be dissipated by damping, resulting in an ever-growing response (secular growth).

Although nonlinear systems cannot be described in the Fourier or Laplace domain, the response amplitude-dependent excitation frequency $\omega(A)$ and attenuation properties $\sigma(A)$ can be defined locally. By only introducing elastic nonlinearity in the mechanical system (no damping involved), the strict mathematical resonance with infinite response for a single frequency vanishes. However, there are still certain frequency and amplitude pairs, where inertial forces cancel elastic forces with a phase lag of $\pi/2$. These pairs are the BBC by definition, resulting in an amplitude A dependent resonant frequency $\omega(A)$. On the same note, a $\sigma(A)$ function can be introduced to describe the attenuation dependency of the response amplitude, keeping the phase locked to $\pi/2$.

Figure 1 demonstrates the response amplitude-dependent functions introduced above and visualises isoli formation. Every response of a smooth dynamical system is somehow connected and can be traced back to a known trivial solution, including the mentioned isoli. In that sense, the proposed technique can predict and explain the formation of isoli from conventional frequency sweep measurements. Furthermore, it can approximate the unstable periodic orbits,

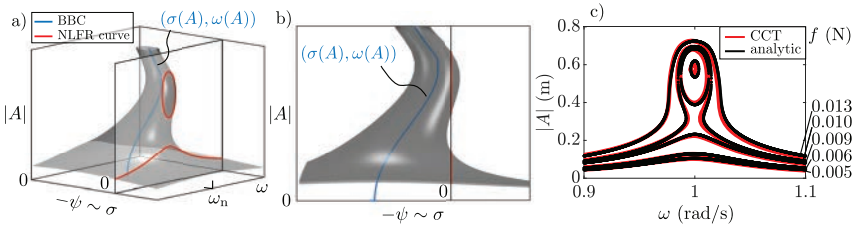

Figure 1: Visualisation of the nonlinear resonance in the space of local attenuation (σ) and frequency (ω) properties. Panels a) and b) show the formation of an isola by slicing the surface at zero corresponding damping. c) The NLFR curves, extracted from the surface.

resulting in complete NLFR curves.

First, we extend the definition of the backbone curve (BBC) [5] to account for nonlinear damping (Fig. 1 b) from the exclusively frequency-related description by defining a parametric BBC as $(\sigma(A),\omega(A))$. Then, the coordinate transformation proposition is demonstrated through the Lindstedt-Poincaré (LP) solution of the Duffing oscillator similar to [1] but for the damping in a Laplace-domain-like space (Fig. 1 a), instead of the frequency. This transformation enables the fitting of linear resonances to nonlinear ones and the ability to transform the fitted surfaces back to the nonlinear space, resulting in complete NLFR curves that capture the isoli. The methodology is numerically validated on the system used in [2], where the analytical solutions are available. The proposed method combined with the techniques in [1] results in a measurement procedure that can approximate unstable periodic orbits and (damping-related) isoli from conventional frequency-sweep measurements.

Model description

The nonlinear system used in this study for demonstrating the proposed transformation technique on a dissipative nonlinear resonance is taken from [2]. The mathematical formulation of this particular system can be written as

$$\ddot{x} + c_1\dot{x} + c_3\dot{x}^3 + c_5\dot{x}^5 = 2f\cos\omega t, \tag{1}$$

where x is the displacement, c_1, c_3, and c_5 are the dissipative terms, f and ω are the amplitude and angular frequency of the forcing, respectively. In [2], they

derive the following equation to extract the periodic solutions of (1).

$$(\omega - 1)^2 R = \frac{R}{256}\left(8c_1 + 6c_3 R + 5R^2\right)^2 - F = 0, \tag{2}$$

where $R = A^2$ is the squared corresponding response amplitude and $F = f^2$ is the squared forcing amplitude. The solutions with zero imaginary parts correspond to the NLFR curves for different forcing levels, which are shown by the black curves in Fig. 1 c).

Conclusion

The transformation of dissipative nonlinearities into a Laplace domain-like representation offers valuable insights into the formation of isolated resonances. By taking the section of the curved surface where the damping capacity is zero, we can derive the complete NLFR curves that characterize the vibrating system. This approach not only explains the conditions under which isolated resonances arise but also provides a visual tool for understanding the dynamic behavior of structures with dissipative nonlinearity.

References

[1] Z. Gabos and Z. Dombovari, "Novel identification technique through the coordinate transform of smooth nonlinear vibrating systems," *11th European Nonlinear Dynamics Conference 2024 (ENOC 2024)*, p. 305, 2024.

[2] G. Habib, G. I. Cirillo and G. Kerschen, "Isolated resonances and nonlinear damping," *Nonlinear Dynamics*, vol. 93, pp. 979–994, 2018. DOI: `https://doi.org/10.1007/s11071-018-4240-z`.

[3] Z. Gabos and Z. Dombovari, "Open-loop swept frequency response of nonlinear structures subjected to weak coupling," *Nonlinear Dynamics*, vol. 113, no. 6, pp. 5091–5108, 2025. DOI: `https://doi.org/10.1007/s11071-024-10546-6`.

[4] G. Kerschen, K. Worden, A. F. Vakakis and J.-C. Golinval, "Past, present and future of nonlinear system identification in structural dynamics," *Mechanical Systems and Signal Processing*, vol. 20, no. 3, pp. 505–592, 2006. DOI: `https://doi.org/10.1016/j.ymssp.2005.04.008`.

[5] D. Wagg, "Understanding the dynamics of multi-degree-of-freedom nonlinear systems using backbone curves," *Procedia Engineering*, vol. 199,

pp. 78–85, 2017, ISSN: 1877-7058. DOI: https://doi.org/10.1016/j.proeng.2017.09.157.

Acoustic fun facts

The loudest observed animal is the sperm whale, capable of emitting 223 dB SPL clicks (1 m, peRMS, re 1 µPa).

(Møhl, B., Wahlberg, M., Miller, L. A., Surlykke, A. & Madsen, P. T. (2000). Sperm whale clicks: Directionality and source level revisited. Journal of the Acoustical Society of America 107(1) 638-648.

In contrast, the loudest terrestrial animal (emitting airborne sound) is the howler monkey, with a peak SPL of 140 dB (1 m, re 20 µPa).

(Richard W. Thorington Jr. et al. (1984). Vocalizations of Howler Monkeys (Alouatta spp.). Journal of Mammalogy 65(2) 319-331.)

NVHH2025-0046

A theoretical study of diameter constraints in circular microphone array beamforming

B. Kocsis[1*], Cs. Horváth[1]

[1]Budapest University of Technology and Economics, Faculty of Mechanical Engineering, Department of Fluid Mechanics, Budapest, Hungary

[*]Corresponding author, e-mail: kocsis.balint@gpk.bme.hu

Summary

Acoustic microphone arrays and beamforming techniques are widely used for the analysis of rotating noise sources, such as those in turbomachinery. In this study, a circular microphone array is employed to investigate these sources, with a focus on the fundamental constraints of the measurement setup. The interdependent relationship between array diameter and measurement distance is examined, defining a theoretical measurement range. Two key limitations – spatial resolution and spatial aliasing – are identified, and practical formulas are derived to estimate the array diameter range for a given distance. These principles are demonstrated through a simple test case.

1. Introduction

The use of microphone arrays in combination with beamforming is a widely applied technique for obtaining not only the amplitude and spectral characteristics of noise sources but also their spatial location. The number and arrangement of microphones have a significant impact on the results. Among the various array geometries, the circular (or ring) arrangement is frequently employed, as it allows installation around ducts or free jets without disturbing the airflow [1]. Circular arrays are particularly well suited for the investigation of rotating noise sources [2]. The present study aims to determine the theoretical limits of the key parameters governing the measurement setup. The obtained theoretical range is then demonstrated through a simplified test case.

2. Theoretical limits of the measurement range

The theoretical measurement range is investigated through a simplified turbomachinery test case, shown in Fig. *3*. For any given turbomachinery, the rotor diameter is fixed. The most important parameters of the measurement setup are the diameter of the microphone array and the distance between the rotor and

the array in the axial direction. These two parameters are interdependent, i.e., variations in rotor-array distance result in changes in the range of array diameter, and vice versa.

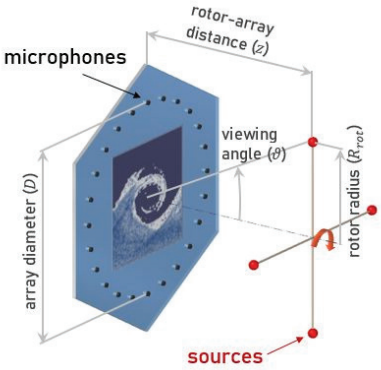

Figure 3. A simplified model of the turbomachinery measurements test case, investigated using a microphone array.

2.1 Limit resulting from the spatial resolution capabilities of a microphone array

Microphone arrays and beamforming techniques, like other imaging methods, are subject to limitations in spatial resolution. According to the Rayleigh criterion, the resolution ρ for on-axis incidence of spatially incoherent waves can be expressed as [3]:

$$\rho = \alpha_R \frac{z}{D} \lambda, \tag{3}$$

where z denotes the rotor-array distance, D is the array diameter, and λ is the wavelength of the incoming wave. The array geometry is accounted for by the shape factor α_R, which takes a value of approximately 1.22 for a circular array. This formulation is applicable to the test case illustrated in Fig. *3*, providing a lower limit for the microphone array diameter range.

2.2 Limit resulting from spatial aliasing on beamforming maps

Due to the discrete sampling of incoming acoustic waves, the issue of spatial aliasing arises. According to the Nyquist criterion, spatial aliasing can be avoided if the spacing between adjacent microphones does not exceed $\lambda/2$ [4]. By narrowing the field of view ϑ from the full angular range of $|\pm\pi/2|$ to the region encompassing the actual noise sources $|\pm\vartheta_s|$ (see Fig. *3*), aliasing can be avoided under the condition:

$$|\Delta x \sin(\vartheta_s)| < \lambda/2 \tag{4}$$

where Δx is the distance between two neighboring microphones. By expressing Δx and ϑ_s in terms of the array diameter D, the rotor-array distance z, and the radius of the sources' path R_{rot}, this criterion can be adapted to the test case under consideration. It thereby provides an upper limit on the microphone array diameter range for a fixed number of microphones.

2.3 Determination of the theoretical measurement range of the microphone array diameter with respect to the rotor-array distance

After substitutions and expressions from Eq. (3) and (4), the array diameter D has the following theoretical range:

$$\frac{\alpha_R \frac{z}{R_{rot}}}{2\sin\left(\frac{\pi}{N}\right)}\lambda < D < \frac{\sqrt{\left(\frac{z}{R_{rot}}\right)^2+1}}{2\sin\left(\frac{\pi}{M}\right)}\lambda \tag{5}$$

where N is the number of evenly distributed sources, and M is the number of microphones. The theoretical measurement range is visually presented in Fig. 4.

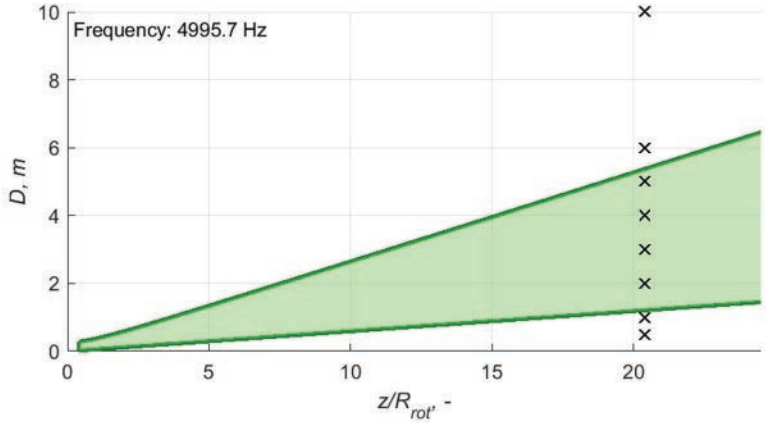

Figure 4. The theoretical measurement range of a circular array of 24 microphones, for a frequency of 4995.7 Hz

The green area shows the ideal range of the array diameter with respect to the rotor-array distance. Although the diameter value is frequency-dependent, the characteristics of the diagram remain invariant with respect to frequency. The measurement distance is normalized by the rotor radius R_{rot}. A lower limit has

also been shown for the measurement distance based on the constraint that the microphones would be in the acoustic far-field of the sources, that is [5]:

$$kz \gg 1 \tag{6}$$

where $k = 2\pi/\lambda$ is the wavenumber.

3. Demonstration of the theoretical measurement range

Fig. *5* presents a series of synthetic beamforming results that demonstrate the effectiveness of the derived formulas. The configuration of the test case is shown in Fig. *3*. Four incoherent simple point sources (marked by black squares in the images) emit white noise while rotating around the center of the image at a radius of $0.245\,m$ and a rotational speed of $50\,rot/s$. The trajectory of the sources is indicated by a black circle in the images. The propagation of the sound is modelled analytically by the convected wave equation [6]. The microphone array, consisting of 24 microphones, is positioned axially aligned with the rotational axis at a distance of $5\,m$ from the rotational plane. For each case, a $30\,s$ recording has been taken at a sampling rate of $44100\,Hz$. Signal processing has been performed using the Virtually Rotating Array (VRA) beamforming algorithm [2], which compensates for the rotational motion of the sources, causing them to appear stationary in the beamforming output. The beamforming code has been implemented in-house and has been employed in other studies conducted by our research group [1,7]. The recorded signals have been processed and analysed for multiple frequency bins, but here only a single frequency bin, centered at $4995.7\,Hz$, is presented. The beamforming results have been computed on a 121×121 point grid, uniformly distributed over an area of $1\,m \times 1\,m$. Beamforming results are considered accurate if they exhibit high amplitudes near the true source locations and low amplitudes elsewhere. In this investigation, the array diameter has been systematically varied. The selected diameters, indicated by black ×-marks in Fig. 4, include two values below and two above the theoretical optimal range, with four values within it. In Fig. *5*, the corresponding array diameters are noted in the top-left corner of each image. In order to provide a clearer representation of both the peak amplitudes and the sidelobe structure, the results are presented over a broad dynamic range of $15\,dB$.

Examining the results at $D = 0.5\,m$ and $D = 1\,m$ reveals the effects of spatial resolution. In these cases, the noise sources are either not resolved or only partially separated, making them difficult to distinguish. This observation aligns with the theoretical lower limit of $1.21\,m$ estimated by the derived formula. In

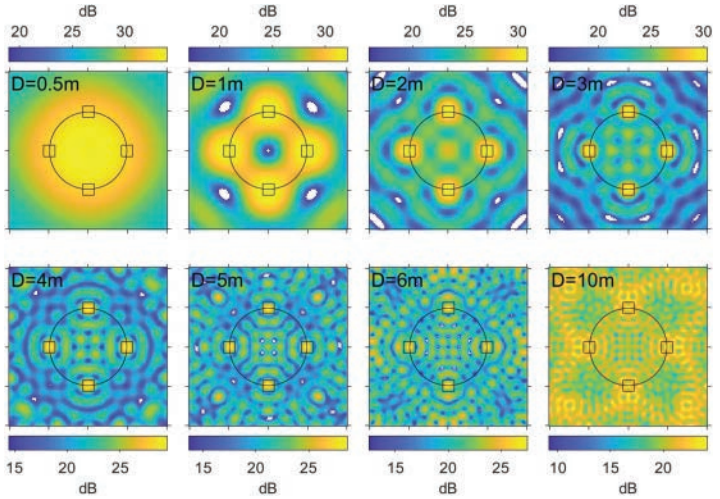

Figure 5. Beamforming results of four rotating point sources emitting white noise, evaluated at 4995.7 Hz.

contrast, the subsequent four beamforming maps – corresponding to $D = 2\,m$, $3\,m$, $4\,m$, and $5\,m$ – successfully localize the noise sources and exhibit a mainlobe-to-sidelobe ratio of at least several dB in the vicinity of each source. However, at $D = 5\,m$, high sidelobe levels are observed in the four corners of the map. While these sidelobes are somewhat removed from the region of interest around the rotor, they are undesirable. This effect becomes more pronounced at $D = 6\,m$, consistent with the theoretical upper limit of $5.38\,m$. The degradation continues at $D = 10\,m$, where the beamforming output no longer displays distinct peaks at the true source locations, further confirming the validity of the derived theoretical limits.

4. Conclusions

In this study, the limits of circular microphone arrays for measuring rotating noise sources have been examined. For a simplified turbomachinery test case, the interdependent limits of microphone array diameter and rotor-array distance have been derived theoretically, based on the constraints imposed by spatial resolution and spatial aliasing. The theoretical estimations have then been validated through beamforming results obtained across a wide range of array diameters at a given measurement distance. The findings confirm that the range identified as optimal through examining the beamforming maps closely aligns with the range estimated by the derived formulas. This agreement supports the

practical applicability of the theoretical measurement range for guiding the design of measurement setups employing circular microphone arrays for rotating noise sources.

Acknowledgements

This project has been partially supported by the European Union and the Hungarian Government in the framework of Competitive Central-Hungary OP (Project ID: VEKOP-2.3.3-15-2017-00017). Project no. 143204 has been implemented with the support provided by the Ministry of Innovation and Technology of Hungary from the National Research, Development and Innovation Fund, financed under the OTKA K 22 funding scheme. Project no. TKP-6-6/PALY-2021 has been implemented with the support provided by the Ministry of Culture and Innovation of Hungary from the National Research, Development and Innovation Fund, financed under the TKP2021-NVA funding scheme. This project was supported by the János Bolyai Research Scholarship of the Hungarian Academy of Sciences.

References

[1] B. Lendvai, T. Benedek, "Experimental and numerical investigation of the blade tip-related aeroacoustic sound source mechanisms of a ducted low-speed axial flow fan," *Applied Acoustics*, vol. 215, 2024, 109705, https://doi.org/10.1016/j.apacoust.2023.109705

[2] G. Herold, E. Sarradj, "Microphone array method for the characterization of rotating sound sources in axial fans," *Noise Control Engineering Journal*, vol. 63, no. 6, pp. 546-551, 2015, https://doi.org/10.3397/1/376348

[3] J. J. Christensen, J. Hald, "Beamforming," BV0056, Brüel & Kjær Technical Review No. 1, 2004.

[4] D.H. Johnson, D.E. Dudgeon, "Array Signal Processing: Concepts and Techniques," Prentice Hall, Englewood Cliffs, New Jersey, 1993, pp. 77-80.

[5] L. E. Kinsler, A. R. Frey, A. B. Coppens, J. V. Sanders, "Fundamentals of Acoustics," Wiley, New York, 1982, pp. 157-159.

[6] P. Sijtsma, S. Oerlemans, H. Holthusen, "Location of rotating sources by phased array measurements," 7th AIAA/CEAS Aeroacoustics Conference and Exhibit, Maastricht, Netherlands, 2001, https://doi.org/10.2514/6.2001-2167

[7] B. Kocsis, Cs. Horváth, "Further Development of Rotating Beamforming Techniques Using Asynchronous Measurements," *Journal of Theoretical and Computational Acoustics*, vol. 32, no. 1, 2024, http://www.doi.org/10.1142/S2591728523400066

NVHH2025-0049

Periodic tail stock pressure modulation in turning of flexible workpiece via piezoelectric actuators

K. Martinovich[1*], D. Bachrathy[1,2]

[1]Budapest University of Technology and Economics,
Department of Applied Mechanics, Budapest H-1111, Hungary
[2]MTA-BME Lendület Machine Tool Vibration Research Group, Budapest
University of Technology and Economics, Budapest H-1111, Hungary
[*]Corresponding author, e-mail: martinovich@mm.bme.hu

Summary

The machining of slender workpieces poses great challenges as it is prone to harmful self-excited vibrations. We propose a feasible control strategy through periodic excitation and optimisation of control parameters to avoid these unstable situations.

Introduction

In manufacturing, the pursuit of greater productivity often leads to chatter vibration, which may ruin the workpiece or damage the tool. To suppress the harmful vibrations of slender workpieces, a few approaches exist in the literature, such as intricate simultaneous machining with multiple tools, using robotic support or advanced control strategies [1]. The well-known spindle speed variation utilises periodic excitations, but it is limited within the control range. A similar but mostly theoretical concept is the stiffness variation [2] with limited laboratory experiments only. We propose its realistic implementation by means of a piezo stack actuator compressing the tailstock of the lathe. By optimising the control, we can maximise the stable operational parameter domain.

Methodology

We investigate the traditional single degree-of-freedom delayed turning model shown in Figure 1, which is extended by parametric excitation, yielding a linear time-periodic delay-differential equation

$$\begin{aligned}\ddot{y}(t)+2\zeta(t)\omega_{\mathrm{n}}(t)\dot{y}(t)+\omega_n(t)^2y(t)\\ =\frac{K_{\mathrm{c,y}}w}{m(t)}(h+y(t-\tau)-y(t)),\end{aligned} \tag{1}$$

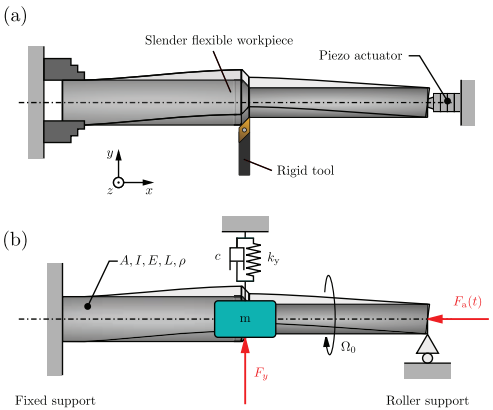

Figure 1: In panel (a) schematic diagram of the turning process of a slender workpiece with periodic tailstock compression, in panel (b) the corresponding one degree-of-freedom mechanical model.

where the parameters are the cutting coefficient $K_{c,y}$, chip width w and chip thickness h. Moreover, the time-periodic parameters according to [2] are the damping ratio $\zeta(t)$, modal mass $m(t)$ and the natural frequency $\omega_n(t)$. Considering the bending vibration of an axially loaded slender beam, the natural frequency reads as

$$\omega_n(t) = \omega_{n,0}\sqrt{1 - \frac{F_a(t)}{F_{a,cr}}}, \tag{2}$$

where $\omega_{n,0}$ is the natural angular frequency of the unloaded workpiece, F_{cr} is the critical axial load of buckling and $F_a(t)$ is the applied periodic axial excitation. Taking into account the application of the piezo actuator, two limit cases exist [3]. If the piezo actuator works against a spring with negligible stiffness, the elongation will be close to the nominal displacement. On the contrary, if the spring stiffness can be considered infinite, the achievable force is close to the blocking force. In this application, the machine's structure in the longitudinal direction k_s, the piezo stack k_p, and the workpiece k_w are built in series. Hence, the achievable force acting on the tailstock of the workpiece can be calculated as

$$F_a = F_p(u)\frac{k_w k_s}{k_s k_p + k_w k_p + k_w k_s} \tag{3}$$

where $F_p(u)$ is the voltage-controlled force of the piezoelectric actuator. We formulate the optimisation of the control parameters by minimising the critical

Floquet multiplier μ_i, which has the largest absolute value, determining the stability of the system

$$\underset{F_\mathrm{a}}{\operatorname{argmin}} \max_{i} \mu_\mathrm{i} \tag{4}$$

considering the periodic force pattern (sinusoidal, triangular, trapezoidal etc.), amplitude and frequency ω. The system in (1) is linear with nonlinear time-periodic excitation. Its linear stability can be directly calculated by the semi-discretisation method [4] or with a more efficient implicit subspace iteration method [5], [6]. The stability charts are showcased for different excitation patterns at two different levels of force amplitude in Figure 2. As the force amplitude is increased, the stable region is shifted and increased which is greatly influenced by the excitation pattern.

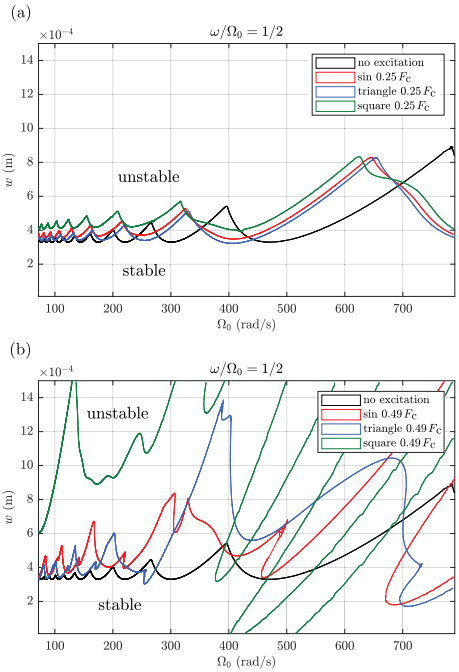

Figure 2: Stability diagram for different tailstock compression patterns: without excitation (black), sinusoidal (red), triangle (blue) and square (green) waveforms with excitation frequency ω half of the spindle speed Ω_0. In panel (a) the amplitude of the waveforms is 25 % of the buckling force, In panel (a) the amplitude of the waveforms is 49 % of the buckling force.

Conclusion

We investigated a feasible implementation of periodic tailstock excitation by means of piezoelectric actuators. We present an effective optimisation of the control parameters by minimising the Floquet multipliers, hence enlarging the stable domain of operational parameters.

Acknowledgements

This project was supported by the Doctoral Excellence Fellowship Programme (DCEP) is funded by the National Research Development and Innovation Fund of the Ministry of Culture and Innovation and the Budapest University of Technology and Economics Hungarian National Research, Development and Innovation Office (NKFI-KKP-133846 and FK-138500).

References

[1] G. Stepan, A. K. Kiss, B. Ghalamchi, J. Sopanen and D. Bachrathy, "Chatter avoidance in cutting highly flexible workpieces," *CIRP Annals*, vol. 66, no. 1, pp. 377–380, 2017.

[2] B. Beri, G. Meszaros and G. Stepan, "Machining of slender workpieces subjected to time-periodic axial force: Stability and chatter suppression," *Journal of Sound and Vibration*, vol. 504, p. 116 114, 2021, ISSN: 0022-460X.

[3] *Piezoelectric actuators: Components, technologies, operation*, Catalog CAT128E, Physik Instrumente (PI) SE & Co. KG, 2025.

[4] T. Insperger and G. Stepan, "Semi-discretization method for delayed systems," *International Journal for numerical methods in engineering*, vol. 55, no. 5, pp. 503–518, 2002.

[5] M. Zatarain, J. Alvarez, I. Bediaga, J. Munoa and Z. Dombovari, "Implicit subspace iteration as an efficient method to compute milling stability lobe diagrams," *The International Journal of Advanced Manufacturing Technology*, vol. 77, pp. 597–607, 2015.

[6] K. Martinovich and D. Bachrathy, "Szimuláció alapú stabilitásvizsgálat állapotfüggő időkésésű modellekben: Simulation based stability analysis in state-dependent delay models (in hungarian)," *Nemzetközi Gépészeti Konferencia–OGÉT*, pp. 252–257, 2024.

NVHH2025-0051

Effect of connection hose on centrifugal coolant pump vibration results

Cs. Báthory[1*], L. Szalma[1]

[1]Robert Bosch Energy and Body System Kft.
Test Center, Miskolc, Hungary

[*]Corresponding author, e-mail: csongor.bathory@hu.bosch.com

Summary

Circulation pumps used in automotive applications are evaluated for NVH (Noise, Vibration, and Harshness) criteria within a closed-loop system filled with a coolant medium. The pump samples should be suspended using elastomer strings attached to hoses. The standard test setup includes differential pressure sensor adapters and safety valves on both the inlet and outlet hoses. The additional weight and bending stiffness of the hoses can significantly influence the stiffness and damping characteristics of the test system. To examine the impact of the connection hoses, a comparison was made between a standard setup, a setup utilizing a smaller diameter EPDM (Ethylene Propylene Diene Monomer) hose and one using a silicone hose. The structure-borne noise results reveal significant differences in the nominal orders of the tested pumps at maximum operational speed. Transfer functions further confirm the variations caused by hoses of differing diameters and materials.

Introduction

In the automotive industry, noise requirements have become increasingly stringent in recent years, with the rise of quieter powertrains such as hybrid or electric motors compared to internal combustion engines [1]. One of the key areas of this concern is the circulation pumps that circulate the coolant for the high-performance batteries built into cars. They must perform this task not only while driving, but also when stationary and charging, which means that there is practically no other source of noise from the car, so the noise emissions of the pump are receiving more attention [2]. A customer informed us, that their measurement result is different from ours, the 2nd and 3rd order noise values of acceleration sensor response are higher than their values. Based on customer feedback, the direction of investigation did go to reduce the system mass and use hoses with lower stiffness. The study focused on examining the effect of the

hose section connected to the pump, comparing the acceleration sensor's octave, FFT (Fast Fourier Transform) analysis and check the mass-line fluctuation between 150 and 500 Hz of the modal analysis FRF (Frequency Response Function) results.

Materials and Method

A centrifugal coolant pump was measured within a closed-loop system filled with a coolant medium. The pump sample was suspended using elastomer strings attached to hoses. Three kind of setups were tested with different hose types. The Standard test setup included differential pressure sensor adapters and safety valves on both the inlet and outlet hoses with a 35 mm outside diameter hose from EPDM material. The Type1 test setup was designed without differential pressure sensor adapters and safety valves with a 26 mm outside diameter hose from EPDM material. The Type2 test setup was designed also without additional weight like differential pressure sensor adapters and safety valves, and the 25 mm outer diameter hose's material was silicone. See the detailed parameters of setup types in Tab. 1*Table 1*. The removal of the differential pressure sensor adapter and safety valves significantly reduced the nominal weight of the connection hose.

Table 1. Measurement setup parameters

Parameter	Standard	Type1	Type2
Material	EPDM	EPDM	Silicone
Differential pressure sensor	With	Without	Without
Outside Diameter [mm]	35	26	25
Inside Diameter [mm]	24	17	19
Wall thickness [mm]	5,5	4,5	3
Bending Stiffness [N/mm]	490	380	220
Nominal weight [g/m]	1570	433	330

A triaxial acceleration sensor (sensitivity: 10 mV/g) was hot glued to the pump sample motor side as Fig. 1 shows. The pump was operated at maximum nominal speed (5360 RPM), operation point was set to 720 l/h and data was collected for 10 seconds. The customer feedback suggested to focus on to the 2^{nd} (180 Hz) and 3^{rd} (270 Hz) order, but from the sample hydraulic and motor topology the 6^{th} (535 Hz) and 7^{th} (625 Hz) order was also included in the FFT

analysis. Modal test was made for detecting the resonance differences of the setup types with an impact hammer. Sample was knocked five times from each direction and averaged their data in the FRF analysis.

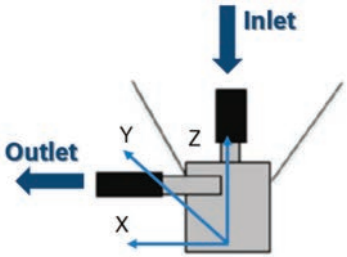

Figure 6. Triaxial acceleration sensor position

Results

The results were calculated with HEAD Acoustics ArtemiS SUITE software. FFT average analysis was made with Hanning window function, 4096 spectrum size and 50% overlapping. The results are presented in the range between 140 and 700 Hz as the study is focusing on this area. FFT average diagram of direction Y (Fig. 2.) indicates with blue arrows the order peaks.

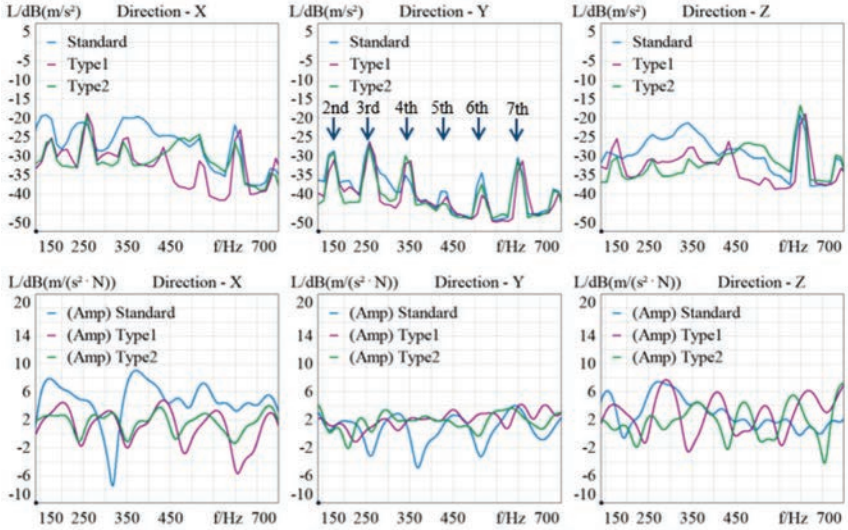

Figure 7. FFT average and FRF results of three setup type, separated by directions. Order numbers are displayed in the FFT average direction Y diagram

FFT results of Standard setup shows higher 2nd, 4th and 5th order in direction X, higher 3rd and 4th order in direction Z. In direction Y 6th order stands out compared to the Type1, but 4th order is lower than Type1 or Type2. Type1 order peaks are close to Type 2 except 5th and 6th in direction X, 6th in direction Y and direction Z, which are lower than Type2. It shows the highest 2nd order in direction Z and between 2nd, 3rd and 4th orders side orders are visible in all three directions.

FRF result shows anti-resonance at 315 Hz in direction X of Standard setup which is more than 10 dB fluctuation between 150 and 500 Hz. Type1 and Type2 shows more stable function, Type1 fluctuation is below 5 dB in direction Y, Type2 is below 5 dB in direction X, but Type1 is over 10 dB in direction Z, while Type2 is around 7 dB, same as Standard.

Conclusion

The modified test setups resulted in a reduction of the main order peaks compared to the standard configuration, which exhibited an anti-resonance at 315 Hz and significant mass-line fluctuations between 150 and 500 Hz. The reduction in mass and the use of alternative hose materials introduced greater damping into the system, as confirmed by the FRF results. Among the tested configurations, the silicone hose—with the lowest bending stiffness—showed the smallest mass-line fluctuations in the X and Z directions. In the Y direction, the smaller-diameter EPDM hose demonstrated the best performance. Type1 setup type shows lower 6th order level in FFT results, but Type2 eliminated the elevated vibration level between the 2nd, 3rd and 4th orders. The introduction of a new test setup still requires further testing, and discussion, since in Type1 and Type2 the differential pressure values and safety options are missing.

References

[1] J. Masri et al., “A survey of modern vehicle noise, vibration, and harshness: A state-of-the-art,” Ain Shams Engineering Journal, Volume 15, Issue 10, ISSN 2090-4479, 2024

[2] A. Alawi et al., “A Comprehensive Review of Thermal Management Challenges and Safety Considerations in Lithium-Ion Batteries for Electric Vehicles”, Batteries, Volume 11, Issue 7, Article number 275, ISSN 2313-0105, 2025

NVHH2025-0054

The effect of slowly varying zeroth order directional factor in the circular milling of a single degree of freedom flexure

A. Bartfai[1,2*], Z. Dombovari[1,2]

[1]Department of Applied Mechanics, Faculty of Mechanical Engineering,
Budapest University of Technology and Economics,
Műegyetem rkp. 3. H-1111 Budapest, Hungary

[2]MTA-BME Lendület Machine Tool Vibration Research Group,
Department of Applied Mechanics,
Budapest University of Technology and Economics,
H-1521 Budapest, Hungary

[*]Corresponding author, e-mail: andras.bartfai@mm.bme.hu

Summary

A circular milling test with slowly varying zeroth order (mean) directional factor is modelled, where crossing from positive to negative mean directional factor results in dynamic stability loss of the governing delay differential equation. However, there is a considerable lag at the point of onsite of high amplitude oscillations after crossing to the asymptotically unstable boundary. An approximate analytical solution of the slowly varying system is given by the WKB method. This is then compared to different numerical schemes highlighting the arising inaccuracies due to the accumulation of numerical errors.

1. Introduction

Machining with industrial robots has a growing interest in industrial application [1]. Although, using robots is beneficiary to reduce the price of machining compared to ordinary machine tools, this arrangement is prone to low frequency, high amplitude chatter vibrations [2], destroying surface quality and tool life. In case of low frequency dominant robotic modes and high speed of revolution, there is an extreme difference between positive and negative mean directional factor (MDF) stability losses, where negative MDF severely limits the maximum achievable stable depth of cut [3]. A single degree of freedom test is simulated with circular path milling, having continuously changing MDF of the dominant mode. Dynamical systems with slowly varying parameters are known

to have a considerable lag of reaching high amplitude oscillations after crossing the asymptotic stability limit [4]. This study focuses on the presence of delayed stability loss due to a slow cross from positive to negative MDF zone, causing dynamic stability loss in robotic milling applications.

2. Mathematical model of circular milling experiment

We consider a milling process with evenly spaced and Z number of teeth rotating with constant spindle speed Ω (Hz). Then, the resulting tooth passing, here the principal, period is given as $T_1 := T_Z = 1/(\Omega Z)$. Linearizing structural dynamics and cutting force around the stationary solution $\mathbf{x} = \overline{\mathbf{x}} + \mathbf{u}$ and transforming into the modal domain by $\mathbf{u} := \mathbf{P}\mathbf{q}$ gives the system of variational delay differential equation

$$\ddot{q}_j(t) + 2\zeta_j \omega_{\mathrm{n}j} \dot{q}_j(t) + \omega_{\mathrm{n}j}^2 q_j(t) = \frac{aZK_{\mathrm{ct}}}{2\pi M_j \sin\kappa} \sum_{k=1}^{n} \beta_{j,k}(t)(q_k(t-\tau) - q_k(t)), \quad (1)$$

where $[\beta_{j,k}(t)]_{j,k} := \boldsymbol{\beta}(t) = \mathbf{P}^{\mathsf{T}} \boldsymbol{\alpha}(t) \mathbf{P}$ defines the directional factor matrix in the modal coordinate system and $\boldsymbol{\alpha}(t)$ is the spatial directional factor matrix. The time delay is given by $\tau = T_1$.

The developed flexure has a single dominant mode, which means that the main dynamic behavior can be accurately represented in a single equation. High tooth passing frequency relative to the natural frequency of the mode enables zero-order approximation (ZOA), replacing the directional factor $\boldsymbol{\beta}(t)$ by its temporal mean $\boldsymbol{\beta}_0$ w.r.t. the fast (rotary) time. Finally, in the high speed of revolution range, the time delay τ is tiny; therefore the delayed state is approximately $q(t-\tau) \approx q(t) - \tau\dot{q}(t)$ by first order Taylor expansion [5], arriving to the final ODE form.

$$\ddot{q}(t) + \left(2\zeta\omega_{\mathrm{n}} + \frac{aZK_{\mathrm{ct}}\beta_0}{2\pi M \sin\kappa}\tau\right)\dot{q}(t) + \omega_{\mathrm{n}}^2 q(t) = 0. \quad (2)$$

The flexure dominant mode has a simple geometric mode shape vector in the form $\mathbf{P}_1(\theta) := \begin{bmatrix}\cos(-\theta) & \sin(-\theta) & 0\end{bmatrix}^{\mathsf{T}}$, where the rotation $-\theta$ represents a rotation in the feed direction to the workpiece by θ. Considering $\kappa = \pi/2$ lead

angle, the mean directional factor is computed as

$$\begin{aligned}\beta_0 = \frac{1}{4}(&2\sin(2\theta-\varphi_{\text{en}}-\varphi_{\text{ex}})\sin(\varphi_{\text{en}}-\varphi_{\text{ex}})-\kappa_{\text{cr}}(2\varphi_{\text{en}}-2\varphi_{\text{ex}}\\&+\sin(2(\theta-\varphi_{\text{en}}))-\sin(2(\theta-\varphi_{\text{ex}})))).\end{aligned} \tag{3}$$

In the circular milling scenario the angle describing mode direction varies in time as $\theta(t) = 2Zf_z\Omega t/d$ (rad) and the time period of passing a full circle is $T_2 = d\pi/(Zf_z\Omega)$, where f_z is the feed per tooth and d is the diameter of the circular milling process. This results in a time varying mean directional factor $\beta_0(\theta(t))$ along the circular path.

3. Approximate solution of the time varying model

Introducing the slowly varying time as $s = \varepsilon t$, where $\varepsilon := f_z/d \ll 1$ gives a system with time varying parameters by considering $\beta_0 \to \beta_0(s)$ in (2). An approximate solution can be given using the zeroth order WKB method [6], which results in the fundamental solutions

$$x_1 = \exp(\sigma_1(s)/\varepsilon),\ x_2 = \exp(\sigma_2(s)/\varepsilon), \tag{4}$$

where

$$\sigma_1(s) = \int_0^s \lambda_1(\xi)\,\mathrm{d}\xi,\ \sigma_2(s) = \int_0^s \lambda_2(\xi)\,\mathrm{d}\xi, \tag{5}$$

while $\lambda_{1,2}(s)$ are the frozen-time eigenvalue functions. These eigenvalue functions can be calculated exactly for the single degree of freedom case; however, generally it cannot be obtained and integrating them are not a simple task. Therefore, curve fitting is applied here in the form

$$\operatorname{Re}\lambda_{1,2}(s) \approx A + B\sin(Cs+D), \tag{6a}$$

$$\operatorname{Im}\lambda_{1,2}(s) \approx \pm(A_0 + A_1\sin(ws+\vartheta_1) + A_2\sin(2ws+\vartheta_2)), \tag{6b}$$

which approximates the original eigenvalue functions accurately.

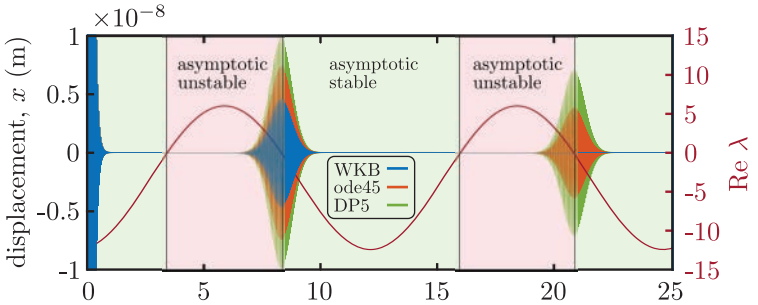

Figure 1: Analytical and numerical simulations of the circular milling operation with diameter $d = 0.4$ m. The numerical simulations are not accurate compared to the analytical solution, while they are also not consistent with each other. Initial conditions: $x_0 = 10^{-6}$ m, $\dot{x}_0 = 0$.

4. Comparing analytical and numerical solutions

The analytical solution is compared to two different numerical schemes: Matlab's ode45 and Julia's DP5. For both methods, relative tolerance of 10^{-13} m and absolute tolerance of 10^{-16} m were used. The modal parameters of the flexure dominant mode was obtained by means of modal testing resulting in

$$\omega_\mathrm{n} = 23.09 \text{ Hz}, \ \zeta = 0.097 \ \%, \ M = 206.57 \text{ kg}. \tag{7}$$

The parameters of the milling process was chosen as

$$\begin{aligned} &Z = 3, \ \kappa = \pi/2, \ a = 10 \text{ mm}, \ K_\mathrm{ct} = 774 \text{ MPa}, \ \Omega = 10000 \text{ rpm}, \\ &\varphi_\mathrm{en} = 0, \ \varphi_\mathrm{ex} = \pi/2, \ f_\mathrm{z} = 0.1 \text{ mm/tooth}, \end{aligned} \tag{8}$$

while two different circular path diameters were simulated in Fig. 1(a) $d = 0.4$ m; (b) $d = 0.5$ m.

Earlier studies showed that there can be a large discrepancy between numerical and analytical solutions, when ε is small (i.e. the solution time interval is large) [4], [7], due to the accumulation of numerical errors. Therefore either decreasing f_z or increasing d makes the performance of numerical solutions poorer. This is verified in Fig. 1, a large circular diameter results in significant differences of the numerical solutions compared to the analytical results. This highlights the importance of semi-analytical solutions in dynamical systems with time varying

parameters and high frequency oscillations.

The simulations show that there is a considerable lag in the asymptotically unstable zone to reach high amplitude oscillations e.g. compared to the initial condition.

5. Conclusions

An approximate analytical solution was obtained by means of the WKB solution for the circular milling operation with slowly varying mean directional factor. This was compared to two different numerical schemes with high precision settings for increasing simulation time intervals by means of circular path diameters. The numerical results showed large discrepancies compared to the analytical solution. Furthermore, the lag effect of reaching high amplitude oscillations after dynamic stability loss was also verified.

References

[1] M. Hagele, "Robots conquer the world [turning point]," *IEEE Robotics & Automation Magazine*, vol. 23, no. 1, pp. 120–118, 2016.

[2] A. Verl, A. Valente, S. Melkote *et al.*, "Robots in machining," *CIRP Annals*, vol. 68, no. 2, pp. 799–822, 2019.

[3] Z. Dombovari, I. Laka, A. Bartfai *et al.*, "Directional factor as the key for chatter free robotic milling of light alloys," *submitted*,

[4] S. M. Baer, T. Erneux and J. Rinzel, "The slow passage through a hopf bifurcation: Delay, memory effects, and resonance," *SIAM Journal on Applied Mathematics*, vol. 49, no. 1, pp. 55–71, 1989.

[5] T. Insperger, "On the approximation of delayed systems by taylor series expansion," *Journal of Computational and Nonlinear Dynamics*, vol. 10, no. 2, p. 024 503, 2015.

[6] C. M. Bender and S. A. Orszag, *Advanced mathematical methods for scientists and engineers I: Asymptotic methods and perturbation theory*. Berlin, Germany: Springer Science & Business Media, 1999, vol. 1.

[7] A. Bartfai, E. F. Ponce-Vanegas, S. J. Hogan, R. Kuske and Z. Dombovari, "Semi-analytical framework for the computation of finite-time stability of forced dynamical systems with slowly varying parameters and high frequency oscillations," *submitted*,

MÜLLER-BBM

Müller-BBM Industry Solutions is your Partner for NVH Engineering Services and Software Products

Our Services

- Experimental modal analysis (EMA)
- Operational vibration analysis (OVA)
- Operational transfer path analysis (OTPA)
- Panel-Contribution-Analysis (PCA)
- Rotary oscillation analysis
- Array measurement technology
- Intensity measurement technology
- Blocked Forces Testing
- Numerical Simulation

Applications in

- Automotive
- Ship and Offshore
- Aerospace
- Railway, Rail Vehicles

Sales, Support and Consulting
Müller-BBM Industry Solutions GmbH
Johannes Guggenberger
Helmut-A.-Müller-Straße 1 – 5
82152 Planegg
info@mbbm-ind.com
Phone +49 89 85602-241
www.mbbm-ind.com

Software Products

FEMtools

FEMtools is a multi-functional family of CAE software to integrate simulation and test.

- Structural Dynamics Toolbox
- Pretest Analysis
- Experimental Modal Analysis (EMA)
- Correlation Analysis
- Sensitivity Analysis
- Model Updating
- Optimization

DDS Dynamic Design Solutions

ME'scope

ME'scope is a universal toolbox for the test engineer

- Evaluation of Test Data
- Operational Deflection Analysis
- Experimental Modal Analysis
- Shape Animation

VIBRANT

NVHH2025-0057

Logarithmic frequency scale filter design using fixed-pole parallel filters

Balázs Bank[1*]

[1]Budapest University of Technology and Economics,
Department of Artificial Intelligence and Systems Engineering, Budapest, Hungary
[*]Corresponding author, e-mail: bank@mit.bme.hu

Summary

In the field of acoustic and audio signal processing the performance of an application is often evaluated based on the perceptual user experience. Therefore, it is important that such signal processing algorithms take into account the properties of the human auditory system. One such property is the logarithmic frequency resolution of the human ear. This case study demonstrates how fixed-pole parallel filters can be efficiently used for logarithmic frequency resolution filter design and compares their performance to traditional FIR and IIR filter design methods. The application examples in the presentation will include the modeling and equalization of a loudspeaker response and the modeling and equalization of a room response.

Introduction

Digital signal processing plays an important role in today's audio applications. One of the most commonly used forms of such processing is the application of digital filters. These can be used to limit the frequency content of the signal (e.g. to cut out unwanted low frequencies or to split the frequency band as required for crossover filters in loudspeaker systems), leading to classic low-pass, high-pass, band-pass or band-reject filters [1], [2]. However, digital filters can be used to approximate any specified frequency response, thus, they can be used to model or to compensate any linear system. In the field of audio, such applications include the compensation of the frequency response inaccuracies of headphones, loudspeakers, entire PA systems, room responses, or a car audio system.

In audio or acoustic signal processing, often we would like to optimize the perceived quality at the given computational resources. One common practice to

achieve this is to evaluate the frequency response of audio systems in a logarithmic scale, since this approximates the quasi-logarithmic frequency resolution of human hearing [3].

Design algorithms for FIR (Finite Impulse Response) or IIR (Infinite Impulse Response) filters are covered in almost all digital signal processing textbooks [1], [2]. However, these general-purpose design techniques minimize the error (approximate the target response) in a linear frequency scale, and it seems that they cannot be easily modified to lead to logarithmic frequency resolution. The reason can be easily understood for FIR filters, where the frequency response of the filter corresponds to the DFT (Discrete Fourier Transform) of the filter coefficients. Since the frequency resolution of the DFT is linear, so is the frequency resolution of the FIR filter. In theory, IIR filters could have an arbitrary resolution due to the fact that pole locations can be chosen freely, however, logarithmic frequency resolution would require such a high pole density at low frequencies that cannot be achieved traditional IIR filter design methods (e.g., Prony or Steiglitz-McBride) [4], [5].

This is demonstrated in Fig. 1, where it is clear that the modeling accuracy is unevenly distributed in logarithmic scale and even the $N = 300$ order filters cannot model the measured room response (thin line) at low frequencies.

Therefore special filter structures and design methodologies have been developed to achieve logarithmic frequency resolution. The most common options are frequency warping [6], Kautz filters [7] and fixed-pole parallel filters [8]. An overview and comparison of these techniques can be found in [5], [9], demonstrating the benefits of fixed-pole parallel filters above the other two methods. Therefore this case study will concentrate on highlighting the key properties of fixed-pole parallel filters.

Fixed-pole parallel filters

Parallel second-order sections have been traditionally used for their better numerical properties, and the coefficients are converted from direct form IIR filters. However, the key idea of fixed-pole parallel filters is that the poles of the second-order sections are fixed (predetermined), and only the numerator coefficients are optimized during filter design [5], [8], [9]. It turns out that by doing this, we gain complete control over the frequency resolution of the design: e.g., by setting the pole frequencies according to a logarithmic scale, logarithmic frequency resolution filters can be designed.

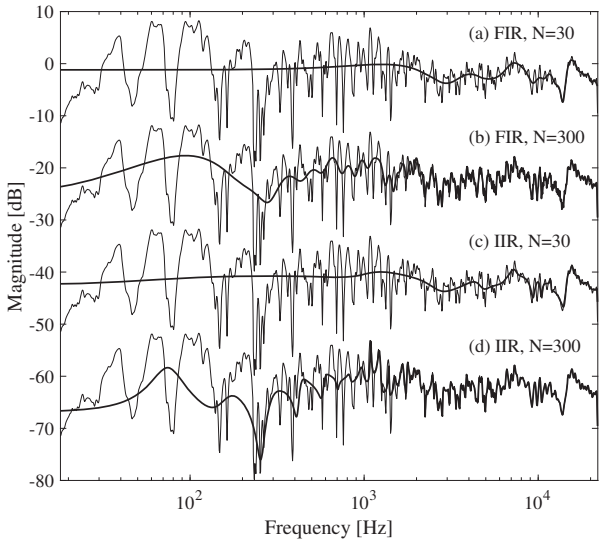

Figure 1: Modeling a room response by FIR and IIR filters. The filter order is marked by N. The target response is displayed by a thin line while the filter responses by thick lines.

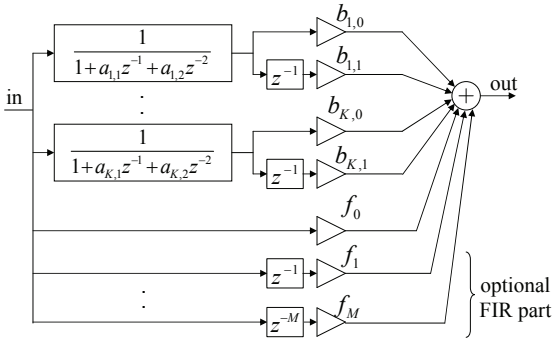

Figure 2: The structure of the fixed-pole parallel filter

The structure of the fixed-pole parallel filter can be seen in Fig. 2. Once the poles are chosen, the denominator coefficients $a_{k,1}$, $a_{k,2}$ become fixed and the output becomes a linear combination of signals with the weights $b_{k,1}$, $b_{k,2}$, f_n.

Filter design

By looking at Fig. 2 and substituting $z^{-1} = e^{-j\vartheta_n}$, the frequency response for a finite set of ϑ_n angular frequencies can be computed as

$$H(\vartheta_n) = \sum_{k=1}^{K} \frac{b_{k,0} + b_{k,1}e^{-j\vartheta_n}}{1 + a_{k,1}e^{-j\vartheta_n} + a_{k,2}e^{-j2\vartheta_n}} + \sum_{m=0}^{M} f_m e^{-jm\vartheta_n}. \tag{1}$$

Equation (1) can be written in a matrix form

$$\mathbf{h} = \mathbf{M}\mathbf{p}, \tag{2}$$

where $\mathbf{p} = [b_{1,0}, b_{1,1}, \ldots b_{K,0}, b_{K,1}, \ f_0 \ldots f_M]^T$ is a column vector composed of the free parameters. The columns of the modeling matrix $\mathbf{M}$ contain the transfer functions of the second-order sections $1/(1 + a_{k,1}e^{-j\vartheta_n} + a_{k,2}e^{-j2\vartheta_n})$ and their delayed versions $e^{-j\vartheta_n}/(1 + a_{k,1}e^{-j\vartheta_n} + a_{k,2}e^{-j2\vartheta_n})$ for the ϑ_n angular frequencies. The last columns of $\mathbf{M}$ are the transfer functions of the FIR part $e^{-jm\vartheta_n}$ for $m = [0 \ldots M]$. Finally, $\mathbf{h} = [H(\vartheta_1) \ldots H(\vartheta_N)]^T$ is a column vector composed of the resulting frequency response.

Now the task is to find the optimal parameters $\mathbf{p}_{\text{opt}}$ such that $\mathbf{h} = \mathbf{M}\mathbf{p}_{\text{opt}}$ is closest to the target frequency response $\mathbf{h}_{\text{t}} = [H(\vartheta_1)_{\text{t}} \ldots H_{\text{t}}(\vartheta_N)]^T$. If the error is evaluated in the mean squares sense

$$e_{\text{LS}} = \sum_{n=1}^{N} |H(\vartheta_n) - H_{\text{t}}(\vartheta_n)|^2 = (\mathbf{h} - \mathbf{h}_{\text{t}})^H (\mathbf{h} - \mathbf{h}_{\text{t}}), \tag{3}$$

the minimum of Eq. (3) is found by the least-squares (LS) solution:

$$\mathbf{p}_{\text{opt}} = \mathbf{M}^{+}\mathbf{h}_{\text{t}}, \tag{4a}$$

$$\mathbf{M}^{+} = (\mathbf{M}^H\mathbf{M})^{-1}\mathbf{M}^H, \tag{4b}$$

where $\mathbf{M}^{+}$ is the Moore-Penrose pseudoinverse, and $\mathbf{M}^H$ is the conjugate transpose of $\mathbf{M}$.

Controlling the frequency resolution by the choice of pole frequencies

It has been demonstrated in [8] that the frequency resolution of the filter design can be directly controlled by the choice of pole frequencies. A simple choice for pole positioning is to set the pole frequencies according to the desired resolution by putting more poles at those frequencies where we wish to achieve higher

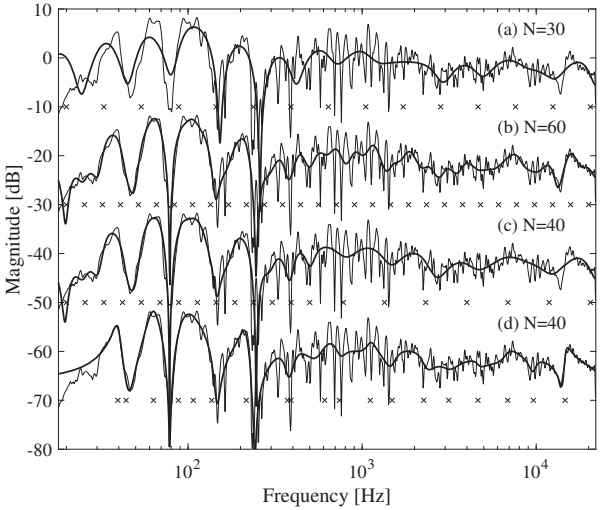

Figure 3: Modeling a room response by fixed-pole parallel filters: logarithmic pole set (a) and (b), stepwise logarithmic pole set (c), and custom warping (d). The filter order is marked by N. The target response is displayed by a thin line while the filter responses by thick lines. The pole frequencies are displayed by crosses.

resolution. The pole angles are then set so that the transfer functions of the second-order denominators cross approximately at their -3 dB points [8].

Figure 3 (a) shows an example when the pole frequencies are set to a logarithmic scale with 1.5 poles per octave, leading to a third octave resolution (the pole frequencies are marked by crosses). When the pole density is doubled (3 poles per octave), a sixth octave resolution can be achieved, displayed in (b). It can be seen in Fig. 3 (a), (b) that the modeling detail is evenly distributed in the logarithmic scale and the low frequency part of the room response is also properly modeled which was not possible for traditional FIR and IIIR filters (compare with Fig. 1).

It is also possible to use different pole densities in different regions, allowing a flexible fine-tuning of modeling detail, as shown in (c). In addition, the pole frequencies can be also chosen automatically, leading to an even better fit [5], [9]. One such example is custom warping, the results of which is shown in Figure 3 (d).

While the examples here only included the modeling of a specific transfer function, it is also possible to design compensation or equalization filters in the same way [5], [9], as will be shown in the presentation.

Conclusion

This case study has demonstrated that traditional FIR and IIR filters cannot be used for logarithmic frequency resolution filter design that would be desirable in audio applications. For that, one of the most efficient design methodology is the fixed-pole parallel filter. It has been shown that by the choice of pole frequencies the frequency resolution can be directly controlled and thus logarithmic frequency resolution is easily achieved.

The method has been used in various industrial applications, in a digital piano, in measurement equipment, and in room equalization systems, to name a few.

The interested reader is referred to the overview paper [5] or the MTA Doctorate thesis [9] of the present author for more details. MATLAB code and a tutorial video can also be found at `http://www.mit.bme.hu/~bank/parfilt/` .

References

[1] T. W. Parks and C. S. Burrus, *Digital Filter Design*. USA: John Wiley and Sons, 1987, p. 341.

[2] A. V. Oppenheim, R. W. Schafer and J. R. Buck, *Discrete-Time Signal Processing*. Upper Saddle River, New Jersey, USA: Prentice-Hall, 1999, p. 870.

[3] E. Zwicker and H. Fastl, *Psychoacoustics: Facts and Models*. Heidelberg, Germany: Springer-Verlag, 1990, p. 354.

[4] M. Waters and M. B. Sandler, "Least squares IIR filter design on a logarithmic frequency scale," in *Proc. IEEE Int. Symp. on Circuits and Syst.*, 1993, pp. 635–638. DOI: `https://doi.org/10.1109/ISCAS.1993.393801`.

[5] B. Bank, "Warped, kautz, and fixed-pole parallel filters: A review," *J. Audio Eng. Soc.*, vol. 70, no. 6, pp. 414–434, 2022.

[6] A. Härmä, M. Karjalainen, L. Savioja *et al.*, "Frequency-warped signal processing for audio applications," *J. Audio Eng. Soc.*, vol. 48, no. 11, pp. 1011–1031, 2000.

[7] T. Paatero and M. Karjalainen, "Kautz filters and generalized frequency resolution: Theory and audio applications," *J. Audio Eng. Soc.*, vol. 51, no. 1–2, pp. 27–44, 2003.

[8] B. Bank, "Audio equalization with fixed-pole parallel filters: An efficient alternative to complex smoothing," *J. Audio Eng. Soc.*, vol. 61, no. 1/2, pp. 39–49, 2013.

[9] B. Bank, *Logarithmic frequency resolution filter design for audio applications*, Doctor of the Hung. Acad. of Sci. thesis, Hungarian Academy of Sciences (MTA), URL: `http://www.mit.bme.hu/ ~bank/mta`, Hungary, 2021.

Acoustic fun facts

You can clearly hear anglers speaking on the other side of the lake, and a concert across Lake Balaton can sound as if it were only 500 meters away? This is not a perceptual illusion but the result of real acoustic phenomena.

On the one hand, acoustic waves with a low angle of incidence are effectively reflected by the water surface. On the other hand, a cold air layer forms just above the surface, acting as a corridor for sounds: Because of the temperature gradient, sound waves that would normally diverge are bent back toward the surface.

As a result, sound is guided on the surface in much the same way as light is guided in an optical fiber.

This effect is especially pronounced at low frequencies, where air absorption is extremely small – on the order of just a few tenths of a decibel per kilometer – and therefore negligible compared with geometric spreading.

NVHH2025-0061

Impact of measurement variables on product sound power levels

A. Kiss*[1],

[1]Robert Bosch Kft.,
ME/ECF-NVH, Budapest, Gyömrői út 104. H-1103 Hungary

*Corresponding author, e-mail: Andras.Kiss@hu.bosch.com

Summary

Various microphone hemisphere measurement setups are available as industrial standard for assessing active sound sources with an emphasis on sound power measurements. Increasing the number of microphones further enhances accuracy by providing more detailed spatial data on sound distribution.

Theoretically the interplay between reflective surfaces, microphone quantity and configuration, and the characteristics of the blower fan collectively determines the accuracy and reliability of the sound power level determination. The main goal of this investigation was to determine the impact on measured values. During the measurements as a noise source we used a serial blower fan. In this case study the impact from different reflective surfaces and the impact from different standardized microphone positions were investigated. The surfaces had maximum ~0.5dB(A), the microphone positions only ~0.2dB(A) impact on determined sound power level. Based on results low difference was visible between different setups. During further blower fan measurements any of the options can be used.

Introduction

A hemisphere with a 1-meter radius offers a compact configuration where microphones are positioned close to the source, enabling precise measurement of direct sound energy.

The impact of reflective surfaces is critical, as they can distort the measurements by reflecting sound waves back into the microphone array. During the

measurements we checked different surfaces (official semi anechoic floor – epoxy resin, asphalt, Mitteldichte Holzfaserplatte "MDF" and Oriented Strand Board "OSB") and their impact on measured values. Consequently, careful management and selection of materials for these surfaces are essential during the setup.

The measurement setups see on *Figure 1*.

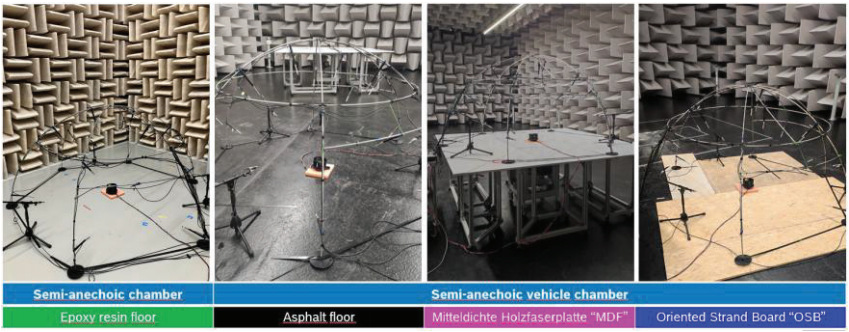

Figure 1: Hemisphere measurement setup with a 1-meter radius (different surfaces)

The measurement results – measured sound pressure levels and calculated sound power levels – see on *Figure 2*.

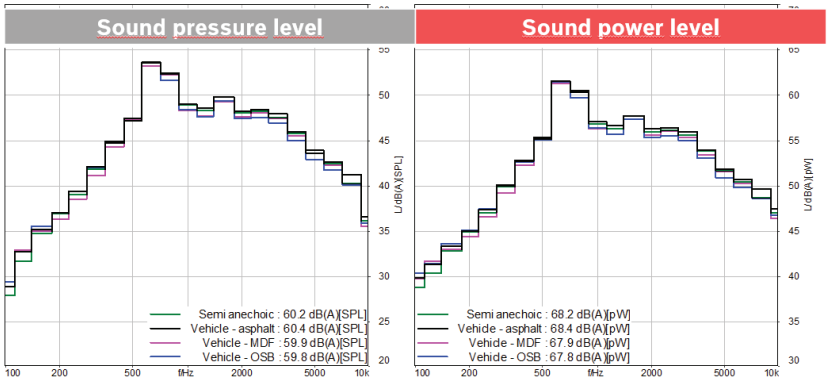

ISO 3745 Table E.1 (Microphone positions on the hemispherical measurement surface – general case)

Figure 2: Measurement results (different surfaces) – 3rd octave spectrum

Other hand increasing the number of microphones further enhances accuracy by providing more detailed spatial data on sound distribution. This is particularly important when testing a blower fan, where airflow and mechanical vibrations can influence the results. The precise arrangement of the microphones is vital to mitigate interference and ensure accurate capture of the fan's acoustic profile. Calibration of the measurement system and careful positioning of the microphones guarantee that the results adhere to strict sound power measurement standards. [3]

During the measurements we have checked the microphone position impact on measured values based on:

- ISO 3744:2010 Acoustics – Determination of sound power levels and sound energy levels of noise sources using sound pressure – Engineering methods for an essentially free field over a reflecting plane [1], Table B.2 (Microphone positions on the hemispherical measurement surface for a broadband noise source).
- ISO 3745:2012 Acoustics – Determination of sound power levels and sound energy levels of noise sources using sound pressure – Precision methods for anechoic rooms and hemi-anechoic rooms [2], Table E.1 (Microphone positions on the hemispherical measurement surface – general case).
- ISO 3745:2012 Acoustics – Determination of sound power levels and sound energy levels of noise sources using sound pressure – Precision methods for anechoic rooms and hemi-anechoic rooms [2], Table E.2 (Microphone positions on the hemispherical measurement surface for broadband omnidirectional sources).

The measurement setups see on *Figure 3*.

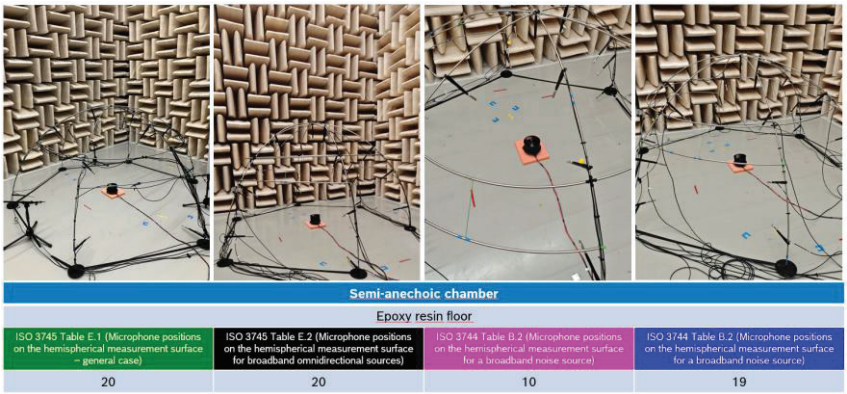

Figure 3: Hemisphere measurement setup with a 1-meter radius (different microphone positions)

The measurement results – measured sound pressure levels and calculated sound power levels – see on *Figure 4*.

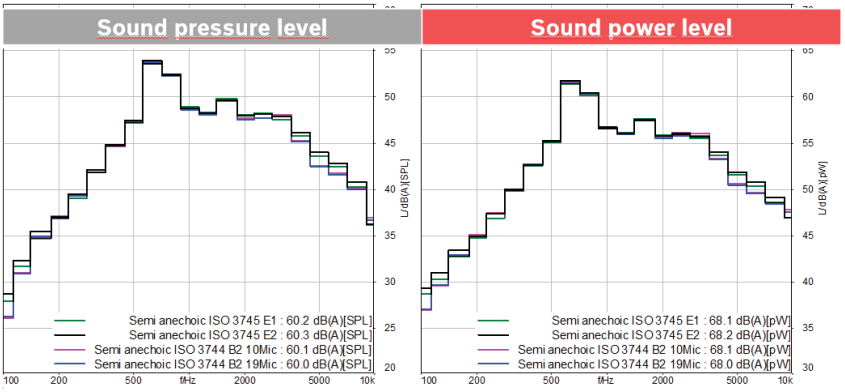

Figure 4: Measurement results (different microphone positions) – 3rd octave spectrum

Conclusions

Overall, the interplay between reflective surfaces, microphone quantity and configuration, and the characteristics of the blower fan collectively determines the accuracy and reliability of the sound power measurements. In this case study the impact from different reflective surfaces and the impact from different microphone positions were investigated. The surfaces had maximum

~0.5dB(A), the microphone positions only ~0.2dB(A) impact on determined sound power level. Based on results low difference was visible between different setups. During further blower fan measurements any of the options can be used.

References

[1] ISO 3744:2010 Acoustics – Determination of sound power levels and sound energy levels of noise sources using sound pressure – Engineering methods for an essentially free field over a reflecting plane https://www.iso.org/standard/52055.html

[2] ISO 3745:2012 Acoustics – Determination of sound power levels and sound energy levels of noise sources using sound pressure – Precision methods for anechoic rooms and hemi-anechoic rooms https://www.iso.org/standard/45362.html

[3] J.R. Hassall, K. Zaveri, and M. Phil, Acoustic Noise Measurements, Brüel&Kjaer, Sweden, 1988.

INNOVATIVE, PRODUCTION-READY SOLUTIONS

AVL Mobility Engineering

We are a leader in the development of innovative mobility systems, including hydrogen engines, hybrid powertrains, battery electric vehicles, and fuel cells.

With expertise in driving functions, subsystems, and components, we are perfectly set to help you integrate systems into vehicles for production. We also focus on Advanced Driver Assistance Systems and fully automated driving, offer technology consulting and stationary energy application development.

www.avl.com

NVHH2025-0063

Case study of forming complete FRF from incomplete data using impulse dynamic subspace

Z. Dombovari[1*,2]

[1] MTA-BME Lendület Machine Tool Vibration Research Group,
Department of Applied Mechanics,
Budapest University of Technology and Economics,
Budapest, Hungary

[2]Department of Applied Mechanics,
Faculty of Mechanical Engineering,
Budapest University of Technology and Economics,
Budapest, Hungary

[*]Corresponding author, e-mail: X.Author@edu.bme.hu

Summary

Autonomous characterization of machine tools often relies on incomplete dynamic responses. This is especially true for next-generation machine tools, which not only control geometric precision but also operate resiliently to prevent harmful oscillation growth. The limited number of sensors and actuators available for excitation and sensing poses additional challenges. Crosstalk is frequently recorded, while key direct dynamic characterizations are missed to maintain a simpler, more cost-effective measurement environment. The method presented here enhances the rank of an incomplete frequency response matrix, enabling a feasible approximation of direct dynamics without relying on parametric fitting, which is commonly used for synthesizing such results

Introduction

It is well known in the theory of modal analysis [1] that unknown directions can be reconstructed due to the rank-one representation of each residue of a given multi-input multi-output (MIMO) linear dynamic system. There are plenty of different conventional methodologies to fit modes in its general non-proportional manner, first usually determining spectral behavior comprising natural frequencies and damping factors. Later, additional fitting determines the amplitude behavior in which the residue matrices serve as an unequivocal description of the modes. This can be further decomposed to e.g. modal scaling factor, mode

shapes, and modal participation vectors, or to derive a nearly proportional description using the more understandable modal mass definition.

These methods are all based on least squares fitting of some mathematical description with different describing function sets and weights determining a rational fraction MIMO description of the system. The most well-known methods are the rational fractional method (RFP, [2]), polyreference (polyMAX, [3], [4]) or least squares (LS) methods [5]. All of these methods can be considered as a family of methods, which require a stability chart to select modes.

Another way of describing the method is based on the kernel of the integral form of dynamical description based on Ibrahim's method [6]. The impulse dynamic subspace (IDS) description uses a linear coordinate transform that uses the so-called principal impulse response functions (IRFs) as a base. It is important to emphasize this methods are explicit methods, without performing least square approximation; this is based on the singular value decomposition (SVD) of the corresponding Green kernel.

The following method is capable of performing synthetization of frequency response functions (FRFs) in the unknown direction without performing any least squares fitting. The method is the combination of the IDS with the so-called symmetric SVD [7] algorithm.

Impulse Dynamic Subspace

Due to the rules of theoretical modal decomposition [1] of linear mechanical systems it is enough to measure an incomplete version of the corresponding frequency response functions (FRF's). This results in a nonsquare representation of the acquired FRF's in the following form

$$\mathbf{H}(\omega) : \mathbb{R} \to \mathbb{C}^{m \times n} \text{ with } m \neq n, \tag{1}$$

where m represents the sensing, while n the excitation dimension including spatial directions and positions. Without sacrificing generality for the given linear mechanical system, we can assume $m \geq n$ for most of the practical cases.

The corresponding impulse response function (IRF) can be determined with $\mathbf{h}(\theta) = (\mathscr{F}^{-1}\mathbf{H}(\omega))(\theta)$. This can play the role of the kernel of the integral

form of a homogeneous linear system as

$$\mathbf{x}(t+\theta) = \int_0^\infty \mathbf{G}(\theta,\vartheta)\,\mathbf{F}^-(t-\vartheta)\mathrm{d}\vartheta \quad \Rightarrow \quad \mathbf{G} = \begin{bmatrix} \mathbf{h}_0 & \mathbf{h}_1 & \dots & \mathbf{h}_N \\ \mathbf{h}_1 & \mathbf{h}_2 & \dots & \mathbf{h}_{N+1} \\ \vdots & \vdots & \ddots & \vdots \\ \mathbf{h}_N & \mathbf{h}_{N+1} & \dots & \mathbf{h}_{2N} \end{bmatrix}, \tag{2}$$

where $\mathbf{G}$ is the discrete Hankel version of the anyway continuous kernel $\mathbf{G}(\theta,\vartheta) = \mathbf{h}(\theta+\vartheta)$ containing samples of the IRF as $\mathbf{h}_j := \Delta\theta\,\mathbf{h}(j\,\Delta\theta)\,(\mathrm{m/N})$. The vector $\mathbf{F}^-(t-\vartheta)$ represents the initial forcing that replaces the role of initial conditions for the well known differential formalism. Whilst $\mathbf{x}(t+\theta)$ represents the transient free response of the mechanical system described by the kernel $\mathbf{G}$.

The impulse dynamic subspace (IDS) is described by the left and right principal-IRF functions $\mathbf{V} \in \mathbb{C}^{mN_V}$ and $\mathbf{W} \in \mathbb{C}^{nN_W}$ (complex values kept for generality). These are the left and right eigenvectors of the nonsquare singular value decomposition (SVD) of the sampled and truncated kernel $\mathbf{G} \in \mathbb{R}^{mN_V \times nN_W}$ with $N_V \leq N$ and $N_W \leq N$ samples as

$$\mathbf{G} = \mathbf{V}\,\Sigma\,\mathbf{W}^{\mathsf{H}}, \tag{3}$$

where Σ contains the singular values having compliance units.

The method to predict the complete Green kernel can be derived by assuming linear relation between the left and right principal IRF's and between the direct and complete left principal IRF's. These assumptions results in the following form to determine the complete sampled Green kernel

$$\mathbf{G}_\mathrm{c} = \mathbf{V}\,\Sigma\left(\mathbf{V}_\mathrm{d}^{\mathsf{H}}\mathbf{V}_\mathrm{d}\right)^{-\mathsf{H}}\left(\mathbf{V}_\mathrm{d}^{\mathsf{H}}\mathbf{V}_\mathrm{d}\right)^{-1}\mathbf{V}_\mathrm{d}^{\mathsf{H}}\,\mathbf{W}_\mathrm{d}\,\mathbf{V}^{\mathsf{H}}. \tag{4}$$

The complete IRF can be derived from (4) using $\mathbf{h}_\mathrm{c} = \mathbf{G}_\mathrm{c}(:,1:n)$, out of which the complete FRF $\mathbf{H}_\mathrm{c}$ can be determined with a simple element-wise (discrete) Fourier transformation (DFT). (The notation $\mathbf{A}(a:b,c:d)$ is the OCTAVE / MATLAB matrix element choice notation.)

Having the original assumption on the dimensions $m \geq n$ one can define the direct (or driving) segment of the left-singular IRF vector as $\mathbf{V} =: [\cdots\mathbf{V}_\mathrm{d}^{\mathsf{T}}\cdots]^{\mathsf{T}}$, where the direct segment has the dimension of $\mathbf{V}_\mathrm{d} \in \mathbb{C}^{nN_W}$. This might require a special indexing sequence considering how large those vectors can be.

Single DOF case study

Here the intention is to present a simple enough example to show how the method performs in ideal and not ideal circumstances, when we deliberately remove a known spatial dimension and predict those back as a benchmark with the method shown in (4).

A single DOF, proportionally damped, but multi dimensional case is defined here with the following formula for the FRF and for the corresponding IRF

$$\mathbf{H}_\mathrm{c}(\omega) := \frac{1}{M}\frac{\mathbf{v}\mathbf{v}^\mathsf{T}(1+\sigma\Gamma(\omega))}{-\omega^2+2\zeta\omega_\mathrm{n}\omega\,\mathrm{i}+\omega_\mathrm{n}^2}, \quad \mathbf{h}_\mathrm{c}(\theta) := \frac{\mathbf{v}\mathbf{v}^\mathsf{T}(1+\sigma\Gamma(\theta))}{M\,\omega_\mathrm{d}}\mathrm{e}^{-\zeta\,\omega_\mathrm{n}\theta}\sin\omega_\mathrm{d}\theta, \tag{5}$$

respectively. Here M is the modal mass, while ω_n and $\omega_\mathrm{d} = \omega_\mathrm{n}\sqrt{1-\zeta^2}$ are the undamped and damped natural frequencies originated from the viscose definition of the damping factor ζ. Later, adding noise plays an essential role modeled by a $\Gamma(\theta)$ Wiener process (white noise) and its intensity σ, while $\Gamma(\omega) := \mathscr{F}(\Gamma(\theta))(\omega)$ [8]. The direction of the modes are considered with the mode shape vector $\mathbf{v}$.

Once the sampled complete Green kernel $\mathbf{G}_\mathrm{c}$ is constructed, one can leave away deliberately one of the dimension - lets say the jth one - to have a benchmark example as

$$\mathbf{G} := \mathbf{G}_\mathrm{c}(:, \mathrm{row}_{k=1}^{N}\,((k-1)m+[1\ldots j-1\;j+1\ldots m])). \tag{6}$$

The incomplete Green kernel can be further truncated to have the dimension $\mathbf{G}\in\mathbb{R}^{mN_V\times nN_W}$, where $N_W \le N_V \le N$. This helps to perform the decomposition presented in (3) promptly without loosing too much of accuracy. Note that for good representation of the dynamics N_V should be kept somewhat colse to N, while N_W can be reduced much greatly to speed up the numerical calculation.

In this benchmark comparison the formula (4) has been applied and compared with the original exact complete function pointing out the quality of the re-synthetization on the left out directions.

The single DOF benchmark test environment

A single DOF is defined with two dimensions with the mode shape vector (5) defined by a single angle ψ with $\mathbf{v} := [\cos\psi\ \sin\psi]^\mathsf{T}$. Since the second dimension is going to be dropped for benchmarking the method presented in (4) 0 deg angle means the mode is physically in the x direction, that is, no prediction is

expected. Whilst, 90 deg will not have any crosstalk to the first dimension, thus, the method presented in (4) will not have any information to predict the mode. In this manner purely 0 and 90 deg cases are going to result in no prediction in the second dimension at all.

The question may arise what deviation from this two values will results in any meaningful prediction. To examine this artificial 'measurement' noise was added to the FRF quantified with σ in (5).

Result of the single DOF benchmark test

The added noise was essential, because in the pure, say normalized case using e.g. $\omega_\mathrm{n} := 1\,\mathrm{rad/s}$ and $\zeta := 10\,\%$ damping the prediction was basically able to predict the second dimension with good quality with very tiny angle variation.

This is shown in the Fig. 1a, where the pure noise-free case is located in the left side of the diagram when $\sigma = 0$ (5). One can recognize both the $0 + \varepsilon$ and $90\,\mathrm{deg} - \varepsilon$ cases are predicted with great precision. That means a sufficiently small deviation is enough to predict ideally the unknown direction.

Noise $\sigma > 0$ is introduced to mimic realistic cases in (5) testing how robust are these tiny deviation to added noise at the 0 and 90 deg bounds. It is important to note that the quality of the prediction is tested in the unknown direction, that is, the signal noise ratio will be much more important in this predicted unknown direction. Actually, this is the reason why it is less robust around 0 angle where an actual geometric/physical projection has naturally less valuable information into the second dimension to predict. This means the prediction might submerge in the noise added. When the mode is more pointing to the second dimension 90 deg the added noise disturb less the prediction, which is naturally more prominent in the unknown direction. After a certain noise level there is no prediction possible which provide good correlation with the original FRF as expected, see large σ values in Fig. 1a.

In the Fig. 1b we can see the effect of the truncation on the second dimension characterized by $N_W = N/p_W$. Interestingly it does not affect the prediction around the 0 angle, which physically have small projection in the unknown dimension.

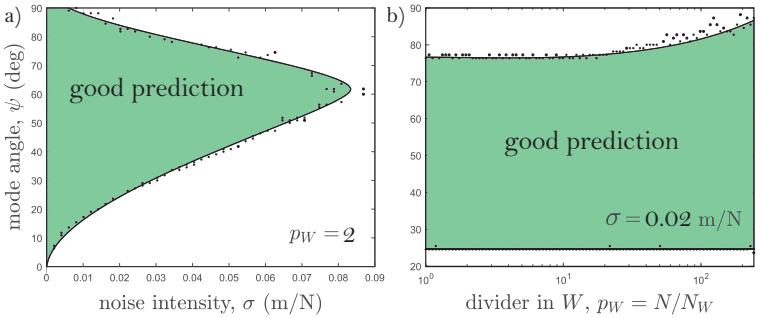

Figure 1: a) shows the sensitivity for noise according to the definition presented in (5), while b) presents the sensitivity of the method on applied truncation.

Conclusion

The presented work summarizes a methodology, with which it is possible to reconstruct the unknown directions using only the measured information in the form of frequency response functions (FRF's). In this manner, this method is a data driven method, which is based on the construction of the Green kernel originated from impulse response functions (IRF's).

The method can be important to provide synthetized FRF data to methodologies which are solely data driven, like the well known zeroth order approximation (ZOA, [9]) or multi-frequency solution (MF, [10]). These methods are important to perform predictions of stability of machining processes included the IDS description [11].

Performing modal analysis usually good noise signal ratio can be achieved suggesting that the presented synthetization can be performed quite well. According to the current study the prediction of unknwon direction can be determined even in a less ideal circumstances when noise is more apparent or/and insufficient sampling is available.

References

[1] D. Ewins, *Modal Testing: theory, practice, and applications*. Research Studies Press, 2000.

[2] H. M. Richardson and D. L. Formenti, "Parameter estimation from frequency response measurements using rational fraction polynomials," in *1st IMAC Conference, Orlando, FL*, 1982.

[3] F. Lembregts, J. L. Leuridan and H. Van Brussel, "Frequency domain direct parameter identification for modal analysis] state space formulation," *Mechanical Systems and Signal Processing*, vol. 4, pp. 65–76, 1989.

[4] V. D. Auweraer and J. Leuridan, "A new testing paradigm for today's product development process–part 2," *Sound and Vibration*, vol. 39, no. 11, pp. 18–21, 2005.

[5] R. R. Craig, A. J. Kurdila and H. M. Kim, "State-space formulation of multi-shaker modal analysis," *Journal of Analytical and Experimental Modal Analysis*, vol. 5, pp. 169–183, 1990.

[6] S. Ibrahim and E. C. Mikulcik, "A method for the direct identification of vibration parameters from the free response," *Shock and Vibration Bulletin*, vol. 47, pp. 183–198, 1977.

[7] A. Bunse-Gerstner and W. B. Gragg, "Singular value decompositions of complex symmetric matrices," *Journal of Computational and Applied Mathematics*, vol. 21, no. 1, pp. 41–54, 1988.

[8] G. Fodor and D. Bachrathy, "Efficient approximation of stochastic turning process based on power spectral density," *The International Journal of Advanced Manufacturing Technology*, vol. 133, no. 1, pp. 5673–5681, 2024.

[9] Y. Altintas and E. Budak, "Analytical prediction of stability lobes in milling," *CIRP Annals - Manuf. Tech.*, vol. 44, pp. 357–362, 1995.

[10] S. D. Merdol and Y. Altintas, "Multi frequency solution of chatter stability for low immersion milling," *Journal of Manufacturing Science and Engineering*, vol. 126, no. 3, pp. 459–466, 2004.

[11] Z. Dombovari, "Stability properties of regenerative cutting processes, based on impulse response functions expressed in the impulse dynamic subspace," *International Journal of Machine Tools and Manufacture*, vol. 162, no. 1, p. 103 691, 2021.

NVHH2025-0064

Case study of nonlinear vibration prediction via LS-DYNA in airbag control units

Horváth Gergely Zoltán[1*], Stéger Zsolt[1], Gazdagh Zoltán Gábor[2]

[1] Robert Bosch Kft., Airbag Electronic Control Unit Mechanical Development, Budapest Gyömrői út 104. H-1103, Hungary

[2]Robert Bosch Kft., Engineering Acoustics – Noise Vibration and Harshness, Budapest Gyömrői út 104. H-1103, Hungary

[*]e-mail: hgz1998@gmail.com

Summary

Sensor signals of the Airbag Electronic Control Unit can be disturbed by the higher harmonics of a nonlinear resonance. A typical source of the nonlinear resonance is related to the sheet metal baseplate of the Airbag Electronic Control Unit, which deforms significantly upon external excitation leading to changing stiffness and instability. In this case study we have been using Ansys LS-Dyna finite element simulation with a nonlinear solver to model the nonlinear resonance of the baseplate aiming to predict the presence of nonlinearity in different design variants, moreover if the nonlinearity source is related to the geometry, contact or material.

Introduction

In this study, we focus on the impact of nonlinear resonance on the Airbag Electronic Control Unit (ECU) and its sensor signals. Nonlinear resonance may caused by the deformation of the sheet metal baseplate of the ECU under external excitation. To investigate this phenomenon, we used Ansys LS-Dyna for finite element simulation (see Figure 1.), utilizing a nonlinear solver to accurately model the behaviour of the baseplate [1].

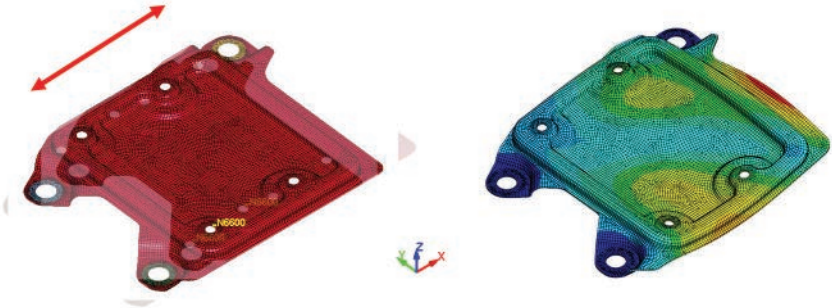

Figure 1: LS-DYNA finite element model of sheet metal baseplate

Results and discussion

The result of the simulation confirms the presence of nonlinearity, identified as contact-related and/or geometry-based, reducing the effort required in the testing phase.

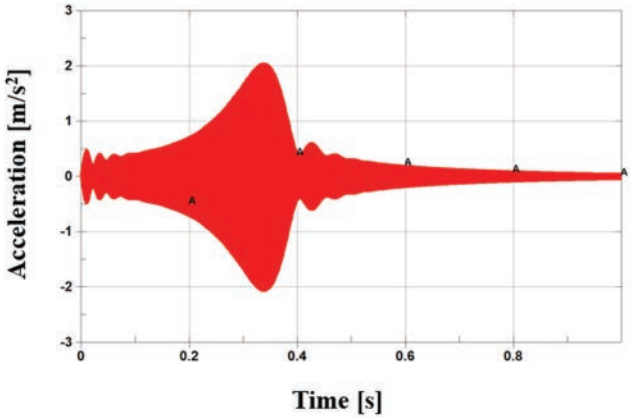

Figure 2: Acceleration time response based on sine-sweep excitation [4]

The approach began with determining the system's vibration modes using Ansys Modal, followed by applying different sinusoidal-sweep excitations in LS-DYNA. [1], [3] Through post-processing, the acceleration response signals from specific nodes in the finite element analysis (FEA) model were selected for further analysis, searching for signs of nonlinearity. [2]

References

[1] Liu, Yucheng. "ANSYS and LS-DYNA used for structural analysis." *International Journal of Computer Aided Engineering and Technology* 1.1 (2008): 31-44.

[2] Levy, Robert, and William R. Spillers. *Analysis of geometrically nonlinear structures*. Springer Science & Business Media, 2013.

[3] Novak, Antonin, et al. "Nonlinear system identification using exponential swept-sine signal." *IEEE Transactions on Instrumentation and Measurement* 59.8 (2009): 2220-2229.

[4] Z. Gazdagh, D. Ács, B. Vehovszky, B. Fukker, “Control of transfer function distortion during RPM-sweep testing of e-drive systems”. In: Conference Proceedings of ISMA2024 - USD2024. 2024, pp. 3779–3787. URL: https://m2.mtmt.hu/api/publication/35498927

NVHH2025-0068

Electroacoustical System of the Puskás Arena

G. Balogh
INTERTON Group, Budapest, Hungary
e-mail: geza.balogh@intertongroup.com

Summary

After 6 years of preparation, design and implementation, the 67,000-seat Puskás Arena was handed over in November 2019. This paper presents the electroacoustical system design and implementation, focusing on challenges, standards, and the correlation between the original concept and the final solution in terms of SPL, STI, and their uniformity.

Introduction

Electroacoustical systems in large venues such as stadiums play a critical role in ensuring intelligible and uniform sound coverage. Professional practice requires compliance with international standards such as UEFA and domestic regulations, focusing on parameters like Sound Pressure Level (SPL) and Speech Transmission Index (STI). Modern systems often rely on IP-based infrastructure, line array loudspeakers, and advanced modeling tools to achieve optimal performance.

Design Challenges and Objectives

The Puskás Arena project was unique due to its scale and the strict requirements set by UEFA 2020 [7]. The design phase (2013–2017) had to ensure compliance with STI = 0.7 (and STI > 0.5, empty stadium) and SPL > 110 dBA (total, continuous SPL, for min. 120 sec) across all seating areas in the stands. The system needed to be highly directional to avoid acoustic overlap between zones. Using EASE (3D acoustic simulation software) was essential to simulate and validate the design before implementation. [1], [2], [3] Furthermore, UEFA 2020 rulebook requires so called avoidance zones (media/press areas, pitch), where SPL level must be adjusted independently from other seats for visitors.

Implementation and Results

Between 2017 and 2019, the system was implemented using over 2,000 loudspeakers and 75,000 meters of cabling. The solution included QSC and d&b

audiotechnik components, centralized control, and IP-based operation. Measurements confirmed SPL of 110.5 dBA (total, continuous) and STI of 0.505 (empty stadium), meeting all requirements. The system was divided into zones to manage acoustic challenges effectively. The final implementation closely matched the original design simulations.

Conclusion

The electroacoustical system of the Puskás Arena demonstrates how modern technology and careful planning can meet stringent performance criteria in large venues. The project serves as a benchmark for future stadium audio system designs. [4], [5], [6]

References

[1] AES Technical Committee on Acoustics, 'Sound System Design and Performance Criteria,' AES, 2018.

[2] d&b audiotechnik, 'System Design Guidelines,' 2020.

[3] QSC, 'Q-SYS Platform Overview,' QSC Technical Documentation, 2021.

[4] https://intertongroup.com/az-audio-rendszer-teljesitmenye-a-puskas-arenaban/

[5] https://www.dbaudio.com/global/en/applications/sports-venues/puskas-arena-pitched-for-victory-with-db/

[6] https://www.dbaudio.com/assets/products/downloads/case-studies/dbaudio-case-study-sports-venues-puskas-arena-budapest.pdf

[7] https://documents.uefa.com/r/Technical-Regulations/UEFA-Stadium-Infrastructure-Regulations-Online

NVHH2025-0069

Case study of long boring bars with passive vibration absorber considering bending and torsion

A. Jolamanov[1*], Z. Dombovari[1]

[1]Budapest University of Technology and Economics,
Department of Applied Mechanics, Budapest, Hungary

[*]Corresponding author, e-mail: azat.jolamanov@edu.bme.hu

Summary

This work shows a case of a long boring bar which exhibits bending and torsional modes. The hybrid model consists of an analytical parametric model of the bar and an experimentally measured Frequency Response Functions (FRFs) of machine dynamics. The monolith part of the bar is represented by a parametric model consisting of four separate segments, namely a solid segment, a hollow segment, a cutting head, and a passive vibration absorber. An experimental modal analysis is performed on a special test bench where the torsional mode was emphasized. The coupling of the analytical and the experimental data is done according to the Receptance Coupling Substructure Analysis (RCSA). A passive vibration absorber is introduced into the hollow segment of the mechanical system and the receptances at the tool tip are analyzed.

Introduction

Boring operation is a widespread machining process that is used to enlarge existing diameter holes in high valued parts. As the process also provide surface finishing on a workpiece, the stability of the operation is essential. However, the boring bar is a mechanical system that closely represents a slender cantilever beam, hence the presence of unwanted vibrations, also known as chatter, is unavoidable [1].

The slenderness of a boring bar is defined through a so-called length-to-diameter ratio (L/D ratio), and once this ratio exceeds a value of around 4, the static and dynamic stiffness of the bar decreases significantly. To overcome this issue there exist a number of different solutions that suppress the unwanted vibrations, such as an introduction of a mass absorber or mode coupling effect [2]. However, all the up-to-date literature takes into account only the bending behaviour of the

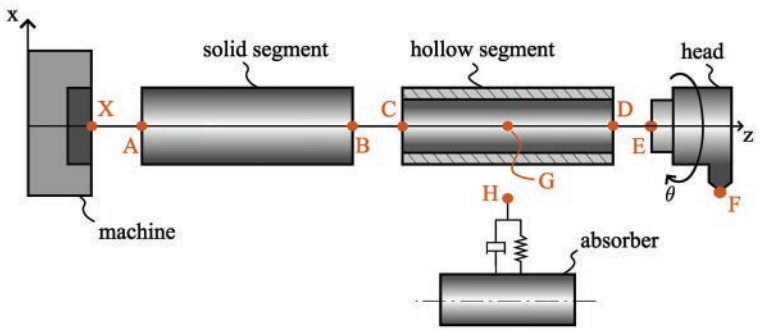

Figure 1: Parametric mechanical model

boring bar system. This work, on the contrary, extends the boundaries of such mechanical systems by introducing the torsional dynamics.

Methodology

Firstly, the parametric mechanical model of the boring bar system is developed. The model consists of separate segments, such as a cutting head, a hollow segment, a solid segment, a mass absorber system, and a machine tool, see Figure 1. The bending behaviour of the beam-like segments is described by the well-known Timoshenko beam model, whereas the torsional behaviour is descried by Euler beam model. The dynamic behaviour of the segments is described in terms of frequency response function matrices (FRFs) and is coupled according to the receptance coupling substructure analysis (RCSA) methodology [3]. For the full bar assembly, the coupling is performed between points $X-A$, $B-C$, $D-E$, and $G-H$. In this work, the FRF matrix for sensing point i and excitation point j is defined as:

$$\mathbf{H}_{i,j}(\omega) := \begin{bmatrix} H_{i,j}(\omega) & L_{i,j}(\omega) & 0 \\ M_{i,j}(\omega) & N_{i,j}(\omega) & 0 \\ 0 & 0 & T_{i,j}(\omega) \end{bmatrix} \begin{pmatrix} \mathrm{m/N} & \mathrm{m/Nm} & \mathrm{m/Nm} \\ \mathrm{rad/N} & \mathrm{rad/Nm} & \mathrm{rad/Nm} \\ \mathrm{rad/N} & \mathrm{rad/Nm} & \mathrm{rad/Nm} \end{pmatrix}, \qquad (1)$$

where the first four elements describe the bending behaviour whilst the fifth element T is related to torsion.

Secondly, a number of parameter optimization schemes is developed. The optimized parameters are described in the following section.

Lastly, a measurement is performed in order to determine the dynamical charac-

teristics of the machine tool segment.

Results

The results of the work are presented in the following subsections.

Parameter optimization

The first optimized parameter is a so-called length ratio which is defined as the ratio of the hollow segment length to the total length of the boring bar:

$$\sigma := \frac{L_{\text{hol}}}{L_{\text{total}}}. \tag{2}$$

The optimization is based on the absorber mass ratio parameter μ, which preferred to be maximized in order to most effectively suppress chatter [4]. It was found that the mass ratio is peaking at around 45-50% of the length ratio σ, depending of the overall bar geometry.

Another parameter that was optimized is the hollow segment wall thickness w. The dependence of the bending and torsional responses on the varying wall thickness was studied. It was found that the amplitude of the torsional response T, when plotted as a function of the wall thickness w, contains a distinct valley. As the current chatter suppression methodologies mainly focus on the dominant bending mode, this finding is believed to be crucial as it provides a possible minimization of the torsion related vibration without affecting the existing mass absorber methodologies.

Lastly, another optimization scheme was performed on the dimensioning of the rubber bushings that provide connection properties between the boring bar and the introduced mass absorber. The radial stiffness of the cylindrical bushings, that is related to the bending behaviour of the bar, is based on the well-known Sims tuning methodology [4]. Later, the dimensioning parameters such as inner and outer diameters as well as length of the rubber rings are varied with keeping the radial stiffness characteristics constant. It was found that the shortest physically feasible rubber bushing design is preferred, as it would provide the most optimal torsional stiffness characteristics.

Analytical calculation

The affect of the introduced mass absorber on the torsional behaviour of the boring bar system has not been studied in the academic literature yet. The analytical calculation results can be seen in Figure 2. The orange and black curves represent the bending tip receptance without and with absorber respectively, whilst the

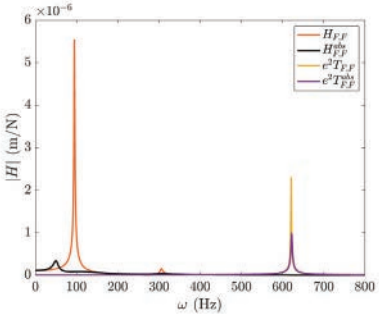

Figure 2: Cutting tip receptance without and with introduced mass absorber

yellow and purple curves represent the torsion tip receptance. It can be clearly seen that the torsional response of the cutting tip becomes the dominant one once the absorber is in place. This finding showcases the importance of the torsional effects on the stability analysis of the long boring bar systems. However, it should be noted that the torsional damping characteristics of the absorber-boring bar connection were approximated according to the up-to-date research into damping, which is considerably limited. Therefore, this parameter should be determined empirically.

Machine dynamics

The machine dynamics are determined based on the modal measurements of a dummy tool. Later, the analytical responses are subtracted from the measurement data according to the inverse RCSA methodology [5]. However, as the current mechanical system is described in a three dimensional space, it was necessary to extend the literature methodology from two to five unknowns.

Another receptance coupling was performed between the determined machine dynamics and the analytical bar of 250 mm. The results were compared to the measured data of similar bar and can be seen in Figures 3. The measured data Φ, the predicted responses based on the determined machine dynamics H and T, and the analytical cantilever cases H^{wall} and T^{wall} are plotted for centre and off-centre direct hits. Also, the acceptable frequency bandwidth is marked with the light grey boundary.

It can be seen that the purely bending prediction of the bar is rather accurate, see Figure 3a. Besides, There exist a numerical antiresonance at around 2500 Hz and a fake mode at around 3500 Hz. These deviations should be studied further and the methodology should be further improved to eliminate such issues. On

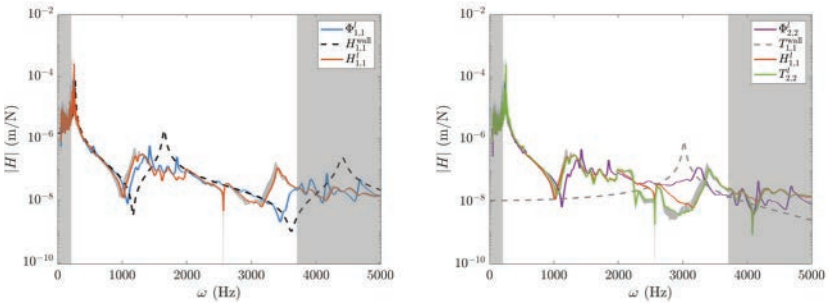

(a) Direct centre response *(b) Direct off-centre response*

*Figure 3: **250 mm long bar**: predicted and measured responses*

the contrary, the presence of the torsional effects on the predicted response is not clear, see Figure 3b. The natural frequency of the torsional mode is rather close to the fake mode. One can argue that the fake mode overwrites the torsional effects, however, the exact reason is still unknown.

Conclusion

The parametric mechanical model of the boring bar system was developed in this work. Later, this system was used to perform a number of optimization schemes with a goal of creating the most stable boring bar design. Lastly, the inverse RCSA methodology was expanded in order to obtain the machine dynamics that would include the torsional behaviour.

References

[1] J. Munoa, X. Beudaert, Z. Dombovari *et al.*, "Chatter suppression techniques in metal cutting," *CIRP Annals*, vol. 65, pp. 785–808, 2016. DOI: 10.1016/j.cirp.2016.06.004.

[2] A. Astarloa, A. Comak, I. Mancisidor *et al.*, "Improvement of boring operations by means of mode coupling effect," *CIRP journal of manufacturing science and technology*, vol. 37, pp. 633–644, Apr. 2022. DOI: 10.1016/j.cirpj.2022.03.008.

[3] T. L. Schmitz and G. S. Duncan, "Three-component receptance coupling substructure analysis for tool point dynamics prediction," *Journal of Manufacturing Science and Engineering*, vol. 127, pp. 781–790, Feb. 2005. DOI: 10.1115/1.2039102.

[4] N. D. Sims, "Vibration absorbers for chatter suppression: A new analytical tuning methodology," *Journal of Sound and Vibration*, vol. 301, pp. 592–607, 2007. DOI: 10.1016/j.jsv.2006.10.020.

[5] S. S. Park, Y. Altintas and M. Movahhedy, "Receptance coupling for end mills," *International Journal of Machine Tools and Manufacture*, vol. 43, pp. 889–896, Jul. 2003. DOI: 10.1016/s0890-6955(03)00088-9.

NVHH2025-0070

Application of Motion Magnification in Automotive Vibration Analysis

K. Horváth[1*], T. Kimpián[1], D. Sulc[2], S. Gungl[1]

[1]thyssenkrupp Components Technology Hungary Ltd.,
Budapest, Hungary

[2]Department of Artificial Intelligence and Systems Engineering,
Budapest University of Technology and Economics, Budapest, Hungary

[*]Corresponding author, e-mail: kristof.horvath@thyssenkrupp-automotive.com

Summary

This study explores the application of motion magnification, a visual technique, for vibration analysis at the automotive component level. Optical methods offer superior spatial resolution and intuitive visual results compared to traditional hammer and accelerometer modal analysis. Although motion magnification provides a robust qualitative tool for developmental insights and troubleshooting, its use for precise measurements is currently limited by camera system constraints: detectable vibration amplitudes are near the threshold typical of vibroacoustic phenomena in automotive steering systems. Here, we detail the applied methodology, present evaluation results from different environments and components, and discuss the inherent limitations and potential bottlenecks.

Introduction

In the automotive industry, noise and vibration control has become increasingly challenging with the shift to electric drivetrains. The removal of the internal combustion engine reduces the overall noise of the vehicle by up to 20 dB, exposing secondary sources such as electric power-assisted steering systems (EPAS). These systems are complex and nonlinear, with multiple potential noise-inducing mechanisms, making accurate characterization essential for meeting strict acoustic targets.

Understanding the dynamic behavior of components is critical to diagnosing issues and validating simulation models. Finite element (FE) methods can predict full-field structural responses, but conventional measurement techniques, such as accelerometers or strain gauges, capture data only at discrete points. This mis-

match limits model correlation, and physical sensors can introduce mass loading, alter structural dynamics, and require labor-intensive installation.

In recent years, video-based approaches have expanded the capabilities of optical methods. Among these, motion magnification has emerged as a powerful qualitative tool, visually amplifying subtle motions in structures to reveal mode shapes and vibration patterns. By providing intuitive insights into complex dynamics without altering the test object, it complements conventional quantitative analysis and can be applied across a range of components and environments.

Motion Magnification

Motion magnification is a technique used to amplify subtle motions in video sequences, making them visible to the human eye. This is achieved by non-photorealistically manipulating the visual motions in the video, either by tracking the trajectories of moving objects (Lagrangian methods) or by manipulating the motions at fixed positions (Eulerian method [1] and phase-based method [2]).

Phase-based Motion Magnification

Phase-based motion magnification works by amplifying small motions through direct manipulation of a signal's phase. To illustrate the principle, consider a one-dimensional sine wave moving along the x-axis. This motion can be expressed as a time-varying phase shift. The image pixel intensity $I(x,t)$ as a function of spatial position and time can be written as

$$I(x,t) = r \cdot \cos\left(2\pi f x + \phi(t)\right) \tag{1}$$

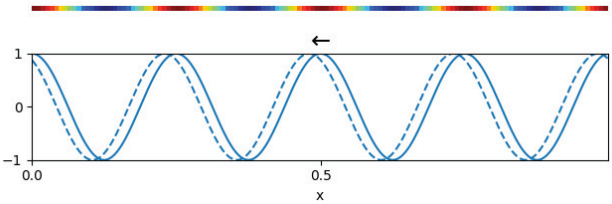

Figure 1: Simple moving sine wave in 1D

From the recorded discrete signal, we can obtain its phase via the analytic signal representation. A real-valued signal has a spectrum with Hermitian symmetry, meaning the negative frequency content is redundant. By discarding the negative

frequencies, we obtain a complex-valued analytic signal, which is equivalent to the original signal plus its 90°-shifted Hilbert transform. The angle of this complex signal gives the instantaneous phase at each position.

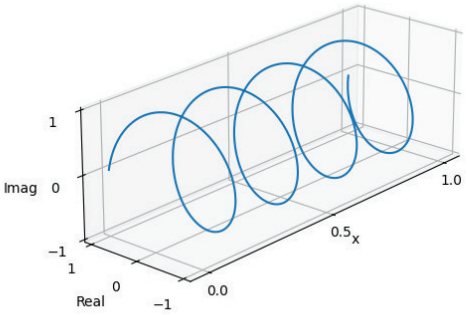

Figure 2: Analytic signal representation

If the signal moves, the change in phase at a fixed spatial position over time directly relates to the displacement. By subtracting the phase at a reference time (e.g., t = 0), we get the relative phase change $\phi(t)$, which tracks the motion. This relative phase can be scaled by a factor λ then used to synthesize a signal with amplified motion:

$$\hat{I}(x,t) = Re\{r \cdot e^{j2\pi fx+\lambda\phi(t)}\} \tag{2}$$

Of course, a real measurement signal will contain many frequency components. Also, extending this idea to images introduces another challenge: motion can occur in any direction on the 2D image plane. Phase-based motion magnification addresses these via complex steerable Laplacian pyramids. The Laplacian decomposition isolates spatial frequency bands, steerability allows orientation-specific motion analysis, and the complex form retains only positive spatial frequencies for straightforward phase extraction similarly as described here. By amplifying the phase in each band and direction, then reconstructing the pyramid, we obtain a video with subtle motions magnified.

Temporal Aliasing

According to the Nyquist–Shannon sampling theorem, a signal must be sampled at least twice its bandwidth to avoid distortion. For accurate temporal analysis, especially in vibration or acoustic studies, a sampling rate of at least ten times the signal frequency is generally recommended. However, most commercially available high-resolution cameras operate below 200 fps, which is insufficient for directly capturing high-frequency motion.

One practical workaround is to exploit temporal aliasing. If the signal of interest is narrowband, the camera's frame rate can be deliberately set below the signal frequency, causing the motion to be aliased into a much lower apparent frequency. This is effectively a form of undersampling, where the high-frequency oscillation is shifted ("folded") into the baseband. By ensuring a short exposure time and precise shutter control, each frame captures a sharp snapshot of the motion at a different phase. Over many periods, this produces a slow-motion sequence that can be analyzed as if recorded at a much higher sampling rate.

Applications

Phase-based motion magnification offers a valuable non-contact alternative for measuring the dynamic response of structures, particularly in cases where traditional sensors may alter the system's behavior. This is especially important for lightweight components or systems where the added mass of accelerometers can significantly shift resonance frequencies and mode shapes.

A first proof-of-concept investigation involved measuring the vibrational orders of an empty electric motor housing. Despite the absence of physical sensors, the method successfully revealed previously identified deformation patterns such as ovalization and triangularization modes.

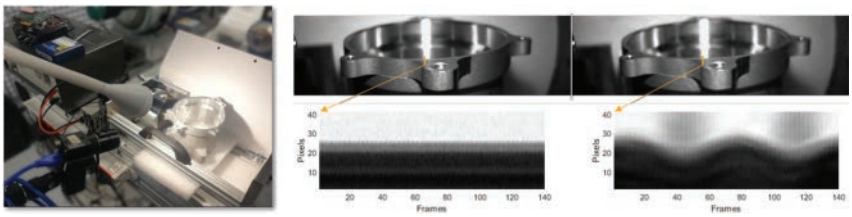

Figure 3: Motor housing shaker measurement

The method also demonstrated its effectiveness in validating FEA simulations, particularly in assessing the shape and frequency of bending modes in the rotor

shaft and pulley assembly.

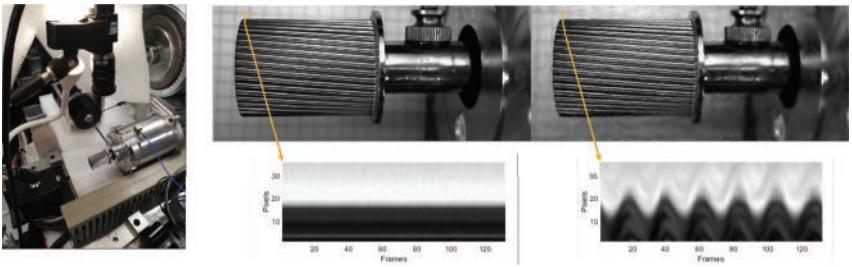

Figure 4: Rotor shaft and pulley mode shape identification

The technique is also highly effective for analyzing rotating or moving parts that are inaccessible to contact sensors. For instance, in automotive electric power steering systems with belt drives, the belt's resonance frequencies can amplify torque ripple harmonics, potentially making them audible in the passenger compartment. Motion magnification enables a detailed visualization of the belt's dynamic behavior, facilitating the identification of dominant orders and resonances that contribute to noise and vibration issues.

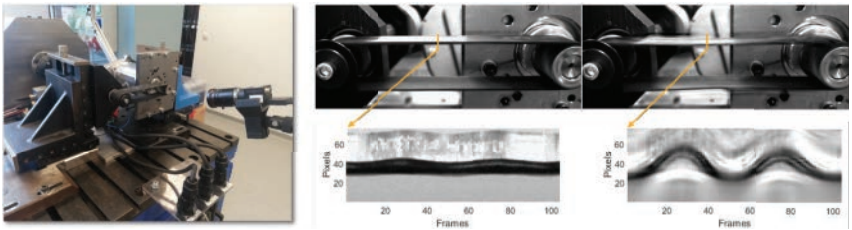

Figure 5: Operational belt measurement

Summary

This work presents an intuitive explanation of phase-based motion magnification, a technique that amplifies subtle motions by manipulating the phase of a signal. To capture high-frequency phenomena with limited-frame-rate cameras, temporal aliasing is employed to down-convert narrowband motion into a lower, observable frequency range. Demonstrated applications include non-contact modal analysis of lightweight structures, propeller blades, and rotating components such as automotive steering system parts.

Acknowledgements

The authors would like to express their gratitude to thyssenkrupp Components Technology Hungary Ltd. for making this research project possible and to all the exceptional colleagues who provided insight and expertise.

References

[1] H.-Y. Wu, M. Rubinstein, E. Shih *et al.*, "Eulerian video magnification for revealing subtle changes in the world," *ACM Trans. Graph. (Proceedings SIGGRAPH 2012)*, vol. 31, no. 4, 2012.

[2] N. Wadhwa, M. Rubinstein, F. Durand and W. T. Freeman, "Phase-based video motion processing," *ACM Trans. Graph. (Proceedings SIGGRAPH 2013)*, vol. 32, no. 4, 2013.

NVHH2025-0071

Stochastic Shimmy in Towed Wheels: Experimental Characterization of Road-Induced Random Vibrations

Xiaolei Du[1*], Akos Miklos[2], Gabor Stepan[2]

[1] Northwestern Polytechnical University, School of Mechanics, Civil Engineering and Architecture, Xi'an, China

[2] Budapest University of Technology and Economics, Department of Applied Mechanics, Faculty of Mechanical Engineering, Budapest, Hungary

[*]Corresponding author, e-mail: duxiaolei970315@163.com

Summary

An experimental setup has been built up to verify stochastic effects on shimmy dynamics of a towed wheel system such as random transitions, with measurements confirming agreement with simulations.

Introduction

Shimmy is a self-excited oscillation that can occur in towed wheel systems, posing significant risks, particularly in aircraft landing gears. In practice, stochastic loads such as road unevenness and crosswinds interact with system nonlinearities, potentially inducing shimmy and leading to stochastic P-bifurcations and random jumps in the dynamic response.

Motivation and goals

A finite element-designed spring as shown in Fig. 3 was attached to the kingpin, with its other end connected to the shaker. A stochastic colored noise signal with the frequency range restricted to 0.1 to 10 Hz shown in Fig. 4 was generated on a laptop and transmitted to the shaker, providing additional stochastic excitation to the towed wheel system to simulate the noise from road unevenness in real world.

As shown in Table 1, the simulation results demonstrate that closer proximity to the kingpin position (l_s) correlates with higher spring stiffness (k), leading to increased stochastic switching and more pronounced stochastic effects.

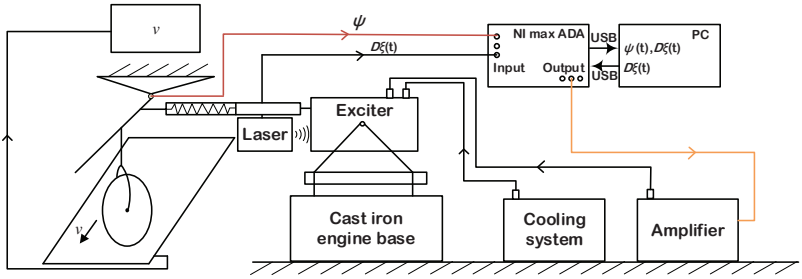

Figure 8: The Schematic of the experiment setup.

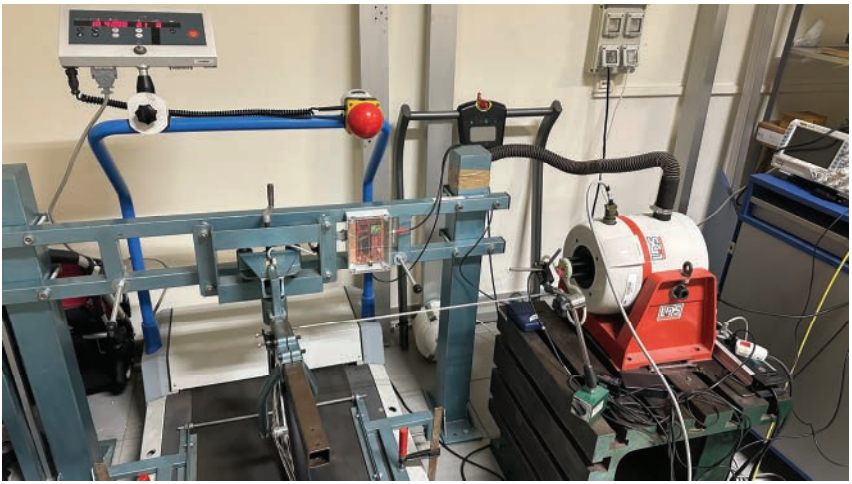

Figure 2: Experiment setup.

Figure 3: The finite element-designed spring.

Table 2: The simulation results.

	l_s=0.005 m	l_s=0.010 m	l_s=0.015 m	l_s=0.020 m	l_s=0.025 m	Time history
k=500 N/m	No transition	No transition	No transition	No transition	No transition	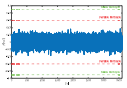
k=750 N/m	One transition	One transition	One transition	One transition	One transition	
k=100 0 N/m	2-3 transitions	2-3 transitions	2-3 transitions	2-3 transitions	1-2 transitions	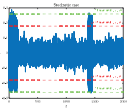
k=125 0 N/m	>10 transitions	>10 transitions	8-10 transitions	8-10 transitions	4-5 transitions	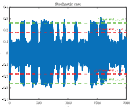

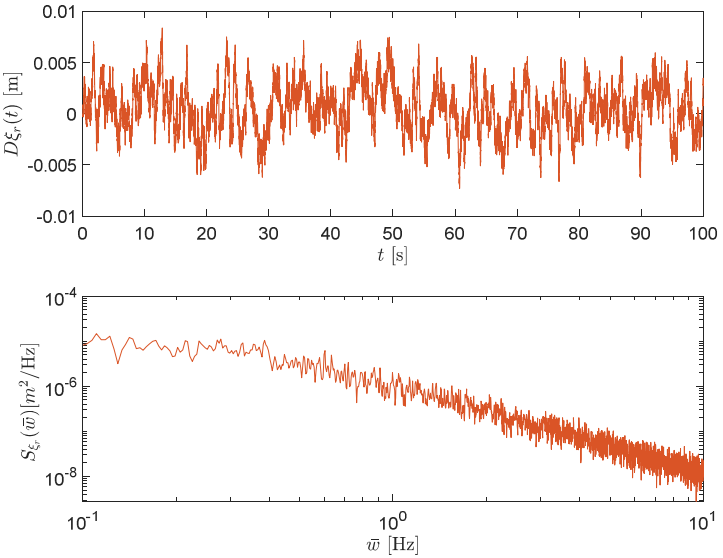

Figure 4: The stochastic colored noise.

Results and discussi□n

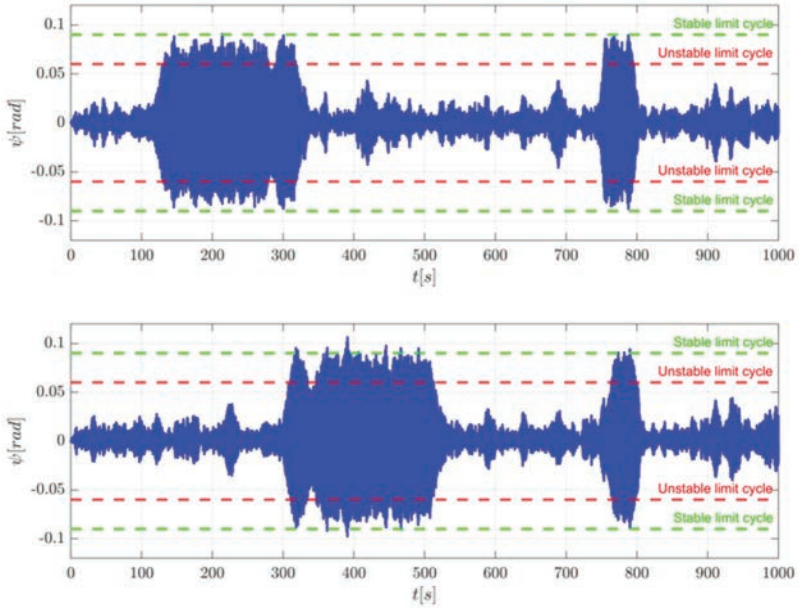

Figure 5: Measurements at v=2.1 km/h.

Experimental data indicates that transitions were observed in the measurements at v = 2.1 km/h, confirming the stochastic effects. These dynamic state transitions, triggered by random excitations, reveal the system's extreme sensitivity to microscopic perturbations. When external excitation amplitudes exceed a critical threshold, the system abruptly shifts from stable straightforward rolling to severe shimmy oscillations.

Conclusions

Shimmy dynamics of a towed wheel model under random excitation is discussed experimentally. It is shown that random transition appears. The stochastic-induced instability poses significant risks to engineering safety, accelerating tire wear and mechanical fatigue while potentially leading to catastrophic consequences such as vehicle directional loss, underscoring the necessity of developing nonlinear dynamic equations with stochastic terms for accurate shimmy predictions and system optimization. The findings highlight the interplay between randomness and nonlinearity in low-speed dynamics, demanding attention in industrial applications to mitigate operational hazards.

References

[1] Yang A, Axas J, Kádár F, et al. Modeling Nonlinear Dynamics from Videos. Nonlinear Dynamics. 2024, 1-29.
[2] Lenkutis T, Cerskus A, Sesok N, Dzedzickis A, Bucinskas V. Road surface profile synthesis: Assessment of suitability for simulation. Symmetry, 2020, 13(1): 68.
[3] Beregi S, Takács D. Analysis of the tyre–road interaction with a non-smooth delayed contact model. Multibody System Dynamics, 2019, 45: 185-201.

Acoustic fun facts

We all know that both random and impulse excitations have a flat frequency spectrum. From an acoustical point of view, they are like twins. But how is that possible, if there is nothing similar in them? Or maybe? Consider a raindrop splashing on a hard surface – it's like an impulse, isn't it? Now imagine the sound of millions of raindrops falling on rocks (i.e. a "continuous" impulse). That is: a waterfall. What is the sound of a waterfall like? ☺

Good to know: even though the frequency spectra of the two signals are quite similar, their phase characteristics are different – random for random noise, and coherent for impulse excitation – resulting in different time-dependent responses.

NVHH2025-0072

A case study on merging dispersed modes due to mass placement using impulse dynamic subspace

T. Kimpián[1], Z. Dombovari[2*,3],

[1]thyssenkrupp Components Technology Hungary Ltd., Budapest, Hungary
[2]MTA-BME Lendület Machine Tool Vibration Research Group,
Department of Applied Mechanics,
Budapest University of Technology and Economics,
Budapest, Hungary
[3]Department of Applied Mechanics,
Faculty of Mechanical Engineering,
Budapest University of Technology and Economics,
Budapest, Hungary
[*]Corresponding author, e-mail: dombovari@mm.bme.hu

Summary

During modal characterisation of a given structure, it is an often-experienced phenomenon that the natural frequency and the damping factor of a particular mode (or multiple modes) varies due to e.g. successive sensor placements over a spatial point grid. This causes a very special mode dispersion of resonances in the describing frequency response matrix, which can reach such a level, where fitting algorithms may identify multiple neighborhooding spurious non-physical modes instead the correct mode with a physical mode shape. The algorithm presented can be the base of an automated method that is able to recognise, group and merge these spurious modes to the physical one ensuring the required orthogonality in the impulse dynamic subspace domain.

Introduction

The measurement circumstances, signal processing barriers and lack of resources typically prevent the accomplishment of the perfect dynamic testing of a given structure. For example, most of the cases, vast amount of sensing points and directions are available for capturing kinematical properties, but only few excitation points and directions can be appropriately utilized [1].

Sensors and exciters do influence the measurement, or more specifically the content of the acquired signal. For example, position and velocity sensors both need

some form of reference point, where isolation might be an issue, while acceleration sensors and electromagnetic exciters (shakers) attach moving mass to the structure. According to the usual measurement practice we rarely place shakers to different locations, rather we relocate the acceleration sensor and eventually its mass with it (rowing accelerometer method). Depending on the reflected mass of the select point and direction of the structure the influence can stretch from drastic or insignificant, but it is always practically present except when a sensor is theoretically on a nodal point or line.

This causes a problem during modal characterisation, when the characteristic exponents (poles), related to the mode, slightly deviate or disperse due to the uneven mass loading effect. This perturbs the resonant 'peaks' preventing any recognition of mode shapes in a conventional manner since all sensor location has slightly different resonant peaks.

The case study presented here shows the possibility to use the so-called Impulse Dynamic Subscpace (IDS, [2]) description to merge modes essentially transforming the base spanned by the so-called singular Impulse Response Functions (IRFs).

IDS description and its modification

The IDS is a modal reduction methodology based on the Green kernel representation of the homogeneous dynamics

$$\mathbf{x}(t+\theta) = \int_0^\infty \mathbf{G}(\theta,\vartheta)\mathbf{F}^-(t-\vartheta)\mathrm{d}\vartheta, \quad \mathbf{G}(\theta,\vartheta) = \sum_k \sigma_k \mathbf{V}_k(\theta)\mathbf{W}_k^{\mathsf{H}}(\vartheta), \quad (1)$$

where $\mathbf{F}^-$ represents the initial forcing, which is the alternative description to the initial condition in differential formalism. The kernel of the free dynamics is represented by the Green function $\mathbf{G}$ in (1), which is simply defined through the IRFs as $\mathbf{G}(\theta,\vartheta) = \mathbf{h}(\theta+\vartheta)$. These are originated as $\mathbf{h}(\theta) = (\mathscr{F}^{-1}\mathbf{H}(\omega))(\theta)$ from the Frequency Response Functions (FRFs), which acquisition is a common practice in the industry.

In this description (1), two consecutive singular values ($\sigma_{2(m-1)+1,2m}$) represent a mode m with its corresponding left- and right-singular IRFs $\mathbf{V}_{2(m-1)+1,2m}(\theta)$ and $\mathbf{W}_{2(m-1)+1,2m}(\vartheta)$, respectively. These vectors form a unitary complete base under a scalar product definition.

The idea of this study lies on the modification of these singular functions with time- and amplitude rescaling mode-by-mode with $\psi_m(x)$ and $\kappa_m(x)$. This gives

a possibility for the reconstruction of the modified dynamics utilizing the above properties given by:

$$\tilde{\mathbf{h}}(\theta) := \tilde{\mathbf{G}}(\theta,0) := \sum_{m=1}^{M}\sum_{l=1}^{2} \sigma_{2(m-1)+l}\tilde{\mathbf{V}}_{2(m-1)+1}(\theta)\tilde{\mathbf{W}}_{2(m-1+1)}(0). \qquad (2)$$

The modified singular-IRF functions defined as

$$\begin{aligned} \tilde{\mathbf{V}}_{2(m-1)+l}(\theta) &:= \kappa_m(\theta)\,\mathbf{V}_{2(m-1)+l}(\psi_m(\theta)) \quad \text{and} \\ \tilde{\mathbf{W}}_{2(m-1)+l}(\vartheta) &:= \kappa_m(\vartheta)\,\mathbf{W}_{2(m-1)+l}(\psi_m(\vartheta)), \end{aligned} \qquad (3)$$

where $\kappa_m(x) := \alpha_m e^{\beta_m x}$ and $\psi_m(x) := \gamma_m x$. The parameters β_m's and γ_m's are modifying the damping and oscillation properties of the given mth influenced mode, while α_m's ensure the unitarity of the modified-IRFs.

Field Study

The following example of a rowing accelerometer modal analysis are from EPAS (Electric Power Assisted Steering) motor NVH (Noise Vibration and Harshness) testing, where the PMSM (Permanent Magnet Synchronous Motor) of the steering system is mounted on a testbench and connected to a hysteresis brake (Fig. 1a).

The measurement points of the angular vibration are numbered and denoted by varying i for sensing and $j = 1$ for excitation shown in Fig. 1. The details of the measurements between the phase currents and the angular acceleration can be found in [3].

Three dominant distinct modes can be recognized in the original FRF set with arbitrary units (a.u.) in Fig. 1bd. The one around 1.2 kHz is very much effected by the acceleration sensor placement spreading the mode in the 1200 and 1240 Hz range.

Applying the above discussed methodology by avoiding appropriate normalization the modes can be corrected by the rescaling of the left- and right-singular IRFs bases shown in (3)

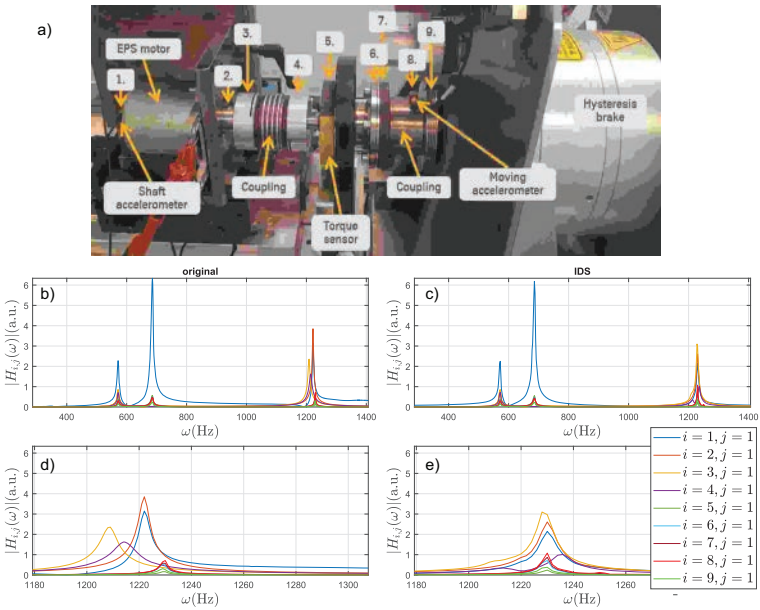

Figure 1: a) shows the measurement setup of PMSM in the NVH test bench loaded by hysteresis brake. Subfigure b and d shows the original measurement, while c and d the corrected measurement by applying rescaling of the IDS base (3).

It can be well seen, that the frequency deviation in the FRFs practically vanishes, therefore the mass loading effect of the accelerometers are corrected.

Conclusion

In this work, we presented a possible application of the Impulse Dynamic Subspace (IDS) to deal with mode dispersion. This scattering of the modes usually appears during acceleration sensor rowing, when the mass of the sensor(s) add(s) to the reflected mass of the structure influencing its dynamic properties. The transformation on the singular-IRFs is capable of compensate the dispersion, however phase compensation might need to be added additionally to avoid the non-physical representation of the mode (see $i = 7$ in Fig. 1e).

By using this methodology multi-input and multi-output (MIMO) dispersed FRFs can be fixed without performing any ad-hoc and/or computationally heavy signal processing or any conventional fitting, which is extremely difficult to perform if disperse modes are apparent.

References

[1] D. Ewins, *Modal Testing: theory, practice, and applications*. Research Studies Press, 2000.

[2] Z. Dombovari, "Dominant modal decomposition method," *Journal of Sound and Vibration*, vol. 392, pp. 56–69, 2017.

[3] T. Kimpián and F. Augusztinovicz, "Torsional modal analysis made easy – methodology and practical examples from electric motor testing," in *Proceedings of ISMA2022-USD2022, International Conference on Noise and Vibration Engineering. Leuven, Belgium*, 2022, pp. 4187–4201.

KNORR-BREMSE
120 YEARS
1905 - 2025

MÁSHOL RUTIN.
NÁLUNK ALKOTÁS.

30
R&D
BUDAPEST
1995 - 2025

KNORR-BREMSE

NVHH2025-0076

Crest-factor-optimized multisine excitation signal for FRF measurements of lightly damped structures

T. Kimpián[1*], F. Augusztinovicz[2]

[1]tyssenkrupp Components Technology Hungary Ltd.,
System and Vehicle Dynamics Department, Acoustics and Signal Processing Team
Budapest, Hungary

[2]Budapest University of Technology and Economics,
Department of Networked Systems and Services, Budapest, Hungary

[*]Corresponding author, e-mail: tibor.kimpian@thyssenkrupp-automotive.com

Summary

A convenient way to characterize a mechanical structure is through its modal description, which can be obtained from measured Frequency Response Functions (FRFs) in various ways. While readily available software packages support the process of modal analysis effectively, tailored solutions can further enhance the quality of measured FRFs in specific situations, leading to more accurate modal models. The acquisition of FRFs for lightly damped structures requires special attention due to their long impulse responses and potentially high vibration amplitudes at resonance frequencies, especially when limited excitation levels or a limited linear range of the tested structure, or both, are factors. In addition to common properties such as bandwidth, resolution, and periodicity, excitation signals can be characterized by their peak-to-RMS ratio, or crest factor, to maximize the Signal-to-Noise Ratio (SNR) of a measurement setup. Several algorithms are available to generate minimum crest-factor multisine signals, which are used to optimize excitation signals for lightly damped structures.

Introduction

Application of multisine signals in FRF measurements are wide-spread and ubiquitous in various fields of engineering. Examples spread from structural dynamics [1], system identification [2] and even radio engineering [3]. The goal of improving the Signal-to-Noise ratio is obtained by maximizing the energy (the RMS value) of the excitation signal while keeping the peak value as low as

possible. This is equivalent to minimizing the crest-factor – the peak over RMS – ratio of the excitation. [2] provides a good example where the excitation and the response crest-factor is minimized at the same time for a known system, however such options are so special, that they are typically not part of commercial measurement software packages.

This work aims to provide a simple online algorithm, that designs the excitation signal in-situ, and reduces the level of excitation where the investigated system has large amplification e.g. at resonances in order to avoid nonlinear distortion in the measured system cased by large vibration amplitudes at those specific frequencies.

The presented algorithm was implemented in MATLAB® using the features of the Audio and DSP toolbox and block processing possibilities utilizing inexpensive hardware components such as a general purpose audio interface hardware and basic passive electrical components for dynamical system modelling.

The online Resonance Response Reduction (R^3) algorithm

Brief outline of the algorithm

In order to determine the necessary excitation spectrum of an arbitrary system, first a rough estimate of the response spectrum is necessary in order to have a starting point for the algorithm. However as the excitation spectrum is getting modified and the amplitude of the excitation is getting reduced at the critical frequencies, the response spectrum also reflects the changes of the excitation spectrum, therefore as the response spectrum changes, it cannot be used as a basis to easily localize the largest amplification of the tested system any longer. If the tested system is close to linear and the SNR is reasonably good, than the FRF preserves the locations of the highest amplification, hence can be used in online algorithms to determine the areas of input excitation reduction explicitly.

Office-testbench setup

In order to manage expensive testbench time, the algorithm has been developed on an “office-testbench” consisting of a high quality USB sound card (ESI U24XL) as audio interface and a very simple electrical circuitry shown in Fig. 1. The only modification that was done on the sound card, is that the internal 33 Ω series output resistors are shorted in order to drive the serial resonator with highest possible current to avoid dips in the excitation spectrum at resonance. The interface was connected to MATLAB® via the Audio Toolbox and the online processing was realized utilizing the system objects from DSP toolbox.

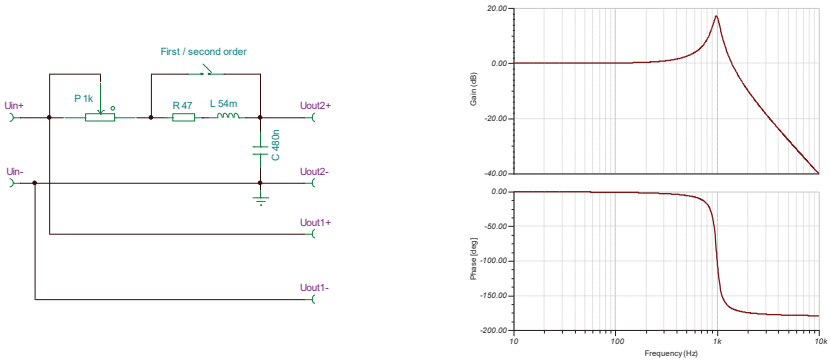

Figure 1: The circuit schematic and the simulated transfer function of the "office-testbench" in second-order, minimum damping mode

The dummy circuitry is essentially a second-order LC low-pass filter with adjustable damping, however by a flip of a switch it can be converted to an adjustable cut-off frequency first order filter as well. The component values have been selected in a way, that the second-order filter can be set to, under-, over-, and critical damping.

Figure 2. shows the experimental setup with the audio interface and the dummy circuitry (left) and the measured FRF in minimum damping condition (right). Of course, for such a simple system the simulated and measured FRFs are close to identical, only the damping differs slightly due to the limited input and output resistances of the sound card.

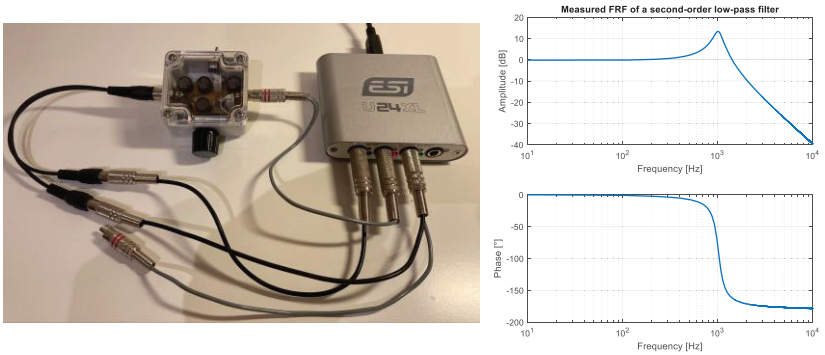

Figure 2: Photo of the "office-testbench" and the measured transfer function of the second-order low-pass filter

Detailed description of the proposed algorithm

As an initialization a random phase multisine is generated according to [4] using the time-frequency domain swapping algorithm with set bandwidth (in this case 10 Hz – 10 kHz) and frequency resolution (2 Hz). The sampling frequency is determined by the audio interface and set to 32 kHz. The most important parameter is the desired amplitude reduction of the peaks in the FRF compared to the highest amplitude point in the specified frequency band.

The generated excitation signal is stored in a circular buffer, from which the necessary amount of samples are passed to the audio interface every cycle, and the acquired data of the two response channels are stored in circular buffers as well. The FRF is calculated between the two recorded channel using an unwindowed H_1 estimator (as the signal is exactly periodic in the circular buffer) and exponential averaging. The peak value of the FRF is determined using maximum search, and the function is cut below the peak values by the user defined maximum reduction parameter. This function is then normalized and inverted thus providing the new amplitude spectrum of the excitation signal and a updated excitation signal is calculated and the circular output buffer is refreshed. After the update of the excitation signal, a few blocks waiting time is inserted, that the response can settle a bit, and the execution of the above sequence is repeated until the excitation spectrum changes less than a predefined threshold. After reaching the threshold, the excitation signal is “frozen”, new spectrum update does not happen, unless, the system changes or the response point is changed (for example as in laser scanning measurements the response measurement point may be altered without switching the excitation off), therefore the data acquisition may begin, and continue until the required amount of data length is reached.

Figure 3. shows the measured transfer function (left column), excitation and response spectra (right column) for different peak reduction values. It can be observed, that the peak of the response spectrum is efficiently “cut-off” avoiding high amplitudes in the response to occur by exactly the predetermined reduction factor shown in the legend. The reason why the response spectra are not exactly flat is because the output impedance of the sound card is not only resistive (e.g. due to a DC decoupling capacitor), therefore a very slight increase can be observed, but otherwise the algorithm performs exactly as expected, and the amount of reduction agrees to the preset value very accurately.

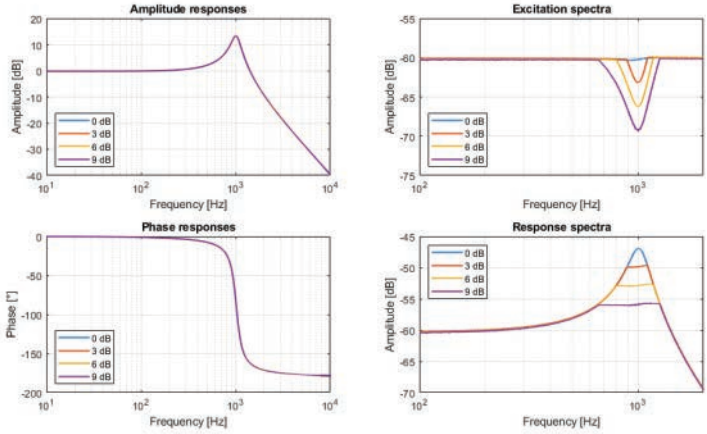

Figure 3: Measured transfer functions of the second-order low-pass filter with different amplitude reduction factors. The measured FRFs are identical (left column), while the excitation and the response spectra (right column) are showing the desired reductions (0, 3, 6, 9 dB) clearly.

Conclusions and future work

This case study introduces the Resonance Response Reduction (R^3) algorithm that generates the amplitude spectrum of a multisine signal in a way that the excitation level of resonant peaks can be reduced by a user defined amount. The proposed algorithm works online, therefore it can adapt to changes in the system, e.g. when the output measurement point is being moved along the structure.

The main idea behind the R^3 algorithm is that it uses the measured FRF to accurately determine the highest amplifications of the measured system, and reduces the excitation in the vicinity of resonances, until a user predefined threshold to avoid non-linear effects to arise due to high response amplitudes. As soon as the FRF settles and the excitation spectrum reaches equilibrium for a specific response point the excitation spectrum update is frozen to provide a stable periodic excitation for the required time to do the necessary averaging for the FRF acquisition. Once the response point and therefore the FRF changes, the algorithm reiterates the excitation spectrum again until a new equilibrium is reached when the measurement of the next response point can be initiated.

The demonstration of the R^3 algorithm is realized on a small “office-testbench” setup, that consists of a resonant system realized using passive electronic

components and an audio interface for excitation and response data acquisition. All calculations are implemented in MATLAB® utilizing Audio Toolbox to stream data to- and from the sound card, and DSP toolbox system objects for the fast blockwise processing of the incoming and outgoing data.

In this case study the phase spectrum of the multisine has not been updated in the optimization loop, therefore the crest-factor of the excitation signal degraded somewhat compared to the originally designed excitation. However with a higher excitation amplitude reduction a small loss of crest-fact does not have any significant impact on the obtained FRF.

Future work may include the complete optimization of the excitation signal with various methods beyond time-frequency domain swapping as many other and possibly more sophisticated algorithms are known in the literature, and testing the algorithm on mechanical structures to prove that high amplitude nonlinear behavior can be avoided using the R^3 algorithm.

Acknowledgement

The author wishes to express his gratitude to many wonderful colleagues at thyssenkrupp Components Technology Hungary Ltd., and special thanks to Zoltan Dombovari for the fruitful discussions on the topic, that gave invaluable ideas inspiring the methods outlined in this study.

References

[1] T. Kimpián, F. Augusztinovicz, “Torsional modal analysis made easy – Methodology and practical examples from electric motor testing” in *Proceedings of ISMA2022 International Conference on Noise and Vibration Engineering USD2022 International Conference on Uncertainty in Structural Dynamics*, W. Desmet, B. Pluymers, D. Moens, S. Neeckx, Place: Leuven, Belgium, 8-10 September 2024, pp. 4187-4201, ISBN 978-90-828931-5-1

[2] P. Guillaume, J. Schoukens, R. Pintelon, I. Kollar, “Crest-factor minimization using nonlinear Chebyshev approximation methods”, *IEEE Transactions on Instrumentation and Measurement*, vol. 10, no. 6, December 1991, pp. 982-989, DOI: 10.1109/19.119778

[3] B. Cseppentő, A. Retzler, Zs. Kollár, “Optimization of the Crest Factor for Complex-Valued Multisine Signals” *Radioengineering*, Vol. 32, No. 2, June 2023, pp. 264-272, DOI: 10.13164/re.2023.0264

[4] E. Van der Ouderaa, J. Schoukens, J. Renneboog, “Peak factor minimization using a time-frequency domain swapping algorithm”, *IEEE Transactions on Instrumentation and Measurement* (Vol. 37, No. 1, March 1988), pp. 145-147., DOI: 10.1109/19.2684

NVHH2025-0077

Dynamic force measurements on flexible workpieces

D. Hajdu[1,2*]

[1]Department of Applied Mechanics, Faculty of Mechanical Engineering, Budapest University of Technology and Economics, Muegyetem rkp. 3., H-1111 Budapest, Hungary

[2]MTA-BME Lendület Machine Tool Vibration Research Group, Department of Applied Mechanics, Budapest University of Technology and Economics, Budapest, Hungary

[*]Corresponding author, e-mail: hajdu@mm.bme.hu

Summary

Dynamic cutting force measurements during milling operations present challenges, particularly at high cutting speeds. The workpieces fixed onto dynamometers are not completely rigid, and the tool-tip-point can be distant from the sensor locations. These factors, along with the modes of the workpiece, affect the measurement signals, while inertial forces further distort the data. To address these issues, special compensation techniques are essential for eliminating the dynamical effects and extracting the real cutting forces during the process. This work proposes a compensation method that utilizes not only the output signals of the dynamometer but also additional sensor data, such as accelerometers.

Introduction

Cutting force measurements in milling operations are key steps in process preparation and planning, tool design, cutting characteristics identification, and validation. The forces determine the power consumption of the machine, the required torque, but they are also important quantities in the mathematical analysis of the dynamical models [1]. The surface quality of machined workpiece, the static deformation, and stability of the process are all affected by the accurate description of the relation between the vibrations, cutting kinematics and empirical force characteristics.

Accurate modelling of the chip formation by means of numerical simulations is extremely challenging and it is also loaded by many uncertainties. Still nowadays, the finite element methods (FEM) are too complicated, complex, time-consuming, and still not reliable enough to replace experimental cutting

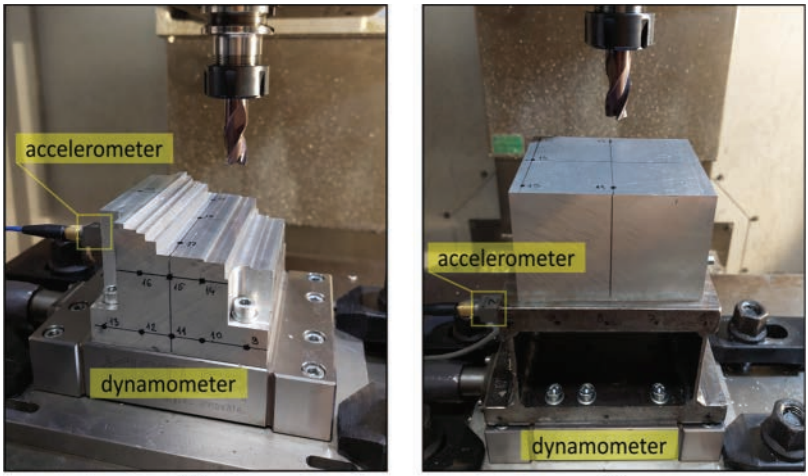

Figure 9: Experimental configuration on a Kistler dynamometer with a (a) relatively rigid workpiece and (b) highly flexible workpiece.

tests performed on real workpieces. Moreover, model validations also need to be done using dynamometers (see Fig. 9), where the workpiece dynamics cannot be completely ignored. The accurate measurements and model validations need the best signal processing techniques that can ensure the highest accuracy.

Dynamic compensation

The compensation technique is based on the experimental modal analysis of the workpiece mounted onto the dynamometer [2]. Impulse hammers are used to generate the excitation force F_e, which is ideally normal to the surface (its normal direction is indicated by $\mathbf{n}$). During the modal analysis, the excitation point coordinate is marked by $\mathbf{r}_e$, which results in the forcing vector $\mathbf{F}_e$ and moment vector $\mathbf{M}_e$ in the frequency domain as

$$\mathbf{F}_e(\omega) = \mathbf{n}F_e(\omega) \quad \text{and} \quad \mathbf{M}_e(\omega) = \mathbf{r}_e \times \big(\mathbf{n}F_e(\omega)\big). \tag{7}$$

The signals of the dynamometer channels are amplified and postprocessed to obtain the measured forces (by the dynamometer sensors) $\mathbf{F}_d$ and moments $\mathbf{M}_d$. Normally, especially at low frequencies, the signal transmission is close to unity if the sensors are accurately calibrated. However, this is far from ideal in the dynamic cases, where the vibrating mass adds the effect of the inertial forces to the signal. To compensate such effects, accelerometers are mounted onto the

workpiece close to the excitation points, where it is possible. The accelerations $\mathbf{A}$ are recorded parallel with the hammer force and dynamometer signals. The transfer function matrix between the input excitation vectors (forces $\mathbf{F}_\mathrm{e}$ and moments $\mathbf{M}_\mathrm{e}$), and output signals (forces $\mathbf{F}_\mathrm{d}$, moments $\mathbf{M}_\mathrm{d}$, acceleration $\mathbf{A}$) is indicated by $\widehat{\mathbf{H}}(\omega)$, i.e.,

$$\begin{bmatrix}\mathbf{F}_\mathrm{e}(\omega)\\ \mathbf{M}_\mathrm{e}(\omega)\end{bmatrix} = \widehat{\mathbf{H}}(\omega)\begin{bmatrix}\mathbf{F}_\mathrm{d}(\omega)\\ \mathbf{M}_\mathrm{d}(\omega)\\ \mathbf{A}(\omega)\end{bmatrix}. \tag{8}$$

In most cases, the experiment requires repetitive measurements at different points of the workpiece to reduce the effect of uncertain excitation, noise, calibration errors, etc. Therefore, all measured data can be ordered into a large redundant linear matrix equation, written shortly as $\mathbf{C}(\omega) = \widehat{\mathbf{H}}(\omega)\mathbf{B}(\omega)$, where the input and output matrices are constructed as

$$\mathbf{C}(\omega) = \begin{bmatrix}\mathbf{F}_{\mathrm{e},1}(\omega) & \cdots & \mathbf{F}_{\mathrm{e},k}(\omega)\\ \mathbf{M}_{\mathrm{e},1}(\omega) & \cdots & \mathbf{M}_{\mathrm{e},k}(\omega)\end{bmatrix} \text{ and } \mathbf{B}(\omega) = \begin{bmatrix}\mathbf{F}_{\mathrm{d},1}(\omega) & \cdots & \mathbf{F}_{\mathrm{d},k}(\omega)\\ \mathbf{M}_{\mathrm{d},1}(\omega) & \cdots & \mathbf{M}_{\mathrm{d},k}(\omega)\\ \mathbf{A}_1(\omega) & \cdots & \mathbf{A}_k(\omega)\end{bmatrix}. \tag{9}$$

The columns contain k number of independent impulse tests. The solution for the linear system of equations gives the matrix $\widehat{\mathbf{H}}(\omega)$, which is used as a calibration matrix (filter) in the rest of the work. Using the Moor-Penrose pseudo-inverse, the formula is given as

$$\widehat{\mathbf{H}}(\omega) = \mathbf{C}(\omega)\mathbf{B}(\omega)^\dagger = \mathbf{C}(\omega)\mathbf{B}(\omega)^\mathrm{T}(\mathbf{B}(\omega)\mathbf{B}(\omega)^\mathrm{T})^{-1}. \tag{10}$$

During the actual cutting force tests, all signals are recorded, transformed into frequency domain, where the compensation (filtering) matrix applies, and transformed back to time domain, where the rest of the postprocessing can be done if needed. Note that the compensation at low frequencies is not accurate due to the technical limitations of acceleration measurements. Therefore, the filter is applied only above a sufficiently small cut-off frequency $\omega_\mathrm{c} > 0$. In the experiments, it was 20 Hz, but it must be adjusted based on the sensors and the system dynamics.

Case study and results

The presented methodology was tested and applied in real case studies, see Fig. 9, where relatively rigid and highly flexible workpieces were machined. The original measured forces (thin black curve) and compensated forces (thick black curve) are shown in Fig. 10. When the highly flexible workpiece was

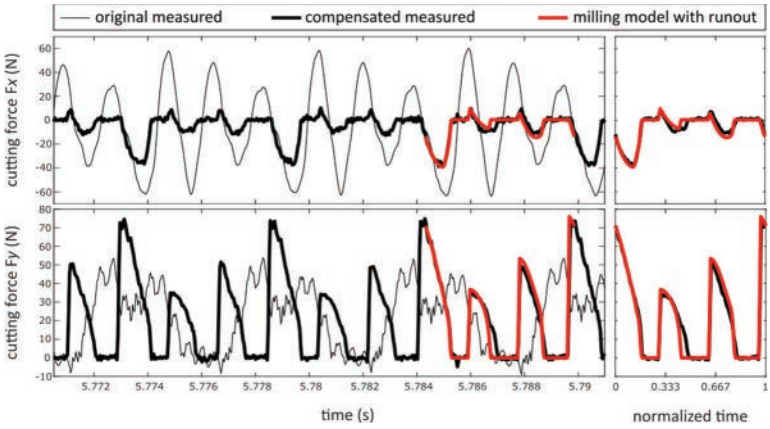

Figure 10: Cutting force signals before and after compensation on a highly flexible workpiece with a three-fluted milling tool, at 10750 rpm.

machined, the low-frequency, but high-amplitude inertial forces could be successfully eliminated using the proposed method (for details, see [**Hiba! A hivatkozási forrás nem található.**]). As a result, only the real cutting forces acting between the tool and the workpiece are seen, which show good agreement with the model-based preliminary calculations (thick red curve). The cutting tool has three symmetrically spaced cutting edges, but the radial tool runout significantly changes the force distribution between the flutes. The magnitude of tool runout can be determined using the compensated signals.

Acknowledgement

The research reported in this paper and carried out at BME has been supported by the Hungarian National Research, Development and Innovation Office (NKFI-KKP-133846).

This paper was supported by the János Bolyai Research Scholarship of the Hungarian Academy of Sciences.

References

[1] D. Hajdu, O. Franco, M. Sanz-Calle, G. Totis, J. Munoa, G. Stepan and Z. Dombovari, “Stable tongues induced by milling tool runout”, *International Journal of Machine Tools and Manufacture*, vol. 206, pp. 104258, 2025.

[2] D. Bachrathy and G. Stepan, “Cutting Force Measurements in High Speed Milling - Extension of the Frequency Range of Kistler Dynamometer”, in *39th International MATADOR Conference on Advanced Manufacturing*, 2017.

NVHH2025-0078

Case-study: comparision of building sound insulation (R'w) and laboratory values (Rw) in lightweight constructions

Jaroslav Hruškovič*

VALERON Enviro Consulting s.r.o.,
Laboratory, Bratislava, Slovakia

*Corresponding author, e-mail: jaroslav.hruskovic@valeron.sk

Summary

The case-study analyzes differences between laboratory sound insulation (Rw) and real-world building sound insulation (R'w) in lightweight constructions. A case study compares multiple construction types, revealing that R'w values are often 10 dB lower than Rw due to flanking and construction imperfections. The study emphasizes that relying on theoretical Rw values is risky. Key recommendations include using advanced calculation methods instead of rough estimates, applying tested and certified materials, and validating designs with real-world measurements. The findings highlight the need for precise simulations and practical testing to ensure effective acoustic performance in lightweight buildings.

Introduction

Lightweight building constructions are more sensitive to sound transmission, where even small structural modifications can significantly impact acoustic performance. A common issue in practice is the incorrect estimation of building sound insulation (R'w), often mistaken for laboratory values (Rw). This miscalculation can lead to serious consequences during construction and design, as real-world performance tends to be lower due to flanking and construction imperfections. This study highlights the gap between laboratory and in-situ sound insulation in lightweight constructions. A case study demonstrates how these differences manifest in practice, emphasizing the importance of accurate predictions and proper acoustic design.

The airborne sound insulation index, Rw, is a key parameter used to characterize the acoustic performance of building elements. While laboratory measurements remain the most reliable method for determining Rw, predictive modeling is

increasingly employed during the design phase to estimate sound insulation properties before construction. However, the reliability of such modeling approaches, particularly in terms of their accuracy and statistical consistency, requires thorough validation to ensure their practical usability.

This study focuses on verifying the reliability of Rw modeling methods by comparing predicted values with measured results across a diverse sample of constructions. The aim is to assess not only the applicability and robustness of these modeling techniques but also to determine their statistical characteristics, such as bias, standard deviation, and confidence intervals. The results will help clarify under what conditions and with what level of certainty these methods can be used in engineering practice.

Aim

The aim of this study is to evaluate the reliability of modeling airborne sound insulation (Rw) as a base for further in situ (R´w) calculations in lightweight floor constructions, using commonly available prediction tools during the design phase. By comparing modeled values with laboratory measurements, the research explores the variability and potential deviations inherent in modeling structural compositions “from scratch,” without relying on predefined databases or templates.

Through a structure modeling exercise and statistical analysis, the study provides insight into the practical limitations of current modeling approaches and highlights the importance of accounting for uncertainty when designing for compliance. The findings aim to inform architects, engineers, and acoustic consultants about the necessary safety margins and the potential benefits of introducing verified reference databases to improve prediction accuracy and reduce design risk.

Methods

This study utilized an internal database provided by AMC Mecanocaucho, which contains a wide range of laboratory-tested floor and ceiling assemblies [4]. These measurements were conducted earlier, under laboratory conditions in accordance with the international standard ISO 10140-2, which specifies the procedures for laboratory measurement of airborne sound insulation of building elements [1]. From this database, we extracted detailed descriptions of floor structures along with their corresponding measured Rw values.

A total of 31 different floor assemblies were selected to represent a cross-section of various construction types, with an emphasis on lightweight building structures. The evaluation involved three engineers who are regularly engaged in building acoustics in their professional practice. Each engineer was tasked with modeling the selected assemblies using Insul version 9 software [2]. Importantly, the engineers had no access to the measured laboratory results and were not informed of the actual Rw values. Their objective was to model each structure as accurately as possible based solely on the construction description.

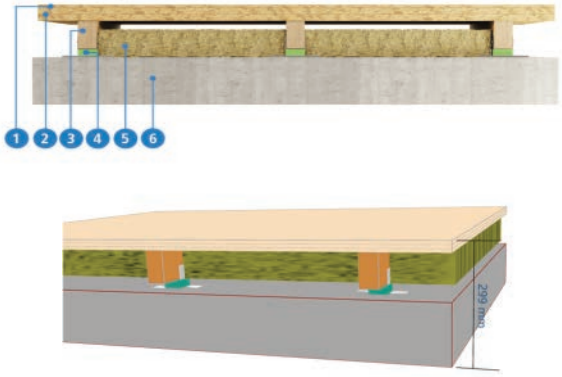

Figure 1: Example of evaluated structure (top) and it's representation in modeling software (bottom)

The results of their simulations were then compared to the laboratory-measured Rw values. In this verification, only the airborne sound insulation index Rw was assessed as a single-number rating. Adaptation coefficients such as C and Ctr, as well as impact sound insulation (Ln,w), were excluded from the scope of this evaluation, due to insufficient data in the AMC internal database.

This process constituted the first iteration of the study. In the second iteration, the engineers were provided with the complete set of their initial modeling results. They were encouraged to compare outcomes together, discuss discrepancies, and apply corrections to their models where appropriate. These revised models were again compared to the measured Rw values.

It should be noted that the engineers started their modeling from scratch, without access to any pre-existing library of known constructions. This ensured that their models were based purely on interpretation of the construction description and not on previous similar cases or incremental adjustments of known assemblies.

The list of all assessed floor assemblies is provided in the Appendix. Each entry includes a textual description of the construction and the corresponding laboratory-measured Rw value. Below is an illustrative example of one of the assessed constructions, along with its representation as modeled in the Insul 9 software environment.

Results

Figure 2. presents a comparison between the measured airborne sound insulation values (Rw) and the results of the first and second modeling iterations. The values were compared without prior access to measured results, and the modeling was based solely on the provided construction descriptions. The second iteration reflects the outcome after the engineers reviewed and discussed their initial results and applied possible corrections to their models.

Some of the assessed constructions, especially those with higher measured Rw values (samples 16-19), show larger differences between measured and calculated values. These instances are visually highlighted for further attention and excluded from the evaluation as during the modeling the modeling software Insul 9 clearly stated that the modelation of such a complex structures is errorneous. In the charts, the x-axis represents the measured Rw values, while the y-axis shows the Rw values obtained through modeling. Each point corresponds to one of the assessed floor assemblies.

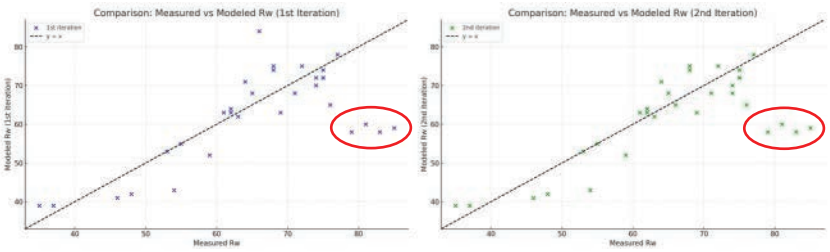

Figure 2: Comparison between the measured and calculated airborne sound insulation values for the first (left) and second (right) iteration

As seen in the graphs, most values are distributed near the y = x line, indicating a general agreement between measured and calculated values. However, a noticeable spread around this line is present, reflecting the variability in modeling accuracy.

Conclusions

This study set out to evaluate the reliability of modeling airborne sound insulation (Rw) using engineering software (in this case, Insul 9 [2]) when the input is based solely on textual and illustrative graphical descriptions of floor assemblies, without access to measured data or pre-calibrated templates. The goal was to understand the magnitude and nature of modeling errors, and to assess whether such an approach is suitable for practical design purposes.

The results show that even experienced professionals, working with diligence and cross-validation, are subject to a significant modeling uncertainty when applying a "from scratch" approach. The standard deviation of the modeling error, after excluding a few extreme outliers, was found to be approximately 4.88 dB. To ensure a 95% probability of success, this uncertainty translates into a required safety margin of nearly 10 dB when designing for compliance. In practical terms, this means that if the target Rw value is 54 dB, a modeled result of 54 dB is only sufficient to offer a 50% likelihood of compliance when measured. To reach a 95% confidence level, the modeled value should instead be approximately 63.8 dB, a +10dB margin.

Such a margin is understandably difficult to justify in many commercial projects. Therefore, the study also points to a promising path forward: the development of a verified and diverse database of typical building constructions. If users could start with pre-modeled structures that closely resemble the design at hand, and apply only small, incremental modifications, the expected modeling error would likely decrease. While this hypothesis still needs verification, additional testing in this study showed that all participants were able to match measured values perfectly, without altering the material or dimensional structure, once they were allowed to fine-tune unspecified input parameters.

In summary, the accuracy of predictive modeling in building acoustics can be significantly improved not only through better tools, but also through better data. A well-maintained database of reference constructions could enable more reliable and efficient acoustic design, reducing the need for overly conservative safety margins while maintaining confidence in compliance.

In practical terms, this means that if the target Rw value is 54 dB, and only the modeling process is considered, a +10 dB margin is needed, resulting in a target of 63.8 dB in software output to ensure a 95% confidence level. This applies only to the laboratory performance.

However, when the objective is to predict in situ performance (R'w) using a full calculation chain, combining the modeling process with the ISO 12354-1 method, the total combined uncertainty must be considered. In that case, the effective standard deviation increases to approximately 5.27 dB, and the required safety margin for 95% confidence becomes approximately 10.55 dB.

In summary:

- For Rw prediction only: use a safety margin of ~10 dB
- For R'w (in situ) prediction using modeling + ISO 12354-1: use a safety margin of ~10.5 dB

These findings underline the need to maintain realistic expectations regarding the accuracy of predictive modeling. In both scenarios, whether estimating only laboratory performance (Rw) or full in situ performance (R'w), it is essential to explicitly account for uncertainty in the design process. By properly incorporating these uncertainties into design targets and safety margins, disappointment after project completion can be avoided, and the acoustic performance of lightweight constructions can be managed with greater reliability and confidence.

References

[1] International Organization for Standardization, *ISO 10140-2: Acoustics Laboratory measurement of sound insulation of building elements Part 2: Measurement of airborne sound insulation*, 2010.

[2] Marshall Day Acoustics, *Insul 9 User Manual*, 2021. [Online]. Available: https://www.insul.co.nz

[3] International Organization for Standardization, *ISO 12354-1: Building acoustics Estimation of acoustic performance of buildings from the performance of elements Part 1: Airborne sound insulation between rooms*, 2017.

[4] AMC Mecanocaucho, *Akustik dBfinder , Laboratory test database*. Online. Available: https://www.akustik.com/en-GB/akustik-dbfinder/

NVHH2025-0082

Comfort-Critical Control in Vehicle Dynamics Using Control Barrier Functions

Adam K. Kiss[1*]

[1]HUN-REN–BME Dynamics of Machines Research Group and
Department of Applied Mechanics, Budapest H-1111, Hungary
[*]Corresponding author, e-mail: kiss_a@mm.bme.hu

Summary

Passenger comfort is a key aspect of vehicle dynamics, influencing user experience and acceptance of automated systems. This paper introduces Comfort-Based Filtering, a novel control strategy that extends Control Barrier Functions (CBFs) to enforce comfort constraints in vehicle motion. The method ensures limited acceleration and jerk by minimally modifying a nominal control input to respect comfort-related constraints.

1. Introduction

Safety-Critical Control (SCC) leverages CBFs to guarantee that system states remain within predefined safe sets [1]. Inspired by this approach, we introduce Comfort-Based Filtering (CBF^2), which extends CBF principles to enforce passenger comfort constraints, ensuring smooth and predictable vehicle behavior.

In vehicle control, abrupt accelerations and high jerks lead to discomfort [2]. The proposed CBF^2 approach integrates these comfort considerations into a real-time control framework that ensures compliance with predefined comfort thresholds while requiring minimal intervention in the nominal control strategy provided by an adaptive cruise control or a human driver.

2. Problem Formulation

We consider a control-affine system:

$$\dot{\mathbf{x}} = \mathbf{f}(\mathbf{x}) + \mathbf{g}(\mathbf{x})\mathbf{u}, \tag{1}$$

where $\mathbf{x} \in \mathbb{R}^n$ is the state vector, $\mathbf{u} \in \mathbb{R}^m$ is the control input, while $\mathbf{f}$ and $\mathbf{g}$ define the system dynamics. Unlike standard safety-critical CBFs, CBF^2 incorporates

constraints on higher-order derivatives such as acceleration and jerk:

$$h_c(\mathbf{x}, \dot{\mathbf{x}}, \ddot{\mathbf{x}}) \geq 0. \tag{2}$$

Forward invariance of the comfort set is ensured by (see more details in [1]):

$$\dot{h}_c(\mathbf{x}, \dot{\mathbf{x}}, \ddot{\mathbf{x}}) + \alpha(h_c(\mathbf{x}, \dot{\mathbf{x}}, \ddot{\mathbf{x}})) \geq 0, \tag{3}$$

where $\alpha(\cdot)$ is a class-$\mathscr{K}$ function enforcing constraint satisfaction.

3. Methodology

CBF^2 modifies a nominal control input $\mathbf{u}_{\text{nom}}$ minimally to ensure comfort-aware behavior. The control input is computed via an optimization problem (OP):

$$\min_{\mathbf{u}} \quad \|\mathbf{u} - \mathbf{u}_{\text{nom}}\|^2 \tag{4}$$

subject to the CBF condition Eq. 3 (see more details and closed form solution in [1]). Higher-order derivatives are approximated using finite differences:

$$\dot{\mathbf{x}}(t) \approx \frac{\mathbf{x}(t) - \mathbf{x}(t - \Delta t)}{\Delta t} \quad \text{and} \quad \ddot{\mathbf{x}}(t) \approx \frac{\dot{\mathbf{x}}(t) - \dot{\mathbf{x}}(t - \Delta t)}{\Delta t}, \tag{5}$$

introducing delay-dependent effects in the CBF condition.

4. Conclusion

CBF^2 extends Control Barrier Functions to enhance passenger comfort in vehicle control systems. By imposing acceleration and jerk constraints, it enables smooth and predictable vehicle maneuvers with minimal controller modifications.

5. Acknowledgements

This project was supported by the János Bolyai Research Scholarship of the Hungarian Academy of Sciences, and by the HUN-REN Hungarian Research Network.

References

[1] A. D. Ames, X. Xu, J. W. Grizzle and P. Tabuada, "Control barrier function based quadratic programs for safety critical systems," *IEEE Transactions on Automatic Control*, vol. 62, no. 8, pp. 3861–3876, 2017.

[2] M. Elbanhawi, M. Simic and R. Jazar, "In the passenger seat: Investigating ride comfort measures in autonomous cars," *IEEE Intelligent transportation systems magazine*, vol. 7, no. 3, pp. 4–17, 2015.

NVHH2025-0094

Analysis of launch-related acoustic loads on a thermal guard assembly

T. Turcsán, PhD[1*], G. Erdős[1], L. Takács, PhD[1]

[1]eCon Engineering Kft., Analysis & Testing Department, Budapest, Hungary

*Corresponding author, e-mail: tamas.turcsan@econengineering.com

Summary

In this paper, we present a Finite Element Analysis (FEA) of a Thermal Guard Assembly (TGA) of an instrument used in space that has to survive a significant amount of vibration loads during the launch of the carrier vehicle. Some of these loads are transferred through the structure, others propagate through the air. The presented FEA concentrates on the latter; the aim was to determine possibly critical stress locations on the TGA structure in frequency range due to acoustic load. For this, an acoustic FE model was built around the TGA structure to model diffuse acoustic loads in a random response analysis with a Power Spectral Density (PSD) profile derived from representative frequency-dependent sound pressure level values. For the random response analysis, a unit acoustic load was determined by using a unit pressure synthetized for all microphone nodes around the TGA structure. The results of PSD analysis are von Mises stresses and relevant accelerations of virtually placed accelerometers on the TGA structure.

Introduction and problem statement

According to the relevant standards (e. g. [1]) there are rigorous criteria for the structures for space applications. Besides other mechanical loads, the structures need to be checked acoustic loads defined by the launch services provides.

As the present thermal guard has large surfaces, the acoustic loads have been deemed critical enough that they need to be checked by calculation already in the design phase – at a later stage, the structure will be tested physically. Such tests are expensive and require specialized hardware: a diffuse acoustic field in the frequency range from 25Hz to 10kHz and an overall noise level of up to 155dB overall sound pressure level (OASPL an equivalent acoustic power of up

to 120 kilowatt) can be achieved in the Large European Acoustic Facility [2]: during the simulation the aim was to reproduce the conditions expected in the measurement scenario as closely as possible.

Model setup

Structure, cavity, measurement points

The acoustic space around of the TGA represented with a 6 m diameter spherical acoustic space as shown in Figure 1. The acoustic space is meshed with a maximal element size that allows the usage of the model up to 1200 Hz with finite elements having pressure degree of freedom only.

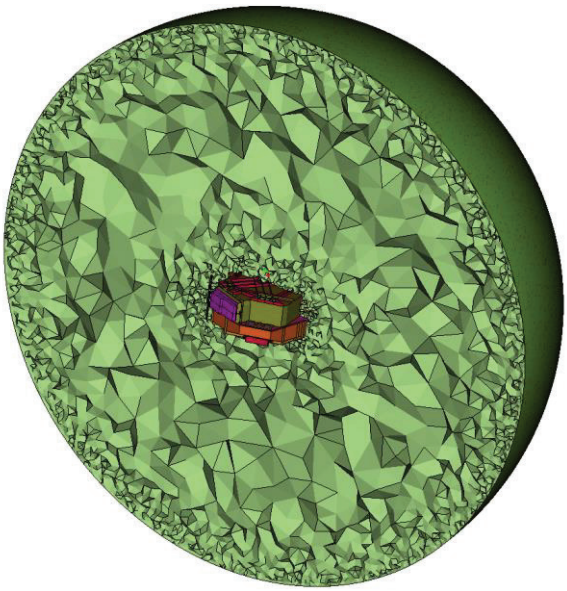

1. Figure Spherical acoustic cavity defined around the structure

The model of the structure itself has been re-used from a previous study focusing on acceleration loads during the launch: the main part of the structure is modelled as mid-surface shell, some additional features are modelled with beams, concentrated and distributed masses and rigid connections.

The material was linear elastic in case of the structure and incompressible air in case of the cavity. There was a uniform 1% modal damping applied. The entire model is linear, thus modal reduction has been possible.

Boundary conditions

The support legs of the structure are fixed rigidly. The boundary conditions of the FE acoustic space are considered as infinite and thus modelled as non-reflecting boundary conditions with Frequency-Dependent Acoustic Absorber Element (CAABSF) with the outer surface of the spherical cavity. The connection between the cavity and the structure were defined with Fluid-Structure Interface Parameters (ACMODL) bulk data entry which assures the coupling.

Loads, simulation setup

The load was defined as diffuse acoustic load. To ensure this, in the physical test 8 microphones are placed at 0.5 m distance from the structure and they should record almost identical pressure levels. The same locations have been used in the model as shown in Figure 2.

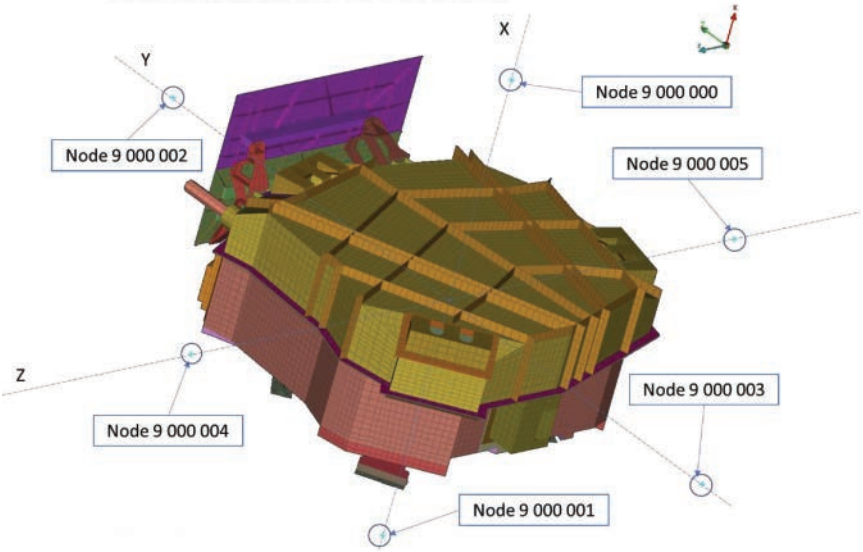

2. Figure Control microphone positions

Acoustic pressure source nodes have been placed on the outer surface of the cavity, and their relative amplitude have been tuned in a pre-simulation to

provide equal pressures in the control points (could be done by algebraic calculations due to the linear model). The final run was a modal frequency response simulation with an upper frequency limit of 1000 Hz and with a prescribed PSD profile provided by the launch service provider.

Evaluation

During the evaluation of the simulation two kind of result quantities have been reported: acceleration as function of frequency in discrete locations and von Mises stress distribution.

Accelerations

Acceleration values were extracted at pre-defined measurement points as function of frequency. The aim of this practice is to provide a validation possibility during the measurement: in a physical test scenario, acceleration sensors are placed in equivalent locations and the values reported can be cross-checked between simulation and measurement.

RMS von Mises Stress

The main result of the calculation has been the RMS von Mises 3σ stress distribution as shown in Figure 3.

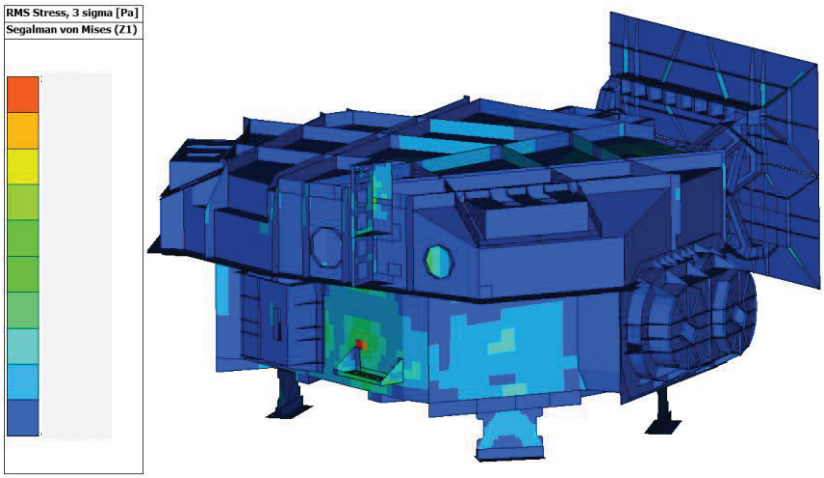

3. Figure Stress field distribution on the structure, exact values hidden

From the stress results, margin of safety has been calculated for the aluminum material of the structure for yield (MoS_y) and for ultimate (MoS_u) strength.

These are calculated according to the following equation (1) and equation (2):

$$\mathbf{MoS_y} = \frac{\boldsymbol{\sigma_{bs,y}}}{\mathbf{\sigma_{ac} \cdot FoS_y \cdot KM \cdot KP}} - \mathbf{1}, \quad (1)$$

and

$$\mathbf{MoS_u} = \frac{\boldsymbol{\sigma_{bs,u}}}{\mathbf{\sigma_{ac} \cdot FoS_u \cdot KM \cdot KP}} - \mathbf{1}, \quad (2)$$

where:

- σ_{ac} is the highest PSD element stress calculated on the investigated part,
- $\sigma_{bs,\,y}$ was the yield strength of the material which value came from material characterization on the aluminum samples,
- $\sigma_{bs,\,u}$ was the ultimate strength of the material which value came from material characterization on the aluminum samples and its results,
- $\mathbf{FoS_y}$ was safety factor for the yield strength,
- $\mathbf{FoS_u}$ was safety factor for the ultimate strength,
- **KM** was model specific safety factor,
- **KP** was project specific safety factor.

The acceptance criteria is a margin of safety above zero. The results in the project provided MoS values around 1 and thus, the design has been accepted.

Conclusions

In the presented case study, the response of a thermal guide assembly has been evaluated for diffuse acoustic load expected during the launch. The structure has been evaluated in a setup mimicking the ground acceptance test, and the stress results have been evaluated. This check in the design phase showed good results thus the design has been accepted for manufacturing. This virtual evaluation ensures that the possible flaws of the structure are identified in an early phase where changes to the design can be implemented with relatively low cost. At a later stage these changes would cause an excessive cost, as due to space industry requirements, the upper and lower shells of the structure are manufactured from large single blocks of aluminum (to avoid welding).

References

[1] ECSS-E-ST-32C Rev. 1 standard, Space engineering - Structural general requirements, ECSS Secretariat ESA-ESTEC, 2008

[2] ESA: Large European Acoustic Facility, technical description, https://technology.esa.int/page/large-european-acoustic-facility

NVHH2025-0099

Experimental study of digital force control with non-proportional damping

Rudolf R. Toth[1*], Daniel Bachrathy[1], Gabor Stepan[1]

[1]Budapest University of Technology and Economics,
Department of Applied Mechanics, Budapest, Hungary
[*]Corresponding author, e-mail: rudolf.toth@mm.bme.hu

Summary

We aim to study the stability of the simple one degree-of-freedom model of digital force control experimentally. This model describes the control task of keeping a constant force between the actuator and a flexible workpiece, while taking into account the effect of using sampled data and zero-order-hold. We use laser based sensors and electromagnetic actuators to achieve force control. The measurements support the theoretical predictions, while some unique scenarios can be identified due to the complex non-proportionally damped nature of the chosen workpiece.

1. Introduction

In this work we investigate the one degree-of-freedom (DoF) model of digital force control experimentally. The digital force control model describes the task of keeping a constant force between the actuator and a flexible workpiece, while taking into account the effect of using sampled data and zero-order-hold (ZOH) [1]. This task has many applications, but achieving stable control is non-trivial due to the sampling delay. In Section 2. we present this model together with our experimental setup. This experimental setup was originally designed for hardware-in-the-loop machining experiments [2], but is programmed to execute force control here [3]. In Section 3. the measurement results are presented that show good agreement with predictions, however the non-proportionally damped nature of the chosen workpiece has some unexpected effects. In the concluding Section 4. some further discussion is granted to these results as well as the challenges and possibilities of accurate modal testing [4].

2. Mechanical model and experimental setup

The one DoF digital force control model is shown in Fig. 1 panel a), while panel b) shows the experimental setup.

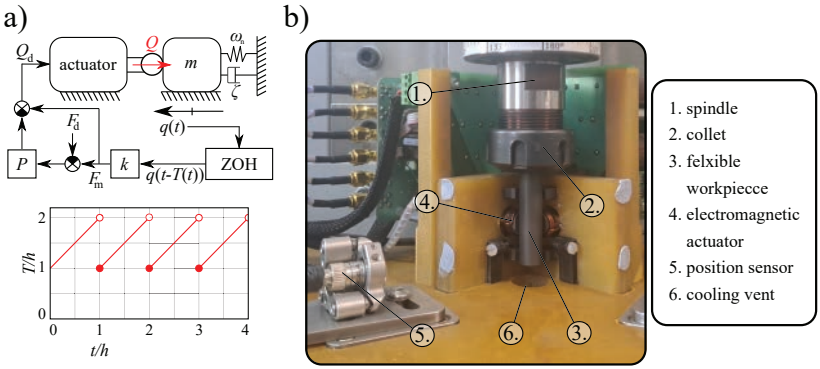

Figure 1: Panel a): The one DoF model of digital force control with the time-dependent time delay due to sampling. Panel b): experimental setup.

The model assumes that the dynamical behavior of the workpiece is captured accurately with a single DoF with angular natural frequency ω_n, damping ratio ζ and stiffness k. In this scenario the discrete-time dynamical system [1] describing the control task with sampling time h and proportional control gain P reads

$$\begin{bmatrix} Q_{j+1} \\ x_{j+1} \\ \dot{x}_{j+1} \end{bmatrix} = \begin{bmatrix} 0 & (1-P)k & 0 \\ \frac{1-\cos(\omega_n h)}{k} & \cos(\omega_n h) & \frac{\sin(\omega_n h)}{\omega_n} \\ \frac{\omega_n \sin(\omega_n h)}{k} & -\omega_n \sin(\omega_n h) & \cos(\omega_n h) \end{bmatrix} \begin{bmatrix} Q_j \\ x_j \\ \dot{x}_j \end{bmatrix}. \quad (1)$$

This equation can be used to predict the stable control parameters h and P by calculating the eigenvalues of the system matrix. The experimental setup presented in panel b) uses laser based position sensors and electromagnetic actuators [2]. The control algorithm is executed on two NI PXIe-8880 real time computers at a 100 kHz sampling rate. This means that we could emulate all sampling rates that are a whole multiple of that 100 kHz [3]. The dominant modal characteristics of the workpiece have been determined to be

$$f_n = 3.1 \text{ kHz}, \ \zeta = 1.95\%. \quad (2)$$

3. Measurement results

Force control was attempted at different sampling time and proportional gain parameters. Stability was determined based on the resulting vibration amplitudes at each measurement point. In Figure 2. panel a) the spectrum of the flexible workpiece is show, while panel b) presents the results of the force control experiments.

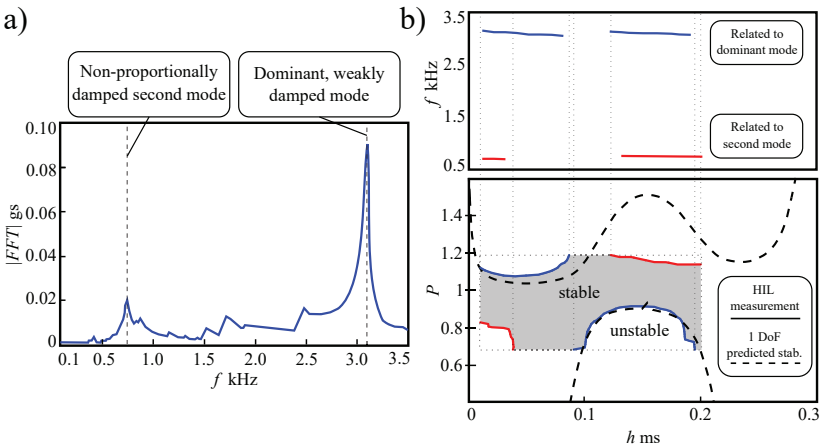

Figure 2: Panel a): Spectrum of the flexible workpiece. Panel b): Digital force control measurement results.

We can see that some of the characteristic curves predicted by the equation (1) were captured accurately (blue curves in Fig. 2. panel b). From the resulting vibration frequencies we can also verify that these stability limits are related to the identified dominant mode with natural frequency of cca. 3 kHz. We can also see, that there are some parameter regions, where the single DoF model is inaccurate (red curves in Fig. 2. panel b). The frequencies also suggest, that these instabilities are related to a non-proportionally damped approximately 700 Hz second mode.

4. Discussion

In this study we experimentally tested sampled data force control. The measurement results were compared to theoretical predictions made by a single DoF model. While some of the predictions proved accurate, the single DoF assumption was not completely adequate as a non-proportionally damped low frequency

mode contributed to unexpected instabilities. We expect that a theoretical prediction made on a two DoF model would resolve the disagreement between our current predictions and the experimental results.

The next step in this study would include building the two DoF model of the workpiece used here. The standard solution is to repeat the modal analysis used to produce the spectrum in Fig. 2. panel a) with measurements made at two points or excitation applied to two different points, ideally both. This would give us the two mode shapes as well as the the two natural frequencies and damping ratios available now.

Consequently, in our experimental setup a two DoF model can be established using an additional sensor or actuator. Generally speaking, in some situations repeating modal measurements might not be possible and predicting the number of DoF in advance can also unreliable. In these cases building models based on limited data would be valuable. This is theoretically possible using delay embedding, however this is outside the scope of this abstract [4].

Acknowledgements

The research reported in this paper has been supported by the Hungarian National Research, Development and Innovation Office (NKFI-KKP-133846).

References

[1] G. Stepan, ”Vibrations of machines subjected to digital force control”, *International Journal of Solids and Structures*, vol. 38, no. 10-13, pp. 2149-2159, 2001.

[2] B. Beri, A. Miklos, D. Takacs, G. Stepan, ”Nonlinearities of hardware-in-the-loop environment affecting turning process emulation”, *International Journal of Machine Tools and Manufacture*, vol. 157, no. 103611, 2020.

[3] R.R. Toth, G. Stepan, ”Robot assisted stabilization for flexible workpieces subjected to highly interrupted cutting”, *MM Science Journal*, 2023.

[4] J. Axås, G. Haller, ”Model reduction for nonlinearizable dynamics via delay-embedded spectral submanifolds”, *Nonlinear Dynamics*, vol. 111, pp. 22079-22099, 2023.

NVHH2025-0100

From concept to construction: how to build fitting noise & vibration test labs

Z. Horváth, M. Rodrigues, P. Pinto

[1]CDM Stravitec NV, Overijse, Belgium

[*]Corresponding author, e-mail: z.horvath@cdm-stravitec.com

Summary

Behind every great man is a great woman, says the old saying. Behind every great R&D center is a great testing facility, which sounds like the transliteration of the above saying into the noise and vibration (N&V) control industry. Research work in the field of N&V technology has taken enormous steps, or instead, leaps, in the last decades. However, the demand for validating calculations or models, or officially classifying a product for noise emission, still requires the same circumstances as in the old times; a measuring space free of N&V. Designing and building it correctly is a task for an acoustic engineer and a challenge to suppliers and contractors, because the stakes are high. This presentation leads the reader into this process and shows some examples of recently realised laboratories.

Introduction

CDM Stravitec, a Belgium-based structural, acoustics and vibration isolation technology company, has been active for over 70 years, since 1951. In collaboration with acoustic engineers, the company was privileged to get involved in some exciting and prestigious laboratory projects and supply solutions by which the stringent requirements could be met. This presentation takes a journey into the design process, highlighting its main challenges, and shows some practical solutions by which different laboratories in different environments could be built.

Authors

The authors with different engineering backgrounds have long years of experience supporting acoustic designers in their endeavours and sharing those experiences at numerous conferences and events. Their practical approach has reinforced the respect of CDM Stravitec in scientific circles, as well.

How to design a good laboratory

Setting the goals

The purpose of the test facility always determines the goal: what it is built for and what is installed in it. Are there any criteria to meet? If yes, who defines them? What are the most typical ones? (VC curves)

Noise & vibration isolation

Creating a space as free from disturbances as possible always boils down to noise and vibration isolation and room acoustical tasks. What is the physics behind the phenomenon of isolation?

What are the physical boundaries to design, and the practical limitations of construction?

Environment

The laboratory environment is the next important factor. These factors determine the size, shape, weight, and necessary acoustic accessories during the design process.

How to design

Modelling or old school methods? What is worth modelling, and what isn't?

Materials to use

The laboratory room, how it is supported (building acoustics, materials), and what comes inside (room acoustics).

Constructional considerations

Building technology and its effect on possible solutions and results. Risks of the design during realisation and how to overcome them (technology, sequence).

Examples of different types of laboratories

General acoustic laboratory
Super silent enclosures
Special equipment testing laboratory

Conclusions

This presentation summarises the design process of a laboratory that will serve as a place where scientific work can be validated or refuted. Careful collection

of information and demand and awareness of available materials and solutions is essential for creating the testing space the R&D process requires. CDM Stravitec can offer decades of experience to acoustic designers to help them achieve their goals in building acoustics and vibration control.

Scientific articles

Only abstracts of the scientific articles are presented here. Full papers are available on the Conference Pen Drive and—if the authors have agreed—will be published in the IOP Journal of Physics: Conference Series (Online ISSN 1742-6596).

NVHH2025-0004

AI-driven solutions to enhance structural dynamics and NVH testing processes

K. Janssens[1*], L. Jia[1,3], A. Tavares[1,3], M. ElKafafy[1], D. Kunte[1,3], D. Gorgoretti[1], W. Vandermeulen[1], M. Brughmans[1], P. Csurcsia[2], S.A. Hosseinli[3,4], R. Vaerenberg[3,4], K. Gryllias[3,4,5], C. Colangeli[1], E. Di Lorenzo[1], F. Deblauwe[1], B. Cornelis[1]

[1] Siemens Industry Software NV, 3001 Leuven, Belgium
[2] Thermo and Fluid Dynamics (FLOW), Vrije Universiteit Brussel (VUB), Pleinlaan 2, 1050, Brussels, Belgium
[3] Department of Mechanical Engineering, KU Leuven, Celestijnenlaan 300, B-3001, Heverlee, Belgium
[4] Flanders Make @ KU Leuven, Belgium
[5] Leuven.AI - KU Leuven Institute for AI, B-3000 Leuven, Belgium

[*]Corresponding author, e-mail: karl.janssens@siemens.com

Abstract

This paper will discuss how artificial intelligence (AI) can be used to enhance physical testing processes in the automotive and aerospace industries, with a specific focus on structural dynamics and NVH. More specifically, the goal is to leverage AI-driven methodologies to improve the efficiency of test campaigns, support quality checks of sensor data, gain insights, and create lumped parameter digital twin models from experimental data. The role of AI in physical testing will be illustrated with several examples. Additionally, the paper will discuss physics-guided data augmentation, which uses simulation and test-based models to generate synthetic datasets that expand the coverage of experimental conditions. This approach addresses the problem of data scarcity, ensures the physical plausibility of augmented data, and improves the robustness of AI models by efficiently simulating different operating conditions and anomalies.

Keywords:

Physical Testing; AI; Physics-guided Data Augmentation; Industrial Applications

NVHH2025-0006

Effect of modal interaction on Close-mode Nonlinear Structures

W-T. Liao[1], H.G.D. Goyder[2], Y.J. Chan[1*]

[1]National Chung Hsing University, Department of Mechanical Engineering, Taichung, Taiwan

[2]Cranfield University, Shrivenham, United Kingdom

[*]Corresponding author, e-mail: yjchan@nchu.edu.tw

Abstract

This study investigates dynamic properties of close-mode nonlinear structures. A 5-DOF system with cubic stiffness is set up. To study the interaction of specific pairs of modes, harmonic excitation of selected profiles are applied in the vicinity of natural frequencies. Results show that the harmonic distortion and shifting resonant frequencies can lead to unexpected resonant peaks for modes with natural frequencies with integer ratio. Also, close natural frequencies leads to extra resonant peaks under higher loads.

Keywords:

Nonlinear vibration; Symmetric structures

NVHH2025-0007

Non-mass loaded excitation technique for precise laser measurements

P. Blaschke

NV Tech Design GmbH, Steinheim, Germany
e-mail: info@nv-tech-design.de

Abstract

The need to measure complex mechanical structures has grown in importance for efficiency in the design process and for structural monitoring. Despite the convenience of using a 3D scanning laser doppler vibrometer (LDV), fixed acceleration sensors are still widely used for industrial applications. However, the effects of sensor attachments cannot be disregarded for lightweight structures. This paper provides a thorough description of how various sensor attachment techniques affect vibration measurements over a wide frequency range (up to 16 kHz). Frequency response function (FRF) measurements were conducted on an aluminum plate of using both the LDV and an accelerometer simultaneously, excited by a scalable automatic modal hammer (SAM). For particular frequency ranges of interest, recommendations for fixation methods are proposed. The study's findings offer practical advice for industrial structure measurement evaluations.

An important outcome of this study is how the fixation method influences the experimental results of the modal properties. The research reveals that the fixation, the contact area, the sensor and the test specimen built a dynamic system that influences the results especially at higher frequencies and should be considered for precise measurements.

Keywords:

Sensor Fixation, Scalable Automatic Modal Hammer, Modal Damping, High Quality FRF

NVHH2025-0008

Practical features and performance of the symplectic time-domain and modal FEM methods of Soundy for car interior acoustic predictions

Cs. Huszty[1*], G. Firtha[1,2], F. Izsák[3]

[1]ENTEL Engineering Research & Consulting Ltd., H-1025 Budapest, Szépvölgyi út 32., Hungary

[2]Department of Networked Systems and Services, Faculty of Electric Engineering, Budapest University of Technology and Economics, Műegyetem rkp. 3., H-1111 Budapest, Hungary

[3]Department of Applied Analysis and Comput. Mathematics & HUN-REN–ELTE NumNet Research Group, Eötvös Loránd University, H-1117 Budapest, Pázmány P. stny. 1.C, Hungary

[*]Corresponding author, e-mail: huszty.csaba@entel.hu

Abstract

Finite Element Method (FEM) predictions for car interior acoustic problems have traditionally been limited by computational costs. In the Soundy framework, we can reduce the computing time by applying the symplectic time-domain approach or by using a modal solution. In this paper, we present and compare the performance of these two FEM solvers of Soundy on car interior problems on a tetrahedral mesh. We also present various practical aspects regarding boundary conditions and stability.

Keywords:

STD-FEM, time domain simulation, finite element method, absorption coefficient, admittance estimation, automotive interior acoustics

NVHH2025-0009

Virtual Prototype Assembly (VPA): an overview of the latest technological advancements

F. Bianciardi[1*], B. Forrier[1], M. Elkafafy[1], N. Salamone[1], D. De Gregoriis[1], K. Janssens[1]

[1]Siemens Industry Software NV, Leuven, Belgium

e-mail: fabio.bianciardi@siemens.com

Abstract

Virtual Prototype Assembly (VPA) is nowadays a key-technology in the vehicle industrial engineering NVH design. It allows full-vehicle NVH predictions early in the design phase by virtually assembling individual component models derived from test bench measurements or numerical simulations. Component-based TPA and substructuring are the core methodologies of the VPA.

To enhance the accuracy and efficiency of the predicted vehicle NVH performance, particularly for e-vehicles, several methodological innovations have been explored in the recent years, including:

- extending the validity of the experimentally identified mount stiffness toward high frequencies;
- addressing the substructuring problem of continuous interfaces between components, such as the case of the battery-to-body integration;
- using parametric reduced order models (pROM) in the VPA framework for efficient component design exploration and optimization;
- developing real-time capable VPA models enabling full-vehicle real-time predictions starting from source components tested on test-rigs.

This paper gives an overview of the latest technological innovations, presenting the achieved results on experimental application cases.

Keywords:

Virtual Prototype Assembly; mount stiffness; hybrid coupling; high-frequency; real-time.

NVHH2025-0015

Design of acoustic absorbers based on local resonant acoustic metamaterials

M. Kaltenbacher[1*], F. Spörk[1], D. Mayrhofer[1]

[1]Institute of Fundamentals and Theory in Electrical Engineering, TU Graz, Austria

*Corresponding author, e-mail: manfred.kaltenbacher@tugraz.at

Abstract

Metamaterials are becoming increasingly popular as a means of reducing vibration and noise. By attaching resonators to a base structure, a so-called stop band can be achieved that suppresses wave propagation in a selectable frequency range. This potential is exploited by finite element simulations to investigate the potential of such metamaterials for noise barriers. The most promising results were obtained with an array of local resonators attached to the base plate having uniform resonant frequency, and by excluding the outermost row of resonators.

Keywords:

Acoustic metamaterial, finite element simulations, sound barrier

NVHH2025-0016

Solution methods comparison for nonlinear structural-acoustic radiation problems: numerical methods – traditional Runge–Kutta method

Q. Xu[1*], Q. Luo[1], Y. Li[1]

[1]Southwest Jiaotong University, School of Mechanics and Aerospace Engineering, Chengdu, China

[*]Qi Xu, e-mail: xuqi@swjtu.edu.cn

Abstract

This study focuses on sound radiation induced by nonlinear structural vibrations under external forcing. Despite its importance, existing research on this topic remains relatively limited. In this regard, a comparative analysis is conducted between a previously developed numerical approach based on the Incremental Harmonic Balance (IHB) method and a conventional semi-analytical method employing the Runge–Kutta scheme. The performance of both methods is evaluated in terms of modeling accuracy and computational efficiency. Numerical results reveal that the IHB method expresses the structural response explicitly as a superposition of trigonometric functions with multiple frequency components, allowing direct substitution into the acoustic radiation formulas without additional frequency-domain transformations. This makes it inherently well-suited for analyzing sound radiation under multi-frequency excitations, particularly in the multiple frequency response, such as the superharmonic resonance region. In contrast, the Runge–Kutta-based method yields time-domain numerical solutions, which require a Fourier transform to extract frequency information before computing sound pressure. Although both approaches can effectively capture nonlinear vibration-induced acoustic radiation, the IHB method exhibits significant advantages in both accuracy and computational efficiency.

Keywords:

Nonlinear vibration; Sound radiation; multiple frequencies; superharmonic resonance radiation.

NVHH2025-0021

Rectilinear and torsional modal analysis of a drone propulsion system using optical methods

Cs. Horváth[1*], Sz. Gungl[2], B. Istók[1], T. Kimpián[2]

[1]Budapest University of Technology and Economics, Faculty of Mechanical Engineering, Department of Fluid Mechanics
[2]thyssenkrupp Components Technology Hungary Kft., System and Vehicle Dynamics Department, Acoustics and Signal Processing Group, Budapest, Hungary

[*]Corresponding author, e-mail: horvath.csaba@gpk.bme.hu

Abstract

Drone noise is a topic of increased interest in the aeroacoustics community. Typical experimental investigations apply microphone measurements to study the aeroacoustic characteristics of drone propulsion systems, often overlooking vibration-induced effects. This investigation applies rectilinear and torsional experimental modal analysis techniques to investigate a drone propulsion system. Rectilinear excitation is carried out using a traditional electrodynamic shaker, while the brushless DC motor of the propulsion system is utilized for the torsional excitation. The structure's response is recorded using a high-speed camera and analyzed with magnification algorithms. The goal of the investigation is to apply well-established experimental modal analysis methods to the new application area of drone propulsion systems to help separate vibration-induced noise sources from aerodynamically induced ones.

Keywords:

Drone noise; modal analysis; image processing; wave-based motion magnification; and torsional vibration analysis

NVHH2025-0026

NVH Modeling and Simulation of Drivetrain Gearboxes

H. Wang[1,2*], F. Naets[1,2]

[1]Department of Mechanical Engineering, KU Leuven, Leuven, Belgium
[2]Flanders Make@KU Leuven, Leuven, Belgium

[*]Corresponding author, e-mail: hongmei.wang@kuleuven.be

Abstract

Gearbox NVH are critical concerns in drivetrain systems, impacting performance, reliability, and user comfort. This study explores the gearbox NVH modeling and simulation approach and provide a framework for efficient NVH prediction. The primary sources of gearbox noise and vibration, including gear meshing dynamics and housing flexibility are investigated. Lumped parameter modeling (LPM), Finite Element Analysis (FEA) and multibody dynamics simulations are employed to model gearbox and drivetrain dynamics, identifying critical vibration modes and the influence of component interactions.

Keywords:

Gearbox NVH, Dynamic modeling, Multi-body dynamics

NVHH2025-0028

The effective reduction of spurious oscillations in the valve closure event of an internal combustion engine

D. Serfőző

Széchenyi University, Department of Applied Mechanics, Győr, Hungary

e-mail: serfozo.daniel@sze.hu

Abstract

The accurate numerical solution of contact-impact problems using finite element method is challenging in multiple aspects. The main difficulty is the effective attenuation of spurious oscillations emerging due to the spatial discretization. As these oscillations deteriorate the accuracy, the elimination of spurious components in the numerical results has a great importance. To achieve it, a damping effect must be contained in the applied numerical scheme. Based on the conducted research in this field, the concrete shape of the damping character plays a crucial role in reducing oscillations with the best possible efficacy. The proposed method operates with viscous damping formulated as Caughey damping. Considering concrete industrial problems, represented as a two-dimensional FEM model, the proposed scheme proved to be effective and more accurate compared to several widely applied numerical methods. Due to the simple formulation combined with good oscillations reduction, the newly developed method has a great potential in practical engineering applications.

Keywords:

Oscillations, Damping, Impact, Contact, Wave propagation

NVHH2025-0031

CT equipment based on sound waves

G. Pór

University of Dunaújváros, Institute of Technology, Dunaujvaros, Hungary
MAID Laboratory
e-mail: porg@uniduna.hu

Abstract

Scanning Acoustic Microscopy (SAM) is a well-known method for detecting flaws in solid materials. It is an ultrasonic testing technique, in which the traditional pulse-echo ultrasound method is combined with precisely driven mechatronics. Using the A-scan as the z-direction reflection at a single point, we collect A-scans at each selected point of the x–y plane, resulting in a three-dimensional dataset. Any 2D slice (i.e., 2D plane) can then be selected, where sound reflections can be identified as flaws in the material. With our newly developed equipment, we can produce a 3D rotating image of all flaws in the material, including flaws, delaminations, and internal structures. In this contribution, we present the results of an examination of a 4 mm-thick, 16-layer composite material, which was pressed to induce delamination between the layers. Excellent 3D rotating images demonstrate that a resolution of 0.1 mm can be achieved, producing CT-like reconstructions based on sound waves..

Keywords

Scanning Acoustic Microscope (SAM), delamination, composite materials, surface corrections

NVHH2025-0039

Exploring stability domains in compressible Ogden's hyperelastic model

A. Kossa

Department of Applied Mechanics, Faculty of Mechanical Engineering, Budapest University of Technology and Economics, Budapest, Hungary

e-mail: kossa@mm.bme.hu

Abstract

Rubber-like materials significantly affect the vibrational behavior and damping behavior of structures. Precise numerical computations in vibroacoustic engineering call for precise modeling of rubber-like materials. The most frequently utilized constitutive mechanical models for such materials are the hyperelastic models, of which the Ogden model is extremely popular since it can simulate well nonlinear stress-strain behavior using a very low number of material parameters. In practical applications, the accounting of volumetric deformation, however small, is crucial to achieve proper simulation. The present study demonstrates that for the compressible Ogden model, stability may be lost even when loading conditions are uniaxial, which can be difficult to simulate. The research aims at determining stability regions for common loading conditions and examining the influence of Poisson's ratio on such stability regions. Through the application of analytical as well as numerical methods, we obtain such stability boundaries, and these are further verified through finite element calculations. Such knowledge of stability limits is significant to ensure that efficient numerical solutions can be obtained in engineering applications. These findings can directly be utilized in improving the accuracy of NVH simulations where rubber components (such as bushings, mounts, or seals) are utilized in vibration isolation and structural noise absorption in vehicles. Our findings provide valuable guidance on enhancing the accuracy of acoustic and vibrational design models, bridging theory with practical engineering needs.

Keywords:

Hyperelasticity, compressibility, Ogden hyperelastic model, stability, constitutive modelling

NVHH2025-0040

Electric machine stator FRFs prediction using Machine Learning

D. Carlino[1*], F. Chauvicourt[1], R. Raia[2]

[1]Siemens Digital Industry Software, ES RTD, Leuven, Belgium
[2]Siemens Digital Industry Software, ROM, Brasov, Romania

[*]Corresponding author, e-mail: davide.carlino@siemens.com

Abstract

In this paper, a Machine Learning surrogate model is developed for Noise, Vibration, and Harshness (NVH) analysis of a 48-slot, 8-pole Permanent Magnet Synchronous Motor (PMSM) stator. A parametric stator model is used to generate a Finite Element based dataset. The resultant Frequency Response Functions (FRFs) due to dedicated force waves are the output to be predicted. To this end, several pre-processing data reduction techniques combined with Machine Learning (ML) regressions are investigated. The findings confirm the workflow ability to generalize effectively, offering a robust and efficient method for NVH analysis of PMSM without the need for an FE model.

Keywords:

Machine Learning; Electric Motor; NVH; Finite Element Analysis; Surrogate Model

NVHH2025-0042

Acoustic excitation for experimental characterization of contact damping in prestressed assemblies

B. Magyar[1], G. Csernák[1], R. Wohlfart[1], Á. Miklós[1*], G. Hénap[1], R. Zana[1], G. Stépán[1]

[1]Budapest University of Technology and Economics, Department of Applied Mechanics, Hungary

[*]Corresponding author, e-mail: miklosa@mm.bme.hu

Abstract

Contact damping contributes significantly to overall structural damping in most engineering systems, yet its prediction remains difficult without physical prototypes. We present an experimental investigation of modal damping in a simplified assembly with adjustable prestress, allowing controlled exploration of contact conditions. Using acoustic excitation, we selectively target individual mode shapes, facilitating precise damping measurements. This method enables direct comparison of damping ratios under free and excited vibrations. Our goal is to identify parameters or physical quantities that can be calculated to predict contact damping well even in case of various geometries.

Keywords:

Contact damping, adjustable prestress, phase resonance

NVHH2025-0043

Optimizing the dynamic behavior of e-Axle test benches by reducing low-frequency vibrations

Z.G. Gazdagh[1,2*], A. Fejér[3], D. Ács[4]

[1]Dept. of Whole Vehicle Engineering, Széchenyi István University, Győr, Hungary
[2]Robert Bosch Kft., Engineering Acoustics – Noise Vibration and Harshness, Budapest, Hungary
[3]Robert Bosch Kft., Electrified Motion – eAxle Layout and Design, Budapest, Hungary
[4]Robert Bosch Kft., Electrified Motion – eAxle Validation, Budapest, Hungary
[*]e-mail: gazdagh.zoltan.gabor@sze.hu

Abstract

In modern automotive testing, controlling vibrations is critical for ensuring system durability and comfort. The inherent low-frequency oscillations of e-axle test benches pose a significant challenge, often leading to unwanted vibrational effects. To address this, our study emphasizes the importance of accurately determining the inertia properties and centre of gravity location. By integrating these measurements into a validated simulation model, we can optimize the assembly position - particularly for rubber mounts - thereby reducing unwanted vibrations. The proposed method involves calculating the moment of inertia and identifying the exact center of gravity coordinates from FRF data and impulse hammer tests. These parameters serve as essential inputs for a simulation model that influences the low frequency dynamic behavior of the test bench. The validated model aims to provide a clearer understanding of the eAxle's operation, thereby aiding in the comprehension of test bench and vehiclelevel behavior. This integrated approach not only enhances vehicle performance but also helps to optimize low frequency performance in test bench measurements caused by output shaft excitations. Ultimately, precise dynamic parameter measurement and simulation-based optimization lead to more reliable and efficient e-axle test bench performance.

Keywords:

Center of Gravity, moment of inertia, eAxle, mass line

NVHH2025-0047

Surface-line contact TPA - Windscreen sensitivity on acoustic transfer at wiper blade positions

T.F. Varga[1*], L.L. Szabó[1]

[1]Robert Bosch Kft, Engineering Acoustics - Noise Vibration and Harshness, Budapest, Hungary

[*]Corresponding author, e-mail: TamasFerenc.Varga@hu.bosch.com

Abstract

Wiper blade and windscreen contact can be considered as a special type of connection in the vibration transfer path of vehicles. Most of connections between vehicle components are point-to-point connections in transfer path analysis, but a wiper blade edge is a line, while the windscreen is a surface on which the blade slides during wiping or is hit by the blade during blade reversal. The presented method uses measured acoustic transfer functions (ATFs) and applies their spatial distribution to describe windscreen sensitivity on wiper blade excitations. Windscreen sensitivity can be related to structural and acoustical modes of the vehicle.

Keywords:

TPA; Acoustic transfer function; wiper system; EMA

NVHH2025-0048

Overview of nonuniform filter bank design methods

B. Ország[1*], L. Sujbert[1]

[1]Department of Artificial Intelligence and Systems Engineering, Faculty of Electrical Engineering and Informatics, Budapest University of Technology and Economics, Műegyetem rkp. 3., H-1111 Budapest, Hungary

[*]Corresponding author, e-mail: orszag@mit.bme.hu

Abstract

This paper investigates the design and implementation of nonsubsampled finite impulse response filter banks, which are commonly utilized in digital signal processing algorithms that demand some timefrequency representation of a signal. Filter bank design is especially difficult if nonuniform bands are required. Most design methods have been developed with the requirement that the input signal must be perfectly reconstructable, but by imposing this, it significantly limits the set of solutions. By permitting a tolerable reconstruction error this requirement can be relaxed. In this paper, we present several of these design methods and give qualitative and quantitative comparisons.

Keywords:

FIR filters, nonuniform filter banks, nonsubsampled filter banks, near perfect reconstruction

NVHH2025-0050

Predicting valve-pipeline instability via impedance equations

Cs. Hős

Budapest University of Technology and Economics Faculty of Mechanical Engineering, Department of Hydrodynamic Systems, Budapest, Hungary

e-mail: hos.csaba@gpk.bme.hu

Abstract

Valve chatter in pipeline systems poses significant challenges in the design and operation of hydraulic and pneumatic networks. This paper introduces a semi-analytical framework for predicting such instabilities using impedance-based methods. Assuming small-amplitude periodic oscillations of pressure and velocity in barotropic fluids, the governing equations are linearised and recast into frequency-domain impedance relations. These relations are extended to include valves, reservoirs, throttle valves, and other components, resulting in a homogeneous algebraic system whose nontrivial solutions determine the critical instability frequencies. Analytical insights are provided for several special cases—including close-coupled valves and quarter-wave instability—along with numerical results to demonstrate the effectiveness of the approach. The proposed method offers a systematic and computationally efficient tool for assessing valve-pipeline stability in systems of arbitrary complexity.

Keywords:

valve chatter, pipeline dynamics, impedance method, pressure relief valve

NVHH2025-0052

Experimental study of self-excited vibrations in broaching operations using strain gauge based stiff load cell technology

Z. Iklodi[1,2*], A. Miklos[1], B. Magyar[1] R. Wohlfart[1], I. Kovacs [3], Z. Dombovari[1,2]

[1]Department of Applied Mechanics, Faculty of Mechanical Engineering, Budapest University of Technology and Economics, Budapest, Hungary
[2]MTA-BME Lendület Machine Tool Vibration Research Group, Department of Applied Mechanics, Budapest University of Technology and Economics, Hungary
[3]Fogaskerekgyár Ltd., Tata, Hungary

[*]Corresponding author, e-mail: zsolt.iklodi@mm.bme.hu

Abstract

In this case study, exploiting a theoretical *infinite length* broaching model, analytic and numeric asymptotic stability predictions are derived to forecast the transient dynamic behaviour of the real, time-limited machining operation. These stability assessments are then validated both numerically and empirically. As instabilities are generally difficult to induce in conventional broaching machines, for conducting cutting experiments, a small scale laboratory test bench is established. To do so, a three-axis milling machine is retrofitted with a custom tool holder, integrated with a stiff, four-axis, strain-gauge-based load cell. This configuration allows accurate monitoring of the process dynamics, and a high degree of control over the operation parameters.

Keywords:

broaching, machine tool chatter, delay, stability

NVHH2025-0053

Investigating passive-side noise in component-based TPA: Insights and recent improvements

B. Gergacz[1*], T. A. Kimpian[1], F. Kadar[2]

[1]thyssenkrupp Components Technology Hungary Kft., Department of Acoustic and signal Processing, Budapest, Hungary
[2]Budapest University of Technology and Economics, Department of Applied Mechanics, Budapest, Hungary

[*]Corresponding author, e-mail: bendeguz.gergacz@thyssenkrupp-automotive.com

Abstracts

The transition from combustion engines to electric motors in the automotive industry has resulted in quieter vehicle interiors, shifting the focus to noise generated by systems such as the electric power-assisted steering system. Component-based Transfer Path Analysis (cTPA) is a key technique for analyzing vibration transmission, investigating the interface between noise-generating active components and the receiving passive structures. In this study, a specialized test setup was developed to assess the impact of passive-side noise on the prediction accuracy of cTPA. To this end, an electric steering motor was mounted on a test bench, and broadband disturbances were introduced to the passive side using an electromechanical shaker. The results were evaluated across different RPMs as well as along spectral orders, providing a comprehensive analysis of the strengths and limitations of cTPA in industrial applications.

Keywords:

Transfer Path Analysis; Blocked force; Vibro-acoustics; Steering; Electric motor

NVHH2025-0055

Vibration characteristics of rolling elements in the presence of different friction and creep models

M. Antali

Széchenyi István University, Department of Applied Mechanics, Győr, Hungary

e-mail: antali.mate@sze.hu

Abstract

Dynamics of wheels and other rolling elements in machines are significantly affected by the friction phenomena between the surfaces. When modeling the transitions between rolling and slipping motion, the simplest choice is applying the Coulomb friction model or the similar but improved models like the Stribeck model. However, when the local deformations are not negligible, often the so-called creep force models are used, which contain a coupled nonsmooth effect of the kinematic variables. This study investigates the different and sometimes surprising effect on the different contact models on the properties of the vibrations. The models are demonstrated on 2D test problems of rolling elements. Mathematical methods of nonsmooth dynamics and singular perturbation are utilized to explore the details of the phenomena.

Keywords:

Dry friction; Creep force; Nonsmooth dynamics

NVHH2025-0056

Compensation of inharmonicity of pianos strings with added masses

P. Szalai[1*], M. Antali[2]

[1]Széchenyi István University, Department of Machine Design, Győr, Hungary
[2]Széchenyi István University, Department of Applied Mechanics, Győr, Hungary
[*]Corresponding author, e-mail: szalai.peter@ga.sze.hu

Abstract

Bass strings of piano consists of a core string and a wire wound around the core. Although this construction is essential for creating strings with low frequency in the presence of moderate tension force, the increased bending stiffness shifts the overtones of the strings. This inharmonicity is more significant for upright pianos with shorter string lengths. In the literature, we can find conceptual ideas for compensation of this effect that is considered acoustically unpleasant. In the present research, we analyse the effect of adding concentrated masses to reduce the amount of inharmonicity. We focus on improvements in the acoustically most significant overtones. The proper parameters are found by using both a finite-element method and experiments.

Keywords:

Piano strings; Inharmonicity; Finite element method; Vibrations

NVHH2025-0060

Dynamic sensors and actuators 3D-printed with filament extrusion

T. Barši Palmić[1], J. Slavič[1*]

[1]University of Ljubljana, Faculty of Mechanical Engineering, Ljubljana, Slovenia

[*]Corresponding author, e-mail: janko.slavic@fs.uni-lj.si

Abstract

3D printing enables the fabrication of multi-material active structures capable of converting mechanical stimuli into electrical signals (sensing) or electrical energy into mechanical motion (actuation). By combining conductive and dielectric polymer composites, it is possible to realize dielectric actuators exhibiting precise displacement control (micro- to nanometer scale) across a broad dynamic range (static to tens of kilohertz). An electromechanical model facilitates precise customization of actuator performance for specific applications, allowing on-demand fabrication. The development of such actuators, together with piezoresistive and piezoelectric sensors, demonstrates significant potential for creating customizable smart structures in a single automated manufacturing process.

Keywords:

3D printing, additive manufacturing, fused-filament fabrication, sensor, actuator, dielectric actuator, electromechanical model, design principles

NVHH2025-0062

Computation of sound radiation by moving sources using the convected boundary element method

P. Rucz[1*], P. Fiala[1]

[1]Budapest University of Technology and Economics, Faculty of Electrical Engineering and Informatics, Department of Networked Systems and Services, Budapest, Hungary

[*]Corresponding author, e-mail: rucz@hit.bme.hu

Abstract

The boundary element method (BEM) is a numerical technique for solving the Kirchhoff–Helmholtz integral equation. Exploiting the Sommerfeld radiation condition, the approach is well-suited for predicting the sound emission of complex sources in unbounded domains. Uniform motion can be incorporated into the formulation, leading to the so-called convected BEM.

This contribution discusses the application of the latter technique for the simulation of noise emission by moving sound sources in practically relevant scenarios. After introducing the basic properties of the formulation, challenges of its application are addressed. Approaches to deal with fictitious eigenfrequencies, half-space problems, and transient sound radiation are presented. The multi-level fast multipole method for solving large-scale problems is implemented and applied. An industrially relevant case study of noise radiation by a vibrating train wheel is demonstrated.

Keywords:

Boundary element methods; Convected Helmholtz equation; Fast multipole BEM; Moving sound sources

NVHH2025-0066

On complex mode shapes and their identification

F. Ponce-Vanegas

Basque Center for Applied Mathematics, Bilbao, Basque Country – Spain

e-mail: fponce@bcamath.org

Abstract

In experimental modal analysis, proportional damping is a convenient simplification that allows practitioners to fit their data to a model. However, this simplification seriously reduces the number of free parameters for fitting, and some systems may be misrepresented by the assumption of proportional damping. We discuss the mathematics behind nonproportional systems, and we propose methods to deal with the computationally demanding problem of fitting data with complex mode shapes.

Keywords:

Experimental modal analysis, Complex mode shapes, Model fitting

NVHH2025-0073

Real-time MRI-based transformer model for articulatory speech synthesis

S. Gonzalez y Gonzalez[1*], M.S. Al-Radhi[1]

[1]Department of Telecommunications and Artificial Intelligence, Budapest University of Technology and Economics, Budapest, Hungary

[*]Corresponding author, e-mail: sgonzalezygonzalez@edu.bme.hu

Abstract

This thesis explores a novel method for articulatory-to-acoustic speech synthesis by leveraging real-time magnetic resonance imaging (rtMRI) data of the vocal tract. The primary objective is to develop a deep learning model that learns articulatory representations directly from sequences of rtMRI frames and generates corresponding acoustic features in the form of mel-spectrograms. The proposed architecture combines convolutional neural networks for spatial feature extraction with a Transformer-based model for temporal sequence modeling, enabling the system to capture both the anatomical structure and dynamic movement of the articulators over time.

The model was trained on paired rtMRI and speech data, achieving promising results in predicting mel-spectrograms that structurally resemble their ground-truth counterparts. Qualitative evaluations show that the system is capable of modeling complex articulatory patterns. However, the final step of converting the predicted mel-spectrograms into audio waveforms with Griffin-Lim algorithm remains with not a good audio quality and is left for future work. This study contributes to the growing field of interpretable and physiologically grounded speech synthesis and provides a foundation for further advancements in multimodal speech technologies.

Keywords:

real-time MRI, articulatory movement, speech synthesis, speech waveform generation

NVHH2025-0074

Optimization of the position and parameters of a tuned-mass damper for flutter suppression applying Bayesian optimization

D.A. Horváth[1*], J. Lelkes[2], T. Kalmár-Nagy[1]

[1]Budapest University of Technology and Economics, Faculty of Mechanical Engineering,Department of Fluid Mechanics, Budapest, Hungary
[2]Robert Bosch Kft., Budapest, Hungary

[*]Corresponding author, e-mail: horvathd1@edu.bme.hu

Abstract

When thin, flexible structures are subjected to airflow, aeroelastic phenomena can occur due to the interaction of elastic, inertial, and aerodynamic forces. Flutter is an aeroelastic instability that leads to dynamic stability loss above a critical flow velocity. This paper investigates a tuned-mass damper (TMD) to attenuate the flutter vibrations and thus expand the stable flight regime. We aim to optimize the parameters and the position of the TMD. To optimize not only the chordwise but also the spanwise position of the TMD, we construct a three-dimensional reduced-order model based on the usual two degrees of freedom model. To determine the optimal position and parameters of the TMD we apply Bayesian optimization. This method assumes only continuity about the objective function (in our case the flutter velocity) and evaluates it less frequently compared to traditional methods. This technique is thus well suited to our problem, where the objective function is costly to evaluate.

Keywords:

aeroelasticity; fluid-structure interaction; vibration attenuation; bayesian optimization

NVHH2025-0075

Flank contact and the stability of cutting processes

Z. Sandor[1*], D. Bachrathy[1], G. Stepan[1]

[1]Budapest University of Technology and Economics, Department of Applied Mechanics, Budapest, Hungary

[*]Corresponding author, e-mail: ksizalan@gmail.com

Abstract

Process damping is a well-documented phenomenon in machining, which is used to explain stability improvement at low cutting speeds. A popular approach is based on the indentation volume beneath the cutting tool, where the contact length between the tool's flank face and the workpiece is assumed to be constant. Although fluctuations in contact length appear to be small, it is crucial to examine whether this has any effect on linear stability. This study introduces a linearization method for the state-dependent delay differential equation derived from the indentation volume under the tool. The mathematical findings indicate that contact length fluctuations do not affect linear stability.

Keywords:

Process damping; Contact length; Linear Stability; Chatter

NVHH2025-0079

Development of tracking methods for nonlinear resonances using a real-time controller

J. Karsai

Budapest University of Technology and Economics, Department for Artificial Intelligence and Systems Engineering, Budapest, Hungary

e-mail: janoskarsai2002@gmail.com

Abstract

Since the first design of the phase-locked loop, various architectures have emerged, as well as new applications0. One of these applications is tracking backbone curves of nonlinear vibrating structures. The focus of this study is to examine what kind of phase-locked loop (PLL) architectures exist for mapping resonances of nonlinear mechanical systems. In the literature, backbone curve measurements have been documented on beam structures, electric components, aircraft and vehicle components, etc. The most common choice is to build the PLL with a mixer phase detector, a PI controller, and a module responsible for generating the output of the control system. However, there exists a variety of options for the phase detector. The choice of whether the phase detection is online (the phase difference is evaluated for every sampling time interval) or offline determines what resources are required and how long a phase tracking experiments takes. In this work, the phase detector options for a digital phase-locked loop design are described, an implementation of an offline PLL is demonstrated and evaluated, and steps of further development are suggested.

Keywords:

Nonlinear resonances, Phase detector, Phase-locked loop, FPGA

NVHH2025-0081

Self-excited oscillations in brake systems: can impact-induced bounce trigger sustained vibrations?

B. Bauer[1*], G. Habib[1]

[1]Budapest University of Technology and Economics,
Faculty of Mechanical Engineering, Department of Applied Mechanics,
Budapest, Hungary

[*]Corresponding author, e-mail: balazs.bauer@mm.bme.hu

Abstract

We investigate transient impacts in drum brakes, where microsecond-scale bounce events can trigger self-excited vibrations. Modeling the shoe as a hinged bar oscillator, we show how friction-induced energy amplification combined with sudden braking can potentially destabilize the system. Analytical and numerical analysis reveals the existence of a self-excited periodic solution, originating from a fold bifurcation. This robust pattern persists across several impact and friction models, demonstrating that impact-induced oscillations are intrinsic to shoe drum brake systems, especially during emergency braking. Our results provide a framework for predicting and mitigating brake NVH while improving transient response – critical for vehicle safety.

Keywords:

Impact; Friction; Fold bifurcation; Drum brakes; Shoe brakes

NVHH2025-0083

Human balancing on SUP board

R.K. Richlik[1*], G. Stépán[1]

[1]Budapest University of Technology and Economics, Department of Applied Mechanics, Budapest, Hungary

[*]Corresponding author, e-mail: richlikrobert@gmail.com

Abstract

Nowadays, the surface of the lakes is covered with people trying to balance and paddle on SUP boards. It is interesting to observe the smaller and larger frequency of stability losses in this form of movement. We present the physical background of these phenomena by approaching the functioning of the human nervous system with PD control, taking into account the time delay of the nervous system. To construct the mechanical model of the system, two 1DoF models are connected: the human body described with a four-joint mechanism, and the SUP board as a floating body supported by the buoyancy force. The general coordinates are the tilt of the SUP board and the tilt of the human hip relative to the board. During the calculations, we assume that the person's feet did not slip on the board. The equations of motion of the coupled system are derived using the Lagrangian equation, which results in a system of delay differential equations. Stability test is performed in the plane of the PD control parameters. The obtained theoretical results are supported by numerical simulation.

Keywords:

Human balancing, Floating body, PD controller, Time delay

NVHH2025-0085

Measuring orientation for visual balancing task of Furuta pendulum

B. Endresz[1*], G. Stepan[1]

[1]Budapest University of Technology and Economics, Department of Applied Mechanics, Budapest, Hungary

[*]Corresponding author, e-mail: endresz.balazs@edu.bme.hu

Abstract

The stability of an unstable system's control depends significantly on measurement accuracy, sensor precision, and time delay. These factors directly influence the system's dynamics and stability requiring careful consideration in both structural design and control algorithm development. This paper presents a comparative analysis of visual orientation detection algorithms from an internal perspective, focusing on their role in controlling a rotary inverted pendulum. It also examines the necessary mechanical calculations for determining the system's critical time delay, which establishes an upper bound for the detection time based on image processing.

Keywords:

balancing, control, image processing, orientation detection, critical time delay

NVHH2025-0088

Sensitivity analysis of tooth microgeometric modifications on vibroacoustic behaviour in helical gears with harmonically distributed variations

K. Horváth[1*], A. Zelei[1]

[1]Széchenyi István University, Audi Hungaria Department of Whole Vehicle Engineering, H-9026 Győr, Hungary

[*]Corresponding author, e-mail: horvath.krisztian@ga.sze.hu

Abstract

The virtual acoustic testing of gear drives has gained growing importance. Fundamentally, the transmission error (TE) is predicted, since it directly affects the vibration and noise characteristics. In this study, the effect of the harmonically distributed tooth microgeometric variations on the TE is investigated via elastic multibody simulations of a helical gear pair. The sensitivity analysis focused on the tip relief, the root relief and the barrelling. The model considered different degrees of linear-, quadratic- and cubic-harmonically distributed variations. The results showed that barrelling with quadratic harmonic microgeometry had the most significant effect on TE. In addition, if harmonic distributions accidentally coincide in the pairing of the gears, the TE is significantly amplified, leading to a pronounced excitation of the system dynamics.

Keywords:

Helical gears; Tooth microgeometry; Transmission error; Sensitivity analysis; Vibroacoustics

NVHH2025-0089

Simulation problems on the state dependent representation of boring bar torsion

L. Radulovic[1*], Z. Dombovari[1]

[1]Department of Applied Mechanics, Budapest University of Technology and Economics, Budapest, Hungary

[*]Corresponding author, e-mail: luka.radulovi@edu.bme.hu

Abstract

The boring process has an important role in the industry, producing fine borehole surfaces with a fairly slender turning tool. This tool is known to be prone to bending, but depending on the geometrical arrangement torsion can cause serious problems. Torsional oscillation is especially dangerous since it directly affects the depth of cut and the regenerative delay. This results in the necessity of state-dependent delay formalism, which greatly complicates the corresponding equations of motion. To have an independent time domain solution we introduce the delay as a state beside two spatial and a single angular positions as well as velocity coordinates. This produces a non-linear delay differential equation with seven state coordinates integrated in time.

Keywords:

vibrations, machine tools, delay differential equations

NVHH2025-0090

Dynamics of low immersion milling subjected to Coulomb friction

F. Bucsky[1*], Z. Dombovari[1]

[1]Department of Applied Mechanics, Budapest University of Technology and Economics, Budapest, Hungary

[*]Corresponding author, e-mail: f.s.bucsky@gmail.com

Abstract

Chatter vibrations are a problem, which plague the manufacturing industry. These self excited vibrations are a result of the regenerative effect and are one of the key limiting factors of manufacturing productivity. Due to this reason many techniques have been explored and applied to attenuate these self excited vibrations. In this work we study the effects of artificially introducing a Coulomb friction based energy dissipation to a flexible workpiece, which is then machined in a low immersion, down milling configuration, and introduce an appropriate measurement environment, where the arising friction can be controlled reliably.

Keywords:

Milling, Chatter, Coulomb friction

NVHH2025-0092

Application of the time-domain boundary element method for acoustic validation of structural NVH simulations

T. Giese[1*], S. Schneider[2]

[1]FunctionBay GmbH, Munich, Germany
[2]Ulm University of Applied Sciences, Ulm, Germany

[*]Corresponding author, e-mail: timo.giese@functionbay.org

Abstract

Predicting radiated noise is a key challenge in NVH development across various mechanical systems. This paper presents a time-domain boundary element method (TD-BEM) approach to compute airborne sound fields directly from structural vibrations. Accurate acoustic prediction requires that structural dy-namics, excitations, and component properties are precisely modeled. Thus, radiated sound serves as a powerful additional criterion to assess overall simulation quality. A validated flexible multibody model provides surface accelerations and therefore the boundary conditions for the TD-BEM. The method is demonstrated on a gearbox test rig in an anechoic environment, showing excellent correlation between measured and simulated sound pressure levels, with deviations below 1 dB. This confirms that accurate modeling of the structural and dynamic behavior is essential for reliable acoustic predictions. The pro-posed workflow establishes acoustic validation as a critical step in simulation-driven NVH development, reducing costly prototyping and enhancing design confidence.

Keywords:

Time-Domain Boundary Element Method (TD-BEM); NVH Simulation; Acoustic Validation; Sound Radiation; Structural Dynamics

NVHH2025-0093

Diffusion-based brain-to-speech synthesis: decoding intracranial EEG into natural speech

F.E. Akaaboune[1*], M.S. Al-Radhi[1]

[1]Budapest University of Technology and Economics, Department of Telecommunications and Artificial Intelligence, Budapest, Hungary

[*]Corresponding author, e-mail: fatimaezzahra.akaaboune@edu.bme.hu

Abstract

Brain-to-speech synthesis is a promising method for helping people with speech impairments communicate. In this paper, we propose a new approach that uses diffusion models to decode speech from intracranial EEG (iEEG) signals. Unlike traditional models that rely on deterministic transformations or direct neural-to-acoustic mappings, diffusion models leverage a generative process that gradually refines noisy latent representations into high-fidelity speech waveforms. This iterative denoising mechanism enables the reconstruction of fine-grained spectral and temporal speech features, enhancing both clarity and naturalness. Our model is trained and evaluated on a publicly available iEEG speech production dataset. By effectively capturing the dynamic variations in speech signals, this work represents an advancement toward real-time, brain-driven speech synthesis, opening new possibilities for neural assistive technologies.

Keywords:

Generative AI; Brain-to-Speech; Diffusion Models; Neural Decoding; Intracranial EEG

List of papers

Keynote speakers – plenary lectures

Industrial case studies

Scientific articles

List of authors

NVHH 2025 – SITE MAP

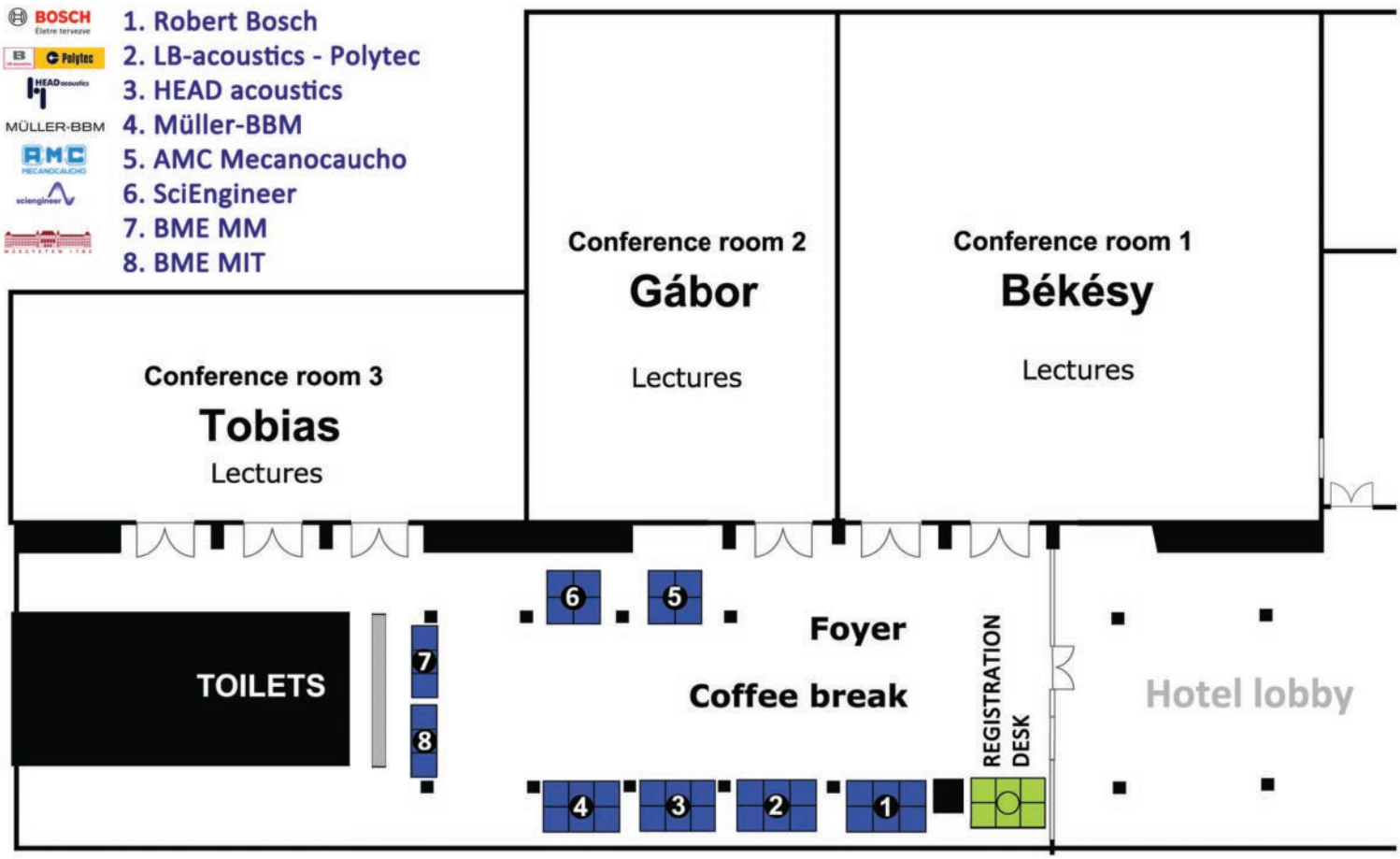

Sponsors:

BOSCH
Életre tervezve
www.bosch.hu

thyssenkrupp
thyssenkrupp.com

AVL
www.avl.com

KNORR-BREMSE
www.knorr-bremse.com

Exhibitors:

LB-acoustics Polytec
lb-acoustics.at

HEAD acoustics
www.head-acoustics.com

MÜLLER-BBM
www.muellerbbm.com/hompage

AMC MECANOCAUCHO
www.mecanocaucho.com

sciengineer
sciengineer.com

Organizing Partners:

MŰEGYETEM 1782

MAGYAR MÉRNÖKI KAMARA

SZÉCHENYI EGYETEM
UNIVERSITY OF GYŐR

National Research, Development and Innovation Office
Hungary

PROGRAM FINANCED FROM THE NRDI FUND

Notes:

Source: Ambrus Apartman Balatonalmádi

NVH 2025

October 8-10, Balatonalmádi

Conference organizing partners:

Sponsors:

Exhibitors:

PROGRAM FINANCED FROM THE NRDI FUND